Inhibition of Nuclear Import of Calcineurin Prevents the Development of Myocardial Hypertrophy

Dissertation zur Erlangung des
naturwissenschaftlichen Doktorgrades
der Bayerischen Julius-Maximilians-Universität Würzburg

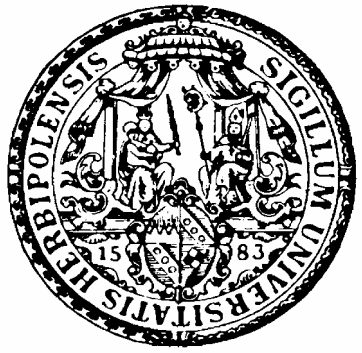

vorgelegt von
Matthias Hallhuber
Vilshofen, Deutschland

Würzburg, 2007

eingereicht am: …….....

Mitglieder der Promotionskommission:

Vorsitzender: .....

Gutachter : .....

Gutachter: .....

Tag des Promotionskolloquiums: .....

Doktorurkunde ausgehändigt am: .....

dedicated to

my Family

Doreen

Christine & Reinhard

Melanie & Christian

Erika, Andrea & Torsten

Acknowledgements

First I would like to thank **Prof. Dr. med. Georg Ertl** for giving me the opportunity to work at the Medical Department I of the Julius-Maximilians-University of Wuerzburg. Additionally, I want to thank **Prof. Dr. rer. nat. Roland Benz,** my custodian from the faculty of biology. Without him, my external PhD study would not have been possible. I want to thank him for listening to my results, reading my thesis and taking responsibility for me and my work.

Especially, I want to thank my custodian during my PhD study, **PD Dr. med. Oliver Ritter**. He gave me the chance to work outside the faculty of biology, to do my external PhD thesis and integrated me friendly in his working group. The very friendly and supportive atmosphere in this group contributed essentially to the final outcome of my studies. Additionally, I want to thank Oliver Ritter not only for helpful discussions but also for private communications and primarily for the possibility to attend diverse congresses, where we had lots of fun. Also, I want to thank **PD Dr. rer. nat. Kai Schuh**. We had lots of discussions about work, but also on things, which the world does not need. It was always funny and I hope, the discussion will go on - at least per telephone.

In this context I would like to thank **Natalie Burkard**, often my right hand in the lab, my bed neighbour on diverse congresses, a very helpful and friendly colleague and - most important - a very good friend. Natalie, I enjoyed the very funny talks often in the late hours in our office and I enjoyed your very good cakes. Also, I want to thank **Jenny Muck**, my left hand during working in the lab. So, did I anything?? When I had questions on labor techniques, Jenny always tried to help me to manage my problem. In this way, I also want to thank her for funny evenings in the Esco-Bar together with Natalie, Claudia and Evi. Another member of my working group is **Claudia Gebhardt**. I want to thank her to do lots of work for me. Especially in the time I wrote my PhD thesis. We had lots of fun discussing about a very special horse, you know Claudia? Without my personal animalhouse keeper **Evi Reichert**, my work would not have been so successful. Evi was not only perfect looking for the animals, Evi was also perfect to hear any Bon Jovi Song, when she was in our office. I would like to thank her for lots of fun in our office – especially our laugh attacks.

Finally, I want to thank Paula, Rongxue, Vijay, Virginija, Theo and all the other people in the Molecular Cardiology – Kai, Marco, Charlotte, Babsi and Helga – for funny talks and helpful discussions.

I want to thank **Thomas Renné** for placing his confocal microscope at my disposal. Without this support the completion of this dissertation would not have been possible. I also want to thank the whole working group around Thomas Renné, containing Melli, Constanze, Peter, Feli and Robert.

In this case, I want to thank my **whole family** and my good **friends**, to have lots of time to celebrate my dissertation certificate. These people often took me out of my hard working day and make me happy once again, especially my soccer guys.

My last thank is dedicated to my lovely **Doreen**. It is not necessary to say more than this. YOU know what I want to say – THANK YOU.

Sources of funding

This work was supported by grants from the Deutsche Forschungsgemeinschaft (DFG, Ri 1085/3-1) and the Interdisziplinäres Zentrum für Klinische Forschung Würzburg (IZKF, E-25 and E-40) to PD Dr. med. Oliver Ritter.

Content

Figures and Tables

Tables

Figures

Summary

The Calcineurin/NFAT signaling cascade is a crucial transducer of cellular function. It has recently been emerged that in addition to the transcription factor NFAT, the phosphatase Calcineurin is also translocated to the nucleus. Our traditional understanding of Calcineurin activation via sustained high Ca^{2+}-levels was also advanced by recent findings from this working group (AG Ritter), which showed that Calcineurin is activated by proteolysis of the C-terminal autoinhibitory domain. This leads to the constitutive activation and nuclear translocation of Calcineurin. Therefore, Calcineurin is not only responsible for dephosphorylating of NFAT in the cytosol thus enabling its nuclear import, its presence in the nucleus is also significant in ensuring the full transcriptional activity of NFAT.

Formation of complexes between transcription factors and DNA regulates the transcriptional process. Therefore, the time that transcription factors remain nuclear is a major determinant of transcriptional activity. The movement of proteins over ~40 kDa into and out of the nucleus is governed by the nuclear pore complex (NPC). Transcription factors and enzymes that regulate the activity of these proteins are shuttled across the nuclear envelope by proteins that recognize nuclear localization signals (NLS) and nuclear export signals (NES) within the amino acid sequence of these transcription factors. In this study, the precise mechanisms of Calcineurin nuclear import and export were identified. Additionally to the nuclear localization sequence (NLS) and the nuclear export sequence (NES) within the sequence of Calcineurin, the respective nuclear cargo proteins, responsible for nuclear import, Importinβ_1, and for nuclear export, CRM1, were identified. Inhibition of the Calcineurin/importin interaction by a competitive peptide, called Import Blocking Peptide (IBP), which mimicked the Calcineurin NLS, prevented nuclear entry of Calcineurin. A non-inhibitory control peptide showed no effect. Using this approach, it was able to prevent the development of myocardial hypertrophy. In Angiotensin II stimulated cardiomyocytes, both the transcriptional and the translational level was suppressed. Additionally, cell size and expression of Brain natriuretic peptide (as molecular marker for hypertrophy) were significantly reduced compared untreated controls. IBP worked dose-dependent, but did not affect the Calcineurin phosphatase activity.

In conclusion, Calcineurin is not only capable of dephosphorylating NFAT, thus enabling its nuclear import, its presence in the nucleus is also important for full NFAT transcriptional activity. Using IBP to prevent the nuclear import of Calcineurin is a completely new approach to prevent the development of myocardial hypertrophy.

Zusammenfassung

Die Calcineurin/NFAT – Signalkaskade spielt eine wichtige Rolle innerhalb der zellulären Funkionalität. Es wurde bereits gezeigt, dass neben NFAT auch die Phosphatase Calcineurin in den Zellkern transportiert wird. Die bisherigen Vorstellungen zur Aktivierung von Calcineurin durch erhöhte intrazelluläre Ca^{2+}-Konzentrationen wurden durch aktuellste Ergebnisse dieser Arbeitsgruppe (AG Ritter) neu diskutiert. Es wurde gezeigt, dass Calcineurin durch gezielte Proteolyse der autoinhibitorischen Domäne konstitutiv aktiviert werden kann und in den Zellkern transportiert wird. Calcineurin ist daher nicht nur verantwortlich für die im Zytosol stattfindende Dephosphorylierung von NFAT, sondern übernimmt auch eine wichtige Funktion im Zellkern. Die nukleäre Lokalisation von Calcineurin ist essentiell für die vollständige transkriptionelle Aktivität von NFAT.
Die Komplexbildung zwischen Transkriptionsfaktoren und DNA reguliert die Transkription. Aus diesem Grund spielt die nukleäre Verweildauer diverser Transkriptionsfaktoren eine tragende Rolle. Der Transport von Proteinen (> 40 kDa) in den und aus dem Zellkern erfolgt über nukleäre Porenkomplexe, wobei die zu transportierenden Proteine mittels nukleärer Lokalisationssequenzen (NLS) / nukleärer Exportsequencen (NES) durch die entsprechenden Transportportproteine (Karyopherine) erkannt werden. In dieser Arbeit wurden die genauen Mechanismen des Imports und des Exports von Calcineurin identifiziert. Zusätzlich konnten die NLS/NES von Calcineurin und die entsprechenden Karyopherine, Importinβ_1 für den Import bzw. CRM1 für den Export, ermittelt werden. Die Inhibition der Calcineurin/Importin Interaktion durch ein kompetitives Peptid, welches als Import Blocking Peptide (IBP) bezeichnet wurde und der NLS von Calcineurin entspricht, verhinderte den nukleären Import von Calcineurin. Durch diesen Mechanismus war es möglich, die Entwicklung kardialer Hypertrophie zu verhindern. In Angiotensin II stimulierten Kardiomyozyten konnten sowohl die transkriptionelle, als auch die translationelle Aktivität reduziert werden. Des Weiteren wurden das Zellwachstum und die Expression von BNP unterdrückt. Das Blockpeptid wirkte konzentrationsabhängig, beeinflusste aber die Phosphatase-Eigenschaft von Calcineurin nicht.
Zusammenfassend lässt sich sagen, dass Calcineurin, nicht nur verantwortlich für die Dephosphorylierung von NFAT ist, sondern die nukleäre Lokalisierung ebenfalls eine entscheidende Rolle für die volle transkriptionelle Aktivität von NFAT spielt. Die Verwendung von IBP, um den nukleären Import von Calcineurin zu verhindern, stellt ein völlig neues Konzept dar, die Entwicklung kardialer Hypertrophie zu unterdrücken.

1. Introduction

1.1. Overview

The year 1999 marked the 20th anniversary of the isolation of the Ca^{2+}- and Calmodulin-dependent protein serine/threonine phosphatase Calcineurin. During the past 20 years, the biological roles of Calcineurin have progressed from a putative inhibitor of the Calmodulin-dependent phosphodiesterase [1] to the ground-breaking discovery that it is the target of the immunosuppressant drugs Cyclosporin A (CsA) and FK506, pharmacological reagents that have been used to define it as a major player in Ca^{2+}-dependent eukaryotic signal transduction pathways [2]. In recent years, several milestones regarding Calcineurin structure have been achieved including the determination of the three-dimensional structure by X-ray diffraction methods [3,4] and biochemical, spectroscopic and physical studies that are beginning to unravel its catalytic mechanism [5-7]. Insight into its physiological functions include mapping of its subcellular localization [8-10], the discovery of its co-localization with other important signaling proteins, and, aside from Ca^{2+}/Calmodulin, the finding of possible endogenous regulators of its activity including redox and/or oxidative stress [6,11] as well as interacting proteins [12-19]. Until now the only known pathway for activating Calcineurin was the Ca^{2+}/Calmodulin-dependent pathway. By an induced conformational switch of the autoinhibitory domain (AID) the phosphatase pattern of Calcineurin is demasked. In this case Calcineurin dephosphorylates its target molecules like the Nuclear factor of activated T-cells (NFAT), which is transported dephosphorylated into the nucleus. Once arrived there, the transcription factor initiates transcription of diverse genes. This signaling cascade was first examined within the T-cell activation, but further studies could demonstrate the cascade also in myocardium. During myocardial hypertrophy, transcripted characteristic genes are e.g. the Brain natriuretic peptide (BNP), the Atrial natriuretic peptide (ANP) or the β-Myosin heavy chain (β-MHC) [20,21]. Current studies demonstrate an alternative pathway of Calcineurin activation based on the targeted proteolysis of Calcineurin by Calpain. Because of its loss of the autoinhibitory domain, the truncated isoform is constitutively active. Additionally, not only NFAT, but also Calcineurin is translocated to the nucleus. Nuclear Calcineurin plays a crucial role within the development of myocardial hypertrophy. In this work a new pharmacological approach is given to prevent the nuclear import of Calcineurin [22,23].

1.2. Calcineurin – a Phosphatase

The protein phosphatase PP2B, also called Calcineurin (Cn), was first described as a Calmodulin-binding protein by Klee et al. in bovine brain [24]. Similar to Calmodulin (CaM), Cn showed a high affinity to Ca^{2+}. In 1982, the phosphatase function was discovered by Stewart et al. The binding of Ca^{2+} and Calmodulin are essentiell for the phophatase activity of Cn [25]. Based on this fact, Cn is called as a Ca^{2+}/Calmodulin-dependent phosphoprotein phosphatase [26].

1.2.1. The Family of Phosphoprotein Phosphatases

Table 1. Overview of the protein phosphatase families (nach Barford D, 1998)

PPP family		PP1 PP2A PP2B *novel protein phosphatases of the PPP family* PPP1, PPP2A, PP5
PPM family		PP2C *Arabidopsis* ABI1, *Arabidopsis* KAPP-1 Pryuvate dehydrogenase phosphatase *Bacillus subtilis* SpoIIE phosphatase
PTP family	tyrosine-specific phosphatases	cytosolic, non-receptor forms: PTP1B, SHP-1 SHP-2 receptor-like, transmembrane forms: CD45, RPTPμ / α
	dual-specific phosphatases	CDC25, MAP kinase phosphatase-1

PPP: phosphoprotein phosphatases P; PPM: phosphoprotein phosphatases M; PTP: protein tyrosine phosphatases

Phosphoprotein phosphatases comprise a large family of enzymes that hydrolyze the phosphoester bonds of phosphoserines, phosphothreonines or phosphothyrosines. These enzymes regulate numerous intracellular processes. Diversity of structure within a family is generated by targeting and regulatory subunits and domains [27]. Based on structual analysis the phosphatases are represented by three distinct gene families. Two of these, the PPP (phosphoprotein phosphatase P) and the PPM (phosphoprotein phosphatase M) families dephosphorylate phosphoserine and phosphothreonine, whereas the protein tyrosine phosphatases (PTP family) dephosphorylate phosphothyrosine amino acids. The catalytic

domains of each family are highly conserved and endowed with functional diversity by regulatory domains and subunits. The members belonging to the PPP and PPM family are metalloenzymes and dephosphorylate each substrate in a single reaction step using a metal-activated nucleophilic water molecule. In contrast, the PTPs catalyze their dephosphorylation by a cysteinyl-phosphate intermediate, which is finally hydrolized [28]. In Table 1 an overview of the named families is given.

1.2.1.1. Protein Serine/Threonine Phosphatases of the PPP Family

The PPP family members PP1, PP2A and PP2B account together with PP2C for the majority of the protein serine/threonine phosphatase activity *in vivo*. Sharing a common catalytic domain of 280 residues is one characteristic of these enzymes, whereas their non-catalytic N- and C-termini are very different and form diverse holoenzyms caused by their associated regulatory subunits [28]. PP1 is involved in different cellular processes, as diverse as glycogen metabolism, calcium transport, muscle contraction, protein synthesis and intracellular transport [29-31]. Diverse mutations in the PP1 gene of various yeast organisms demonstrated the importance within the regulation of mitosis, which has been confirmed by studies of *Drosophila* mutants [32-34]. Similar to PP1 the PP2A is also characterized by several effects in cellular processes, such as metabolism, muscle contraction, synaptic transmission, signal transduction, RNA splicing and the cell cycle progression. Within the cell cycle regulation, PP2A dephosphorylates the cell division Cycle protein 25 (CDC25), keeping it in a low-activity state. On its part, CDC25 is known to activate Cyclin-dependent kinases (Cdks) by removing inhibitory phosphates, which leads to Cdk phosphorylation of multiple substrates that drive the cell division process forward. This negative effect of PP2A on the mitosis is one part of the cell cycle regulation [35]. Further studies point for an important new role for PP2A in the control of chromosome cohesion, mediated, at least in part, through interactions with Shugoshins. The association of sister chromatids during mitosis depends on a multi-subunit complex called Cohesin. Protecting Cohesin from phosphorylation by the Shugoshin protein family prevents separation of the chromatides [36,37]. The demonstrated interaction of these complex with PP2A is required for centromeric localization of Shugoshin proteins and proper chromosome segregation [38].

Calcineurin (PP2B) is characterized by its Ca^{2+} dependence for activity. But Burkard and co-workers identified a Ca^{2+}-independent pathway. Based on a targeted proteolysis of the autoinhibitory domain by Calpain, Cn is activated constitutively [22]. PP2B plays a crucial role within the Ca^{2+} signaling cascade of activated T-cells and is responsible for the dephosphorylation of NFAT [35]. According to its dephosphorylation both NFAT and also the phosphatase Calcineurin are shuttled into the nucleus independent of each other. Nuclear located PP2B is necessary for NFAT to develop its whole transcriptional activity [22,23]. For more details on Calcineurin look from 1.2.2. - 1.2.6.

1.2.1.2. Protein Serine/Threonine Phosphatases of the PPM Family

This is a very variable family of protein phosphatases whose defining member is PP2C. Within the PPM family, the PP2C domain occurs in numerous structural contexts that reflects functional diversity. One important role of PP2C within intracellular processes is to reverse protein kinase cascades that become activated as a result of stress [28]. For example, in mammalian hepatocytes, PP2C prevents the inhibition of Cholesterol and fatty acid biosynthesis resulting from elevated AMP ATP ratios [39]. In yeast, the enzyme negatively regulates the PBS2/HOG1-MAP kinase pathway, which is activated in response to both osmotic and heat shock [40]. The role of PP2C-like protein phsophatases in regulating stress-response pathways is also conserved in prokaryotes. The sequences of protein phosphatases of the PPM family share no similarity with those of the PPP family; however, the structures of these two families are strikingly similar [27,28]. Dephosphorylation is probably catalyzed by metal-activated water molecules that act as nucleophiles and acids in a similar mechanims to that proposed for the PPP family.

1.2.1.3. The Family of Protein Tyrosine Phosphatases (PTP)

Numerous extracellular stimuli – e.g. hormones, growth factors, antigens, and cell-cell and cell-matrix interactions – activate receptor Protein tyrosine kinases (PTKs) and/or receptor-associated soluble protein tyrosine kinases, leading to an increase in the levels of cellular tyrosine phosphorylation and the triggering of downstream signaling pathways. Similary to the PTKs, diversity of the PTP family includes receptor-like transmembrane proteins and

soluble cytosolic proteins. The large family can be divided into three subfamilies – the non-transmembrane PTPs, the receptor-like PTPs (RPTPs) and the dual-specifity phosphatases (DSPs). Each PTP contains a highly conserved catalytic domain that shares high sequence similarity throughout the family. The structural and functional diversity within the family is generated by non-catalytic regulatory and targeting domains attached to the N- and C-termini of the catalytic domain. Such domains are not only responsible for regulating PTP catalytic activity but also for targeting such enzymes to their particular subcellular locations[28].

1.2.2. Calcineurin – Tissue and Subcellular Distribution

Calcineurin (Cn) is widely distributed in mammalian tissues, with the highest level found in brain [9]. In addition, Cn A and B subunits have been observed in adipose tissue, adernal cells, bone osteoclasts, heart, hindbrain and spinal cord, kidney, liver, B and T lymphocytes, lung, medulla, olfactory bulb, pancreas, placenta, platelets, retina, skeletal muscle, smooth muscle, spleen, testis and sperm, thymus and thyroid. Distinct tissue distribution is observed for the various isoforms of each subunit [7]. The γ-isoform of CnA encoded by the *PPP3CC* gene is testis specific [41]. By using polyclonal antibodies that distinguish between the α- and the β-isoforms of CnA (encoded by the *PPP3CA* and *PPP3CB* genes respectively), it was found that CnAα was more abundant than Aβ in the rat brain and heart, but the relative abundance is reversed in spleen, thymus and lymphocytes [9]. Using radioimmunoassay, Anthony and colleagues [8] measured the subcellular distribution of Cn in chick forebrain homogenate. In that study, Cn was highly enriched in the cytoplasmic and microsomal fractions. Further studies confirmed its predominance in the cytoplasm [10]. Politino and King showed that Cn binds small, acidic unilamellar vesicles in a Ca^{2+}-dependent fashion [42]. Time by time there is predominant evidence for Cn in the nucleus. In spermatids, Cn was localized nuclear, and its levels were most abundant during the initial stage of nuclear elongation, with almost no signal present in the cytoplasm [43]. In the context of signaling pathways that activate NFAT, Shibasaki et al. have shown that calcium induces an association between Cn and NFAT that results in co-localization of both molecules in the nucleus [44]. Within the development of myocardial hypertrophy, Burkard et al. also showed nuclear Cn both in human and rodent myocardium [22]. Finally, the protein phosphatase has also been shown to be associated with the cytoskeleton [7].

1.2.3. Calcineurin – Structure and Domain Characteristics

Based on increasing sequence data available, several groups have completed comprehensive sequence alignments of serine/threonine protein phosphatases and have identified a number of residues that are conserved in all members of this family. These studies identified a "phosphoesterase motif" (**D**x**H**$(x)_n$**GD**xx**DR**$(x)_m$**GNHD/E**) that is conserved not only in PP1, PP2A, and Cn, but in many other enzymes involved in the cleavage of phosphoester bonds, including acid and alkaline phosphatases and bacterial exonucleases. Four of the residues in the phosphoesterase motif (underlined letters) are ligands to a dinuclear metal co-factor in PP1 and Cn. Thus, it has been hypothesized that this motif provides a scaffold for an active dinuclear metal center in every member of the phosphoesterase family [7,45]. Using X-ray structure analysis, the three-dimensional structure of the phosphoesterase motif was examined. This motif is represented as a β-α-β-α-β scaffold for an active site dinuclear metal center. The three β-strands of this motif form a parallel pleated sheet that is capped by intervening α-helices. Two metal ions (Fe^{3+} and Zn^{2+}) are positioned at the apex of this fold forming a dinuclear metal center with four of the metal ligands provided by residues in loops between β-sheets and α-helices [7].

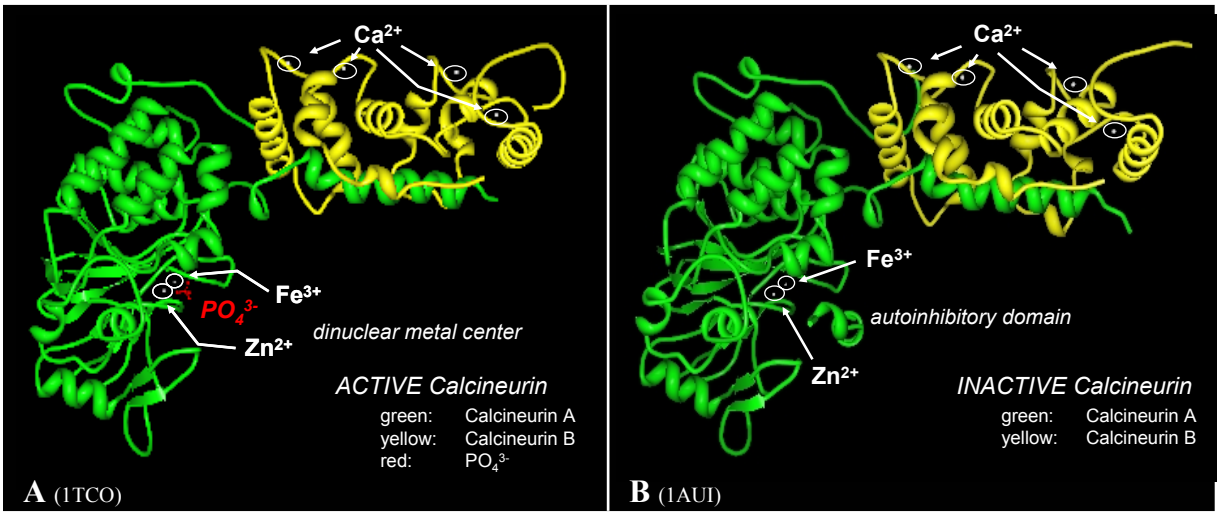

Figure 1. Structure of active and inactive state of Calcineurin A.
In Figure 1A the active form of Calcineurin A is shown (green coloured). The catalytic center is characterized by Zn^{2+} and Fe^{3+} and is free for any phosphate group (PO_4^{3-}; red). In contrast, in Figure 1B the dinuclear metal center is masked by the autoinhibitory domain – Calcineurin A is inactive.

In Figure 1 the three-dimensional structure is shown by a ribbon diagramm. The catalytic subunit CnA (60 kDa) is green coloured whereas the regulatory subunit CnB (19 kDa) is yellow. It is seen that this subunit is forming a complex with CnA via the CnB-binding helix. Also marked, four Ca^{2+} ions, bound by the EF-hand domains of CnB, the dinuclear metal

center (each white bordered) and a bound phosphate group (red coloured). The structures have been taken out of the RCSB protein data bank (www.rcsb.org/pdb/home/home.do; 1TCO and 1AUI respectively).

In Figure 1A the 1TCO structure has been modified. The FK506/FKBP12 complex, inhibiting the phophatase activity of Cn, has been removed for better visualization. This form of Cn is active. With exception of the N-terminal residues 1-16 and the regulatory domain of CnA, missing in the bovine protein, the crystal structure of the Ca $^{2+}$-saturated form of the truncated bovine Cn is similar to that of the full-length recombinant protein [46]. Because of lacking the autoinhibitory domain in 1TCO, the file 1AUI has been taken for showing the way of masking the phosphatase pattern by the autoinhibitory domain (AID) (Figure 1B). Based on masking the dinuclear metal center, the AID is responsible for the autoregulation of Cn. The shown conformation demonstrates the inactive form of Cn. Interestingly, the Calmodulin (CaM) domain was disordered in the X-ray structure, and therefore, the knowledge of how this domain interacts with the active site and autoinhibitory domains to confer CaM-regulation remains rudimentary [7]. For better understanding a linear organization of each domain localized within CnA is drawn in Figure 2.

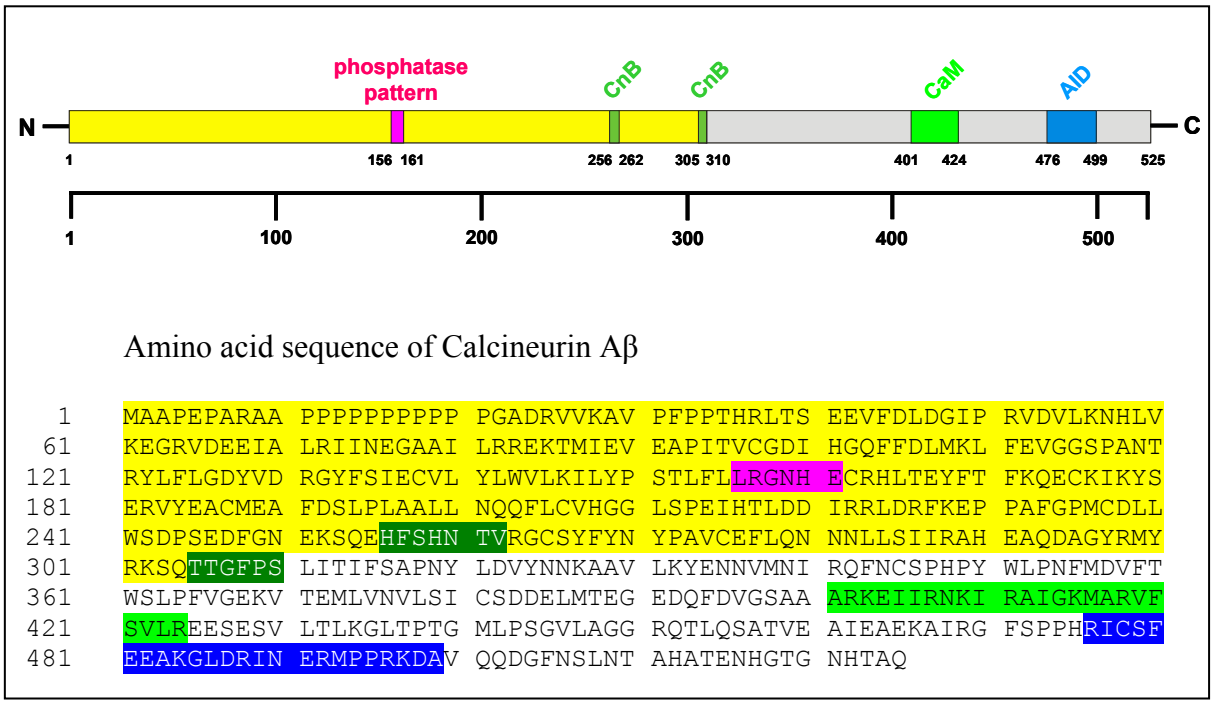

Figure 2. Linear drawing and localization of Calcineurin domains. (Hallhuber M, 2006)
The N-terminal catalytic domain of Calcineurin reaches to amino acid 310 (yellow coloured), containing the phosphatase pattern (pink) and the CnB-binding sites (green). In the C-terminal end the CaM-binding site (lime green) and the autoinhibitory domain (AID, blue) are localized.

Within the catalytic domain, which reaches from the N-terminus to amino acid 310 (yellow coloured), the two CnB binding sites (green, amino acid regions 256-262 and 305-310) and the phosphatase pattern (pink), amino acid region 156-161) are localized. The CaM binding site (lime green, amino acid 401-424) and the autoinhibitory domain (AID, blue, amino acid 476-499) are located within the C-terminal region of Cn.

1.2.4. Calcineurin – Specific Inhibitors

Cyclosporin A (CsA, Sandimmune®) and FK506 (Tacrolimus, Prograf®) are the most important immunosuppressive agents used in organ transplantation and in the treatment of diverse immune disorders. These agents produce similar effects on signal transduction pathways in T-lymphocytes, however, neither they do not share similar chemical structure nor do they react with the same target. CsA is a neutral, lipophilic and very hydrophobic, cyclic peptide of eleven amino acids extracted from *Tolypocladium inflatum Gams*. Following oral or intravenous administration, CsA distributes rapidly between blood cells and plasma. CsA does not cross the blood-brain barrier, but it crosses the placenta and it can be detected in amniotic fluid and fetal blood. The elimination half-life of CsA has been estimated to be approximately six hours. FK506 is a macrolide antibiotic extracted from *Streptomycetes tsukubensis.* This drug can be administrated orally or intravenously. Its elimination half-life is approximately twenty hours. FK506 is approximately 100 times more potent than CsA in its Cn inhibitory characteristics. The mechanism of action of these two immunosuppressive agents has been investigated extensively in immune cells. CsA and FK506 bind with high affinity to the ubiquitous cytosolic peptidyl-propyl isomerases Cyclophilin (CyP) and FK506-binding protein-12 (FKBP12), respectively. CsA-CyP and FK506-FKBP12 associates with Cn and inhibits phosphatase acitivity as well as its interaction with a variety of substrates [47].

To avoid many of the complications arising from the use CsA and FK506 as Cn inhibitors, recent work has involved the use of genetic models with inhibited Cn activity. This has been accomplished by either overexpressing naturally occurring inhibitors of Cn, so-called ´calcipressins`, through dominant-negative strategies, or more recently through gene targeting. The first such approach involved overexpression of the Cn inhibitory domain from two proteins, Calcineurin inhibitor / Calcineurin binding protein 1 (Cain/Cabin-1) and A-kinase anchoring protein 79 (AKAP79). Cain is a ubiquitously expressed 230 kDa protein

containing a C-terminal domain that acts as a non-competitive inhibitor of Cn, while AKAP79 is a scaffolding protein that docks Cn, Protein kinase A (PKA) and Protein kinase C (PKC). Using a recombinant adenoviral approach to infect neonatal rat cardiomyocytes, Taigen et al. demonstrated that the Cn inhibitory domain from either Cain or AKAP79 blocked *in vitro* hypertrophy in response to Phenylephrine (PE), Angiotensin II (AngII) and 1 % serum. These studies were then extended to the *in vivo* setting by the creation of Cain and AKAP79 transgenic mice. Low-copy Cain or AKAP79 mice displayed normal heart function at baseline and an impaired hypertrophic response to abdominal aortic constriction and AngII infusion [13,15,48,49]. A second approach to genetically inhibit Cn involved transgenic over-expression of the Cn inhibitory protein Myocyte-enriched Cn-interacting protein 1 (MCIP1) in the heart. MCIP1 was first identified as Down syndrome critical region 1 (DSCR1), a member of a family of Cn inhibitors conserved from yeast to humans. MCIP1 is highly enriched in cardiac and slow skeletal muscle. Interestingly, MCIP1 expression is transcriptionally regulated by Cn and NFAT, such that the third intron of the human *MCIP1* gene contains a cluster of 15 consensus NFAT binding sites, making it the first known feedback regulator of Cn activity [50]. In accordance with these functions, cardiac-specific MCIP1 overexpressing transgenic mice demonstrated impaired hypertrophy to Isoproterenol infusion, treadmill running and pressure overload [51,52].

Taken together, there exists both exogenous and endogenous Cn inhibitors, which have all in common that they effect the phosphatase activity of Cn. Within these work a new approach is given to prevent the activation of Cn. The critical difference to the previous way of Cn inhibition is that the phosphatase activity remains unaffected.

1.2.5. Calcineurin – Physiological Importance

The complex regulation of Cn is expected from an enzyme, which has now been shown to be a major player in the regulation of cellular processes. None is better understood than the Ca^{2+}-dependent, Cn-mediated regulation of transcription of the T-cell growth factor, Interleukin-2. The translocation of the transcription factor NFAT, in response to an increase of intracellular Ca^{2+} induced by the occupancy of the T-cell receptor, is dependent upon its dephosphorylation by Cn. It was the first example of the transduction of a signal at the plasma membrane to the nucleus. A prolonged Ca^{2+} signal and the co-translocation of Cn and NFAT

to the nucleus ensure the sustained activation of gene expression, which is reversed by the Glycogen synthase kinase 3β (GSK3β), following a decrease of intracellular Ca^{2+}. The involvement of Cn in the regulation of the expression of an array of growth factors like κ3, TNFα, NFκB and TGFβ, is reviewed by Crabtree C. R. and Rao A. [53,54]. As it does in T-cells, Cn plays an important role in the regulation of gene expression in response to Ca^{2+} signals in yeast [55,56]. In this organism, two major sites of action of Cn are the pheromone response pathway and the adaptation to high salt stress. The induction of genes involved in these two pathways has now been shown to be regulated differentially by the Ca^{2+}-dependent and FK506-sensitive interaction of a single transcription factor Tcn1p, or Crz1p, with Cn [57]. Other processes under Cn control include Ca^{2+} sequestration, cytokinesis, sporulation, and mating [55,56]. Identifying the sites of action of Cn in striatal and hippocampal neurons, which are particularly rich in Cn, continues to be a major challenge. The dephosphorylation of the Dopamine- and cyclic AMP-regulated phosphoprotein with a molecular weight of 32 kDa (DARPP-32) by Cn in striatal neurons was the first evidence for a protein phosphatase cascade involving Cn responsible for the opposite effects of Glutamate and cAMP on neuronal excitability. In hippocampal neurons activation of Cn not only results in inhibition of the release of the neurotransmitters, Glutamate and g-Aminobutyric acid, but is also involved in the desensitization of the postsynaptic N-methyl-D-aspartat (NMDA) receptor-coupled Ca^{2+} channels. The complex regulation of the function of the NMDA receptors may be the basis for the proposed role of Cn in long term potentiation and depression and long term memory. Cn-mediated activation of nitric oxide synthase has also been invoked to explain Glutamate neurotoxicity. A role for Cn has also been proposed in apoptosis and in the redistribution of integrins required for the migration of neutrophils on Vibronectin in response to Ca^{2+} transients. The inhibition of the Cn-mediated regulation of the Na^{+}-K^{+}-ATPase by the immunosuppressive drugs in the kidney may be responsible for their nephrotoxicity, whereas in cerebellar neurons, the Cn activation of the Na^{+}-K^{+}-ATPase is required to prevent neurotoxicity because of excessive Na^{+} entry induced by Glutamate binding to NMDA receptors. Regulation of two intracellular Ca^{2+} channels (first, the Ryanodine receptor (RyR) involved in excitation-contraction coupling in skeletal muscle and other excitable cells and second, the IP3 receptor involved in Ca^{2+} release by hormones and neurotransmitters) can potentially affect all cellular processes under Ca^{2+} control [46].

Besides immunology and neuroscience, Cn plays also a crucial role in cardiology. The protein phosphatase works as a regulator of pathophysiological hypertrophy. Studies by

Molkentin et al. provided the first evidence that Cn, when expressed at high levels, can elicit cardiac hypertrophy both *in vivo* in transgenic mouse models and *in vitro* in cardiac myocytes [21,58]. Until now the exact role in potentially regulating physiological growth of the heart is less understood. Indeed, it is often speculated that pathological and physiological hypertrophy utilize similar signaling pathways, although the timing and degree of signaling probably regulate the ultimate phenotype of each response. By definition, physiological hypertrophy generally refers to the clinical phenomenon known as an ´athletic` heart. Phyiological hypertrophy is induced by regular exercise training that promotes myocyte growth changes in the heart that are reversible and do not progress to decompensation. Circumstantial data suggest a potential role for Cn signaling in regulating physiological hypertrophy. *In vivo* Cn inhibition by MCIP1 overexpression attenuates exercise-induced hypertrophy. In addition, athletic hypertrophy is associated with increased IGF-1 production, which was previously shown to cause skeletal muscle hypertrophy through a Cn-NFAT-GATA pathway in cultured myoblasts. Other observations confirm the regulating role of Cn within the development of a physiological hypertrophy. First, Myocyte enhanced factor 2C (MEF2C) gene targeted mice died during embryonic development with a hypoplastic right ventricle [59]. Second, targeted disruption of the calcium regulatory genes *calreticulin* and *connexin-45* each resulted in embryonic lethality that was associated with defective NFAT-mediated transcription in the heart [60,61]. Third, deletion of NFATc1 in the mouse resulted in defective cardiac valve formation and embryonic lethality [62]. Fourth, targeted disruption of NFATc3, but not NFATc4 in mice demonstrated a significant reduction in Cn transgene-induced cardiac hypertrophy at 19, 26 days, 6, 8 and 10 weeks of age. NFATc3-null mice also showed attenuated pressure overload- and AngII-induced cardiac hypertrophy [63]. Although many of these recent studies were focused on either proving or disproving ´Calcineurin` as a major hypertrophy transducer, Cn is believed to have many other cellular targets and functions which are less well understood. The working group around Münch G. report that Cn may regulate the sarcoplasmatic reticulum (SR) Ca^{2+} transport by dephosphorylating Phospholamban (PLB), the regulator of SR Ca^{2+} ATPase (SERCA). The authors suggest that Cn activation during heart failure can have negative effects on SR Ca^{2+} transport function because it can dephosphorylate PLB and decrease Ca^{2+} uptake function. It is well known that unphosphorylated PLB inhibits SERCA pump by reducing its affinity to Ca^{2+} and phosphorylation reverses it [64,65]. Cn could also modulate the function of several other proteins involved in cardiac contractility and Ca^{2+} homeostasis either directly or indirectly. The protein

phosphatase has been implicated in the Ca^{2+} dependent inactivation of L-type Ca^{2+} channel in cardiac myocytes [66]. Current studies postulated that not only nuclear NFAT, but also nuclear Cn is important within the development of myocardial hypertrophy. Additionally to the nuclear translocation of NFAT, Burkard et al. could illustrate a nuclear localization of Cn by immunohistochemistry of human and rodent heart [22]. Unlike the known cytosolic function as a phosphatase, the exact nuclear role of Cn is still unclear.

Taken together, although the exact function of Cn within the signaling cascade causing myocardial hypertrophy is still unclear, it is generally accepted that Cn plays a crucial role within the development of physiological and pathological myocardial hypertrophy.

1.2.6. Calcineurin – Activation Pathways

1.2.6.1. The Ca^{2+}-Calmodulin Dependent Pathway

The Ca^{2+} dependence of the phosphatase activity of Cn is controlled by two structurally similar but functionally different Ca^{2+}-binding proteins, Calmodulin (CaM) and Calcineurin B (CnB) [67]. At less than 10^{-7} M Ca^{2+}, CnB, with its high affinity site occupied, remains bound to CnA, but the enzyme is inactive. Occupancy of the low affinity sites (k_D betwenn 0.5 and 1.0 μM) results in a small activation. The basal activity is stimulated more than 20-fold by the addition of an equimolar amount of CaM. Consistent with the fact that activation is the result of the Ca^{2+} dependent binding of CaM to Cn, the concentration of Ca^{2+} needed for activation decreases with increasing concentrations of CaM, and the CaM concentrations needed for activation decreases with increasing Ca^{2+} concentrations [68]. The highly cooperative Ca^{2+} dependence of the CaM stimulation of Cn allows the enzyme to respond to narrow Ca^{2+} threshold following cell stimulation. As with most CaM regulated enzymes, the mechnism of CaM activation is believed to involve binding to the CaM binding domain, resulting in a displacement of an autoinhibitory domain (AID) [67]. The flexible structure of the CaM-binding domain revealed in the crystal structure of Cn and the blocking of the catalytic center by the AID is compatible with this mechanism. Displacement of the inhibitory domain upon CaM binding can also explain the role of CaM in the oxidative inactivation of Cn. In crude tissue extracts, Cn exhibits a high phosphatase activity that is almost completely dependent on CaM and does not depend on added metals for activity but is subject to a time and Ca^{2+}/CaM

dependent inactivation faciliated by small heat-stable inactivators. The search for factors responsible for the high phosphatase activity and instability of crude Cn led to the finding that, in crude extracts, Cn is protected against inactivation by Superoxide dismutase (SOD). Displacement of the AID upon binding of Ca^{2+}/CaM may expose the metal co-factors in the active site of the enzyme to the damaging effects of superoxide anion. The reversibility of Cn inactivation by Ascorbate suggests that it is the result of the oxidation of Fe^{2+} at the active site. The modulation of Cn activity by the oxidation of Fe^{2+} provides a reversible mechanism to desensitize the enzyme and to couple Ca^{2+} dependent protein dephosphorylation to the redox state of the cells. Clarification of the role of CnB within activation of Cn has been more elusive. CnB is required for reconstitution of an active enyzme from its subunits separated under denaturating conditions. The irreversible inactivation and dissociation of the two subunits accompanying the complete decalcification of Cn indicate that Ca^{2+} binding to the high affinity site of CnB plays a strucural rather than a regulatory role. Ca^{2+} binding to the low affinity sites is apparently not only responsible for the small CaM independent activation but also for CaM activation [46]. In Figure 3A the conformational switch, demasking the phosphatase pattern, is shown. By this structural change, Cn is able to dephosphorylate its target molecules, e.g. NFAT.

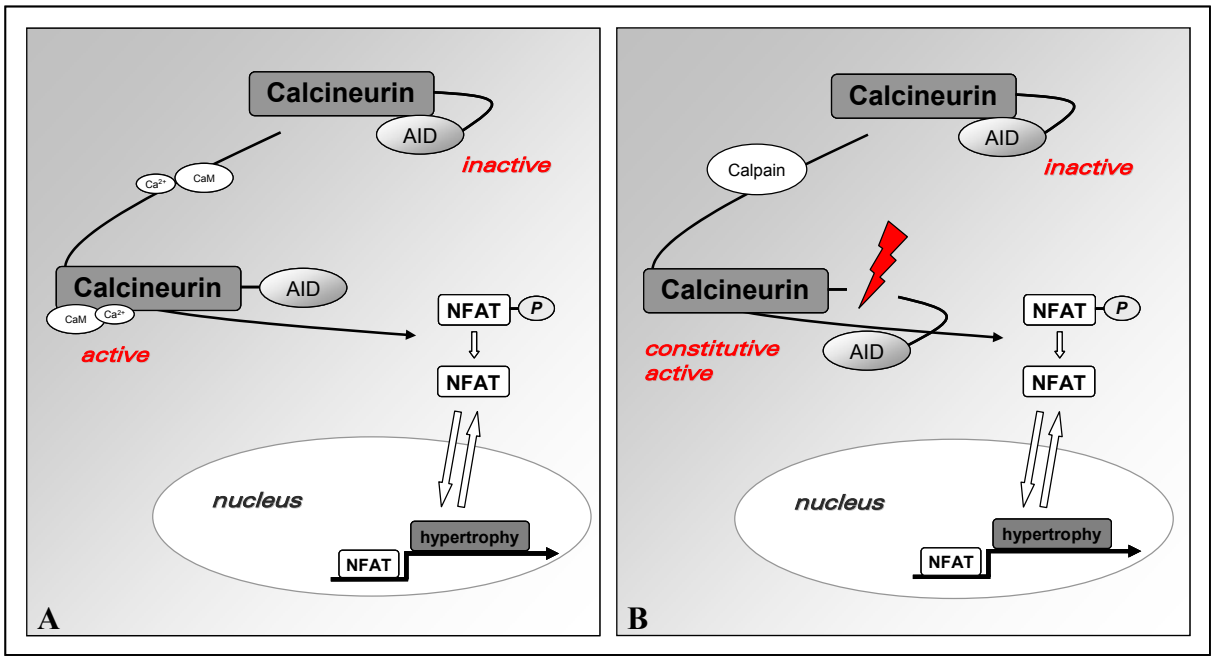

Figure 3. Activation pathways of Calcineurin.
Binding of Ca^{2+} and Calmodulin (CaM) by Calcineurin (Cn) causes a conformational change of the C-terminus containing the autoinhibitory domain (AID). Demasking the phosphatase pattern activates Cn (A). In contrast, the targeted proteolysis of Cn by Calpain causes a constitutive active form lacking the AID. This activation is both Ca^{2+} and Calmodulin independent (B).

1.6.2.2. The Ca^{2+}-Calmodulin Independent Pathway

Current studies identified an alternative pathway for activating the protein phosphatase Calcineurin. This pathway is both Ca^{2+} and CaM independent. Based on a targeted proteolysis of the C-terminal AID by the Ca^{2+}-dependent protease Calpain the phosphatase pattern is demasked. Within the excitotoxic neurogeneration three truncated isoforms of Cn have been detected - 45, 48 and 57 kDa isoform. Two of these isoforms showed whole enzymatic activity. They were activated by physiological Ca^{2+}-concentrations and constitutive active, but they were also suppressed in their activity by the immunosuppressive reagent FK506, a potential Cn inhibitor. Both, the 45 and 48 kDa isoform, are lacking the AID, whereby the 45 kDa fragment only remains the CaM binding site in part. Transgenic mice overexpressing both the 45 kDa and the 48 kDa Cn isoform showed neuronal cell death in hippocampal neurons without Glutamate exposure. Calpain inhibitors blocked not only Cn cleavage but also Glutamate-induced exitotoxic neuronal cell death *in vitro* and *in vivo*. In contrast, the 57 kDa isoforms reacts like the full length Cn (60 kDa) because of lacking only C-terminal irrelevant sequence areas. The authors emphasized that this activation by limited proteolysis is irreversible because of truncation of the AID and the CaM binding site. These and previous studies suggest that Calpain dependent regulation of Cn acitivity may occur only under pathological conditions such as neuroexcitotoxicity, whereas under physiological conditions, the phosphatase activity is regulated by Ca^{2+}/CaM in a reversible manner [69]. In 2005, Burkard et al., confirmed the Calpain-dependent activation pathway for Cn in neonatal rat cardiomyocytes (NRCMs). Recombinant CnA was incubated with recombinant μ-Calpain. The authors showed a time and concentration dependent targeted proteolysis. By MALDI-TOF – MS the cleavage site was localized at amino acid 423. Both fragments, 48 kDa and 11 kDa, have been detected, whereby the 48 kDa isoform was lacking the AID completely and the CaM binding site in part. This isoform was constitutive active. Within the development of myocardial hypertrophy the activation of Cn plays a crucial role. The authors postulate that the targeted proteolysis of Cn by Calpain could represent an additional mechanism to control Cn activity in heart [22]. Faced to the Ca^{2+}/CaM dependent pathway, Figure 3B illustrates the Ca^{2+}/CaM independent pathway.

In human heart failure myocardium and in rodent induced hypertrophied myocardium a nuclear distribution of Cn have been detected [22]. According to this new aspect it has been suggested that within the sequence of Cn a nuclear localization sequence (NLS) and a nuclear

export sequence (NES) could be localized. Depending on this important recognition sites, the import and export could be regulated. In this work, a NLS and a NES have been identified [23]. In the following text the components and the exact mechansims are described.

1.3. Nuclear Import and Nuclear Export

As in everyday life also within the smallest unit of life, the cells, certain barriers sometimes can not be overcome without the help of others. In eukaryotic cells one of these barriers consists of the nuclear envelope that separates the nucleus from the cytoplasm and restricts nucleocytoplasmic exchange of material to nuclear pore complexes (NPCs), which are embedded in the nuclear membranes. For a long time, one of the big questions was the identity of the system, escorting the variety of macromolecular cargoes between the nucleus and cytoplasm. Since more than a decade now, it is known that nuclear transport receptors mediate most of the transport events through the NPC.

1.3.1. The Field: Nucleocytoplasmic Transport

The existence of a nucleus in eukaryotic cells implies the spatial separation of transcription (nucleus) and translation (cytoplasm). This provides eukaryotic cells with additional means to regulate the fundamental process of gene expression. The confinement of transcription and translation to distinct compartments also prevents translation before splicing has been completed. The splicing process is necessary because most eukaryotic genes contain introns. However, nuclei contain many of the components required for translation such as ribosomal subunits, mRNA and even aminoacylated tRNA [70], whereas proteins whose function is clearly nuclear (e.g. histones, transcription factors, DNA polymerases) are synthesized in the cytoplasm. Thus, bidirectional intracellular trafficking of macromolecules between these two compartments is required and consumes a considerable amount of the cell's energy pool. Thereby, selective transport of proteins is a major mechanism by which biochemical differences are maintained between the cytoplasm and nucleus. The site of exchange is the nuclear pore complex (NPC), one of the largest macromolecular assemblies in a eukaryotic cell. It is embedded in the double membrane of the nuclear envelope. The NPC connects the cytoplasm and the nucleus of interphase cells and can be traversed in a passive or a facilitated

manner. The passive mode applies for ions, ATP and small molecules but becomes ineffective for proteins with a molecular weight greater than 40-60 kDa. A single NPC can accommodate about 1000 translocation events per second [71] and the cargoes range in mass from few kDa to almost 50 MDa that equals almost 40 nm in diameter [72]. Unlike translocation across other organelle membranes, passage through the NPC does not require unfolding of the substrates; however, the mechanistic details of the translocation event and the principles of NPC function have not been completely unveiled. In addition, also molecules which potentially may passively diffuse through the NPC are often actively translocated, since this allows a more efficient and regulated transport (for reviews, see references [72-75]). In general, four major categories of active nucleocytoplasmic transport can be distinguished. First, biosynthetic transport, supplying the two different compartments with macromolecules that have been produced in the opposite one [74,76]. The second category includes the so-called recycling reactions in which cargo-free transport receptors or transport adaptors are returned back to the compartment, where the next cargo molecule should be loaded [77]. Third, regulated traffic of cargoes between nucleus and cytoplasm, which is used to control key cellular processes [78]. For instance, the activity of many transcription factors is controlled at least partially by their subcellular localization. Finally, also the nuclear export machinery can be considered as an independent category of active nucleocytoplasmic transport. Exportin-mediated transport counteracts the slow but steady leakage of cytoplasmic proteins into the nucleus [79,80] and removes proteins that have unintentionally entered the nucleus (for review [81]).

1.3.2. The Site of Action: Nuclear Pore Complex

The nuclear pore complex (NPC) is one of the largest protein assemblies in eukaryotic cells, ranging in mass between 50 MDa in yeast and 125 MDa in vertebrates [72]. Three-dimensional structures of the NPC have been derived from electron microscopy studies in yeast [82] and in higher eukaryotes (*Xenopus* oocytes) [83] indicating that the core of the NPC consists of a cylinder with eight-fold symmetry (so-called ´spoke` complex) that spans the nuclear envelope. Cytoplasmic and nuclear ring moiety sandwich the central framework and peripheral filaments originate from each ring moiety, pointing towards the cytoplasm and nucleoplasm, respectively. The eight nuclear filaments are held together in a distal ring

forming a distinct assembly called nuclear basket. The central pore (channel) created by the spoke complex has a length of about 90 nm and a narrowest diameter of 45-50 nm [83-86].

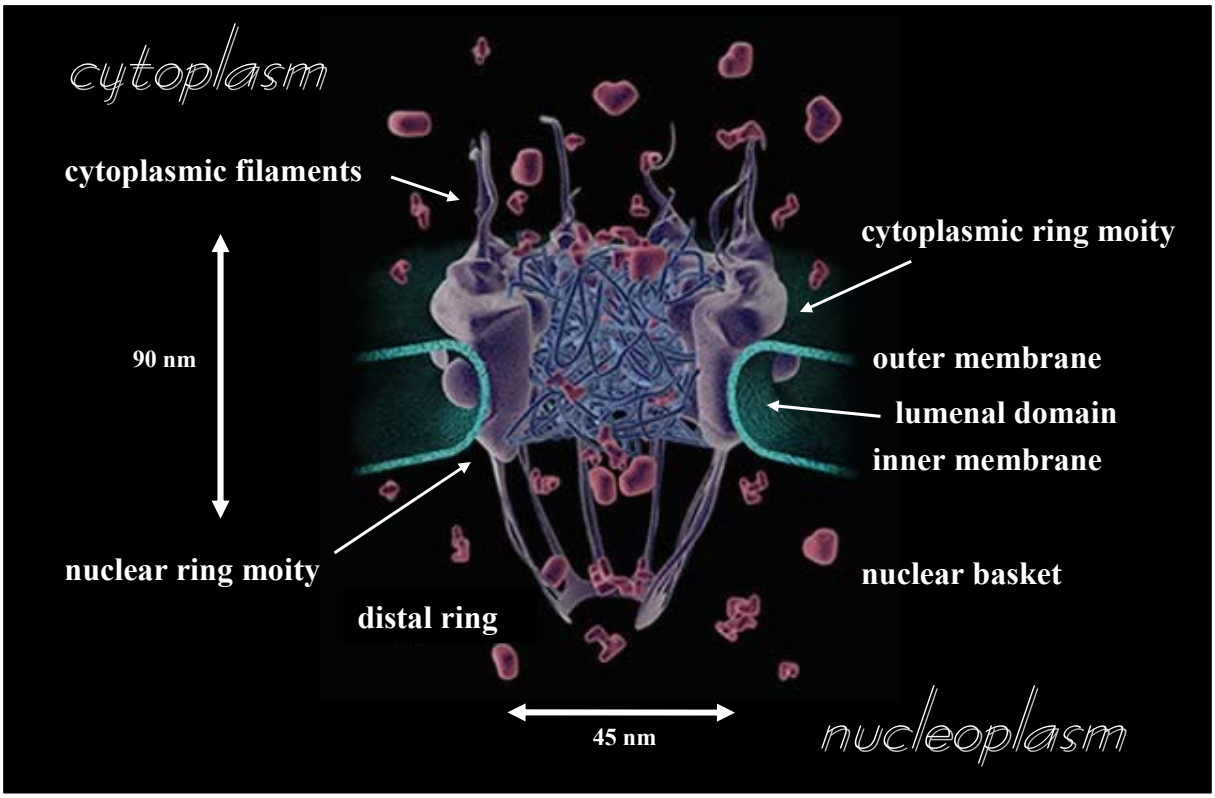

Figure 4. The nuclear pore complex (NPC) – tunnel between nucleus and cytoplasm. (Patel S, 2005)
A model of the 3D architecture of the NPC based on electron microscopy studies. The major structural components of NPC include the central framework with eight-fold rotational symmetry, the cytoplasmic ring and filaments, and the nuclear ring and basket.The cytoplasmic fibrils and the nuclear basket are involved in the initial and terminal stages of translocation.

With regard to the molecular architecture, in yeast and in mammals the NPC is composed of only 30 different components. Most of these componenent proteins, termed nucleoporins or Nups, are present in two copies per spoke (with eight spokes per NPC), each copy located symmetrically on either side of the NPC midplane [87]. The massive NPC can be constructed from few distinct proteins because of the high copy number of the individual nucleoporins, owing to the eight-fold rotational symmetry of the NPC. Approximately one third of all core nucleoporins contains domains of Phenylalanine-Glycine (FG)-repeats [72,87-89] which mediate the main interaction between transport factors and nucleoporins. On the basis of the affinity and the nature of interaction, different models of facilitated translocation through the NPC have been proposed [89,90]. The Brownian affinity gate model [89] proposes that the aqueous NPC channel consists of a narrow central tube. Binding to peripheral FG-repeats facilitates the entry into the pore and then allows translocation by Brownian motion. The selective phase model is based on kinetic data presented by Ribbeck and Gorlich [91]. As the name indicates,

this model proposes that the central channel of the NPC is filled with a selective phase consisting of a meshwork formed by weakly interacting, hydrophobic FG-repeats. This meshwork functions as kind of a sieve; presenting a significant permeability barrier for inert molecules, but becoming selectively permeable for transport receptors that can interact with the FG-repeats and disrupt the meshwork. Very similar to the selective phase model is the 'oily-spaghetti' model suggesting that the NPC channel is filled by hydrophobic, unstructured, non-interacting FG-repeats [90]. These 'oily-spaghetti' can be pushed aside by transport receptors (loaded with a cargo or unloaded) whereas they prevent the translocation of other molecules.

In conclusion, all three models have two things in common: Firstly, the NPC selectivity is exclusively achieved by the conserved FG-repeats. Secondly, transport through the pores occurs via diffusion.

1.3.3. The Mediators: Importins and Exportins

Most nuclear transport processes are mediated by soluble transport receptors that recognize specific sequences or structural characteristics of their cargoes and facilitate the passage of receptor-cargo complexes through the NPC. Transport receptors constantly shuttle between nucleus and cytoplasm thereby rapidly crossing the permeability barrier of nuclear pores [91]. The biggest class of nuclear transport receptors is the superfamily of Importinβ like factors (also named karyopherins) that can be classified as importins (import karyopherin) and exportins (export karyopherin), depending on the direction in which they transport the cargo [74,90,92,93]. Common features of the Importinβ family members are an amino-terminal Ran guanosine triphosphatase (RanGTP) binding domain, a similar large size (90-130 kDa), and an acidic isoelectric point (4.6-5.9) [94]. Twenty members of this Importinβ family were identified in mammals (Table 2). For ten of these (Importin-β1, Karyopherin-β2, TransportinSR1, TransportinSR2, Importin4, Importin5, Importin7, Importin8, Importin9, Importin11), a role in nuclear import was acknowledged, seven were shown to function in nuclear export (CRM1/Exportin1, Exportin-t, CAS, Exportin4, Exportin5, Exportin6, Exportin7), and one can mediate transport in both directions (Importin13), leaving two uncharacterized (RanBP6, RanBP17).

Table 2. Karyopherin-β family members. (Pemberton LF, 2005)

human	cargo	yeast	cargo
Import			
Importin-β1	many cargoes, cargoes with basic NLSs via Karyopherinα, UsnRNPs via Snurportin	Kap95	many cargoes including those with NLS via Karyopherinα
Karyopherin-β2	hnRNPA1, histones, ribosomal proteins	Kap104	Nab2, Hrp1
TransportinSR1	SR proteins	Mtr10/Kap111	NpI3, Hrb1
TransportinSR2	HuR	.....	
Importin4	histones, ribosomal proteins	Kap123	ribosomal proteins, histones
Importin5	histones, ribosomal proteins	Kap121	ribosomal proteins, histones, Pho4, others
Importin7	HIV RTC, Glucocorticoid receptor, ribosomal proteins	Nmd5/Kap119	TFIIS, Hog1, others
Importin8	SRP19	.....	
Importin9	histones, ribosomal proteins	Kap114	TBP, histones, Nap1p
Importin11	UbcM2, rpL12	.....	
.....		Kap122	TFIIA
Export			
CRM1	leucine rich NES cargoes	CRM1	leucine rich NES cargoes
Exportin-t	tRNA	Los1	tRNA
CAS	Karyopherin α	Cse1	Karyopherin α
Exportin4	eIF-5A	.....	
Exportin5	microRNA precursors	.....	
Exportin6	Profilin, Actin	.....	
Exportin7	p50Rho-GAP, 14-3-38	.....	
Import / Export			
Importin13	Rbm8, Ubc9, Pax6 (import), eIF-1A (export)	.....	
.....		Msn5	Pho4, others including phosphorylated proteins (import); replication protein A complex (export)
uncharacterized			
RanBP6	undefined		
RanBP17	undefined	.....	undefined
.....		Kap120	

Members of the Karyopherin-β family (human and yeast) are shown. Orthologue proteins are grouped. Dotted lines indicate orthologues have not yet been identified. NES: nuclear export sequence; NLS: nuclear localization sequence

Considering the low number of transport receptors and the large number of proteins that have to be translocated, most transport factors probably recognize many cargoes. Just the other way around, the identification of multiple import receptors for certain cargoes revealed a significant redundancy between transport pathways (for a review and a cargo list, see Pemberton LF, 2005 [93]). An intriguing question regarding this subject is, how does a given import receptor recognize many structurally different proteins?

Structural studies have focused so far mainly on Importinβ revealing that the structure of this import receptor consists of 19 tandem HEAT repeats forming a superhelical structure (snaillike). HEAT repeats are named after the four proteins (Huntingtin, Elongation factor 3, 'A' subunit of protein phosphatase A, and TOR1 lipid kinase) in which the motif was identified first. Each HEAT repeat consists of two helices A and B connected by a loop (see Figure 5A [95] and 5B (www.rcsb.org; 1QGK)). The A helices are located on the outside of the protein and form the convex face (red coloured), whereas the B helices are located at the inside, forming the concave surface (yellow coloured) [95-97].

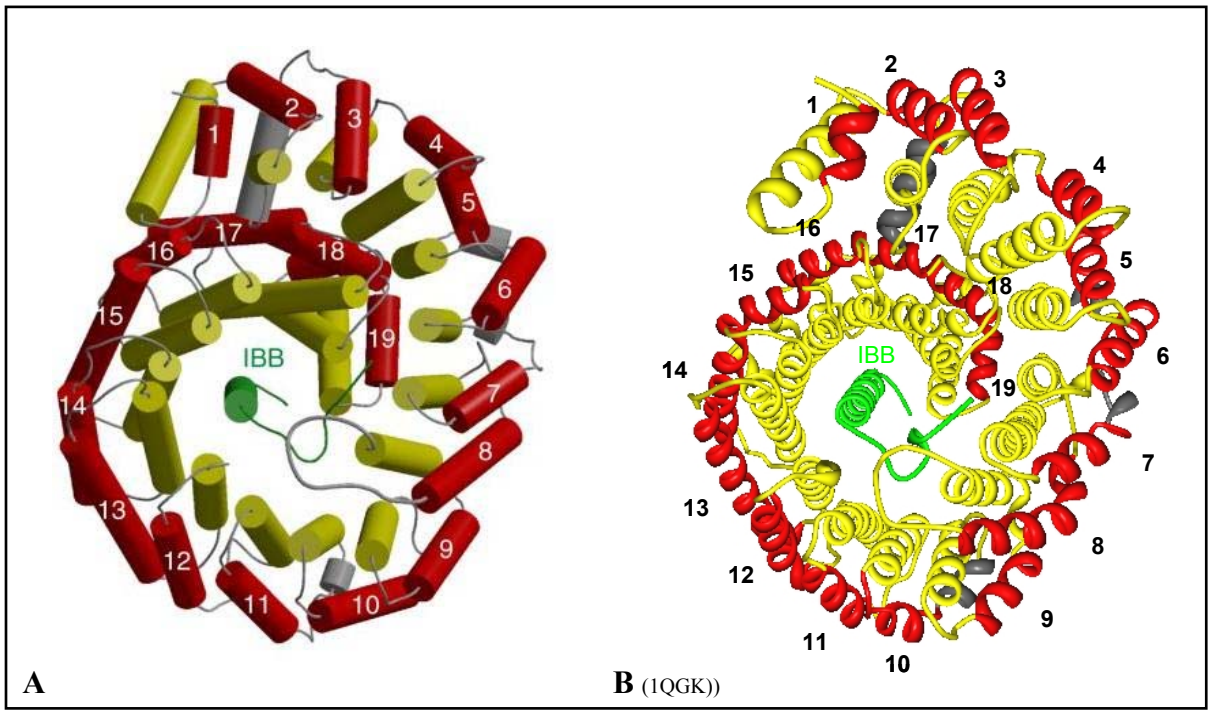

Figure 5. Structure of Importinβ$_1$.
The 19 HEAT tandem repeats form a superhelical structure. Each HEAT repeat consists of two helices, A and B. The A helices are located on the outside (red coloured) whereas the B helices (yellow) are reveting the inner side. For better visualization a schematic draw (A, Cingolani G, 1999) is faced to an ribbon diagramm (B, 1QGK). The Importinβ binding domain (IBB) of Importinα is green coloured.

Interactions with the NPC (FG-repeats) occur on the outer surface of the helical structure [96], whereas cargoes such as the Importinβ binding domain (IBB, green coloured) of Importinα (HEAT 7-19) [95], the Parathyroid hormone-related protein (PTHrP; HEAT 1-11) [97], and RanGTP (HEAT 1-10) [98] bind the indicated regions of the inner concave surface. Furthermore, structural differences were observed between RanGTP bound and unbound Importinβ, suggesting that Importinβ undergoes large conformational changes in the HEAT repeat arrangement upon RanGTP binding. Taken together, structural analysis strongly indicates that the spring-like superhelical conformation of Importinβ has a large degree of

flexibility [99]. This inherited flexibility provides a rational explanation for the existence of many distinct substrate binding sites in Importinβ. Recently, two independent studies have illuminated the structural basis and the molecular mechanisms for the assembly of nuclear export complexes [100,101]. Both studies revealed that exportins (such as Cellular apoptosis-susceptibility (CAS) and Chromosome region maintenance protein 1 (CRM1)) are also constructed from superhelices of HEAT repeats suggesting that presumably all members of the Importinβ family share this structural feature. Further, it was shown that a conformational change in the N-terminal Ran binding site (loop) of CRM1 (Exportin1) accounts for the cooperativity of Ran and cargo binding [101] and that a second (C-terminal) Ran binding site as identified in CAS (Exportin2) may be a general feature of export receptors. In contrast to the N-terminal binding site, formed by the inner surface of HEAT 1-3, there exists no counterpart in Importinβ for the C-terminal binding site, which is formed by HEAT 13-14 together with the long loop in HEAT 19 [100]. CRM1 mediates the nuclear export of proteins exposing leucine-rich nuclear export sequences (NESs). Most NESs bind to CRM1 with relatively low affinity. Recently, higher-affinity NESs contains the motif LxxLFxxLSV. But there exist exceptions, such as the NESs of parvovirus minute virus of mice NS2 protein or the Calcineurin A (in this work), which do not fit the suggested NES consensus. The export sequences are not the only crucial part for the export. Studies on the NES within the HIV Rev protein, which is also exported by CRM1, showed that the isolated NES much more weakly binds to CRM1 than the full protein. This implies that an NES might require an appropriate context to adopt the conformation needed for CRM1 binding, and that flanking residues might also contribute to NES affinity [102]. Additionally to NLS or NES masking, which prevents nuclear import or export, the affinity of importins or exportins for their respective NLSs or NESs can be regulated by phosphorylation. Both the enhance and the blocking of the nuclear import or export is possible through a variety of mechanisms [103] (see chapter 1.3.6.).

Contrary to the structure of the Importinβ family members, Importinα does not consist of HEAT repeats, but consists of ten tandemly repeated hydrophobic 42 amino acid repeats (known as ´ARM` repeats, named after the *Drosophila* gene *armadillo*), forming a cylindrical superhelix. According to its amino acid composition an individual ARM repeat forms three helices [92,93,104,105]. Superposition of individual Importinα ARM repeats with Importinβ HEAT repeats indicates significant structural similarities, suggesting that these two structures belong to the same family of helical repeat motifs. Besides the ARM repeat domain which harbors the NLS-binding site, Importinα contains a short carboxyl terminus and a basic,

autoinhibitory, amino terminal Importinβ binding (IBB) domain. The IBB domain can bind either to ARM repeats (autoinhibition [106]) or to Importinβ, forming the functional Importinα/β heterodimer [107]. In this case, interaction of Importinβ with the IBB domain is analogous to a direct Importinβ - cargo interaction in absence of Importinα adaptor. The Importinα/β-carrier heterocomplex initially contacts the NPC at the distal end of cytoplasmic fibirls, from where it is transferred to the cytoplasmic entry of the central channel [105].

Binding of positively charged amino acid sequences (basic NLSs) is in both cases a result of hydrophobic interactions combined with electrostatic interactions on the surface of the molecule. However, despite the structural similarities regarding the repeating units (HEAT and ARM) and despite using similar binding strategies, Importinα and Importinβ have different NLS sequence requirements for their cargoes. In general, classical positively charged NLSs that bind to Importinα are too short to be recognized by Importinβ (for reviews see [108,109]).

1.3.4. The Key Regulator: Ran

Cargo binding and release of importins and exportins is controlled by a steep RanGTP gradient which is maintained across the nuclear envelope through the asymmetric distribution of factors that regulate the Guanine nucleotide-bound state of Ran [74,75,90]. The Ran guanine exchange factor (RanGEF; also called RCC1), is exclusively nuclear, while the Ran GTPase-activating protein (RanGAP) together with the Ran binding proteins RanBP1 and RanBP2 are cytoplasmic. Recent fluorescence resonance energy transfer (FRET)-based biosensor data confirmed the presence of a RanGTP gradient in interphase nuclei (cells) and the concentration difference between nuclear and cytoplasmic RanGTP was estimated to be at least 200-fold [110]. Importins and exportins interact with RanGTP through their conserved amino-terminal domains, but binding of RanGTP has the opposite effect on these receptors. Importins load cargoes in the absence of Ran in the cytoplasm and release their cargo upon RanGTP binding in the nucleus [73,111,112]. Moreover, an Importinβ mutant which lacks the Ran binding site is unable to discharge cargo into the nucleus [111]. Thus, the role of Ran is not limited to its GTPase activity. Instead, cytoplasmic RanGDP appears to be required at an early stage of NLS protein import, whereas nuclear RanGTP is implicated in terminating the translocation. In this fashion, the asymmetric distribution of RanGDP and RanGTP is likely to

play an important role in determining the directionality of protein import. Following cargo-protein complex dissociation, Importinβ returns to the cytoplasm [105].

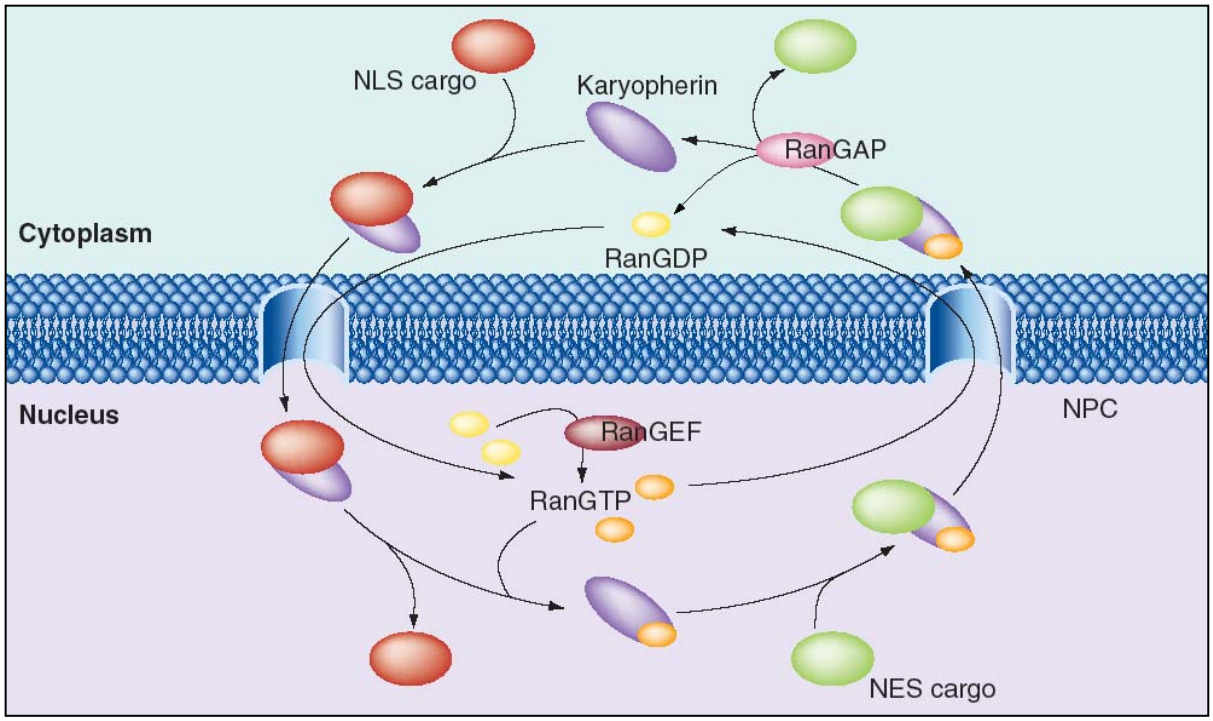

Figure 6. Nucleocytoplasmic trafficking. (Hallhuber M, 2007)
The heterocomplex of cargo protein and karyopherin is shuttled to the nucleus by crossing the NPC. After dissociation the karyopherin recognizes the NES of the cargo and binds RanGTP. Depending on RanGAP, the complex dissociates into its elements once arrived in the cytosol. The resulting RanGDP is shuttled back to the nucleus, whereas the karyopherin remains cytosolic for the next cycle.

GAP: GTPase-activating protein; GDP: Guanine diphosphate; GEF: Guanine nucleotide exchange factor; NES: Nuclear export sequence; NLS: Nuclear localization sequence; NPC: Nuclear pore complex

In contrast, exportins bind substrates only in the presence of RanGTP in the nucleus. Exportins, NES cargoes and RanGTP undergo cooperative binding, resulting in the formation of a trimeric export complex. Although crystallographic structures have been solved for some import receptors together with their cargo or with RanGTP, similar data on exportins that could explain why exportins bind cargo and RanGTP synergistically are not yet available [113]. After translocation through the NPC cargo release is accomplished when the Ran bound GTP molecule is hydrolyzed in the cytoplasm [77,114,115]. For a single round of nuclear import GTP hydrolysis is not needed because translocation through the NPC itself is a fully reversible process. However, directional transport is only achieved by Ran which regulates cargo binding and release of the transport receptors (shown in a simplified illustration; Figure 6). Thus, GTP hydrolysis constitutes the sole input of metabolic energy, in form of at least one molecule of GTP hydrolyzed per transport cycle, which allows import and export cargoes to accumulate against gradients of chemical activities [74,116].

When transport receptors directly bind to their cargo, a single round of RanGTP hydrolysis is expended to translocate one cargo uni-directionally through the NPC. However, in case of transport receptors which carry cargoes bi-directionally across the nuclear envelope, such as Importin13 in mammals [117] and Msn5 in yeast [118], transport of two substrates in opposite directions per RanGTP hydrolysis cycle is achieved. This obvious increase in efficiency because of lesser energy expenditure, however, drastically limits the endpoint of cargo accumulation. The export of one RanGTP molecule down the RanGTP introduction gradient must drive the transport of two cargoes against their gradients of chemical activity [117]. As a result, bi-directional transport by a single carrier is probably an exception rather than the rule. In addition, some importins as Importinβ also use adaptor proteins to interact with their cargo. Classical NLS (cNLS) containing proteins are recognized by the Importinα/β heterodimer, where Importinα binds to the cNLS and Importinβ is required for translocation through the NPC. Since both importins return independently to the cytoplasm in a RanGTP-complex (Importinβ/RanGTP and Importinα/CAS/RanGTP) two RanGTP molecules are expended for this classical NLS import cycle [74,119]. No matter in which way RanGTP depletion from the nucleus occurs, it has to be continuously refilled. RanGDP could theoretically diffuse into the nucleus; however, it was shown that its nuclear uptake is facilitated by the Ran import receptor NTF2/p10 which particularly recognizes the GDP conformation of Ran. In the nucleus, RanGDP is recharged with GTP by the action of nucleotide exchange factor RanGEF which also leads to the dissociation of RanGTP from NTF2. In conclusion, Ran has to cross the nuclear envelope as frequently as all members of the Importinβ family together and therefore probably represents the most rapidly shuttling macromolecule in the cell.

1.3.5. The Signals: NLS and NES

Receptor-mediated, active nuclear transport of proteins between the nucleus and cytoplasm depends on localization signals in the cargoes. Depending on the direction in which the macromolecules are transported, the signals can be classified in nuclear localization sequences (NLSs) and nuclear export sequences (NESs). In general, these signals are defined by amino acid regions (peptide sequences) of the respective cargoes, but the size and structure of transport signals vary considerably. Contrary to other peptide signals or targeting sequences (as for instance ER targeting signals), NLSs and NESs are not cleaved during/after

transport because they (i) are not located at either the N- or C-terminal end, and (ii) are often required to function many times depending on the cargo's duration of life (e.g. shuttling proteins and transcription factors). However, the most dramatic event in the cells of higher eukaryotes is mitosis. Once per cell cycle/division the nuclear envelope breaks down, the content of the nuclear and cytoplasmic compartments becomes completely mixed, and eventually has to be sorted out. Of course, this requires intrinsic protein sorting signals.

1.3.5.1. The Nuclear Localization Sequences (NLSs)

Recognition of the import signals does not occur by a single uniform mechanism and therefore no consensus import signal can be defined as proposed in the early days. However, nuclear localization sequences (NLSs) can be principally divided into two groups, the classical NLSs (cNLSs) and the nonclassical NLSs (ncNLSs). The large number of nuclear proteins bearing a cNLS are imported into the nucleus by the Importinα/β heterodimer [73,105]. In these importin-cargo complexes Importinα represents the adaptor molecule that links the cargo with the actual import mediator Importinβ. Thus, Importinα contains a cargo (with a cNLS) binding site (ARM repeats; see also chapter 1.3.3.) and an Importinβ binding (IBB) domain which consists of approximately 40 % basic residues [107]. The cNLSs consist of short stretches of positively charged, basic amino acids, but they do not fit a tight consensus. They can be monopartite, as in the Simian virus 40 (SV40) large-T antigen (T-ag) that consists of a heptapeptide containing five basic amino acids [73,120,121], or bipartite, as in Nucleoplasmin [73,122]. The NLS in Nucleoplasmin consists of two short basic clusters separated by a spacer of ten amino acids. In addition to the cNLS dependent pathway, importins can also function in the absence of adapter molecules like Importinα. Within this alternative pathway cargo proteins contain a ncNLS which is in general longer than the cNLS [123]. Proteins bearing ncNLSs directly bind to one of the twenty members of the Importinβ family present in higher eukaryotes [124]. The list of adapter independent cargoes is constantly growing and examples include the transcription factors cAMP response element-binding protein (CREB), Jun and Fos [125], Mothers against decapentaplegic homolog 3 (Mad3, also called Smad-3) [126], the retroviral proteins Rev [127] and Tat in HIV-1 [127], the ribosomal proteins S7, L5, and L23a [128], the core histones H2A, H2B, H3 and H4 (www.expasy.org/uniprot/ Q14974), and Parathyroid hormonerelated protein (PTHrP) [129], which all directly bind to Importinβ.

Transportin mediates the nuclear import of M9-containing proteins such as heterogenous nuclear ribonucleoprotein A1 (hnRNP A1). The M9 domain, consisting of ~38 amino acid residues, is quite exceptional because it contains only a single essential basic residue, but is rich in Glycine and comprises many aromatic residues [130]. Besides recognizing M9 domain containing proteins, Transportin also mediates nuclear import of the ribosomal protein L23a (rpL23a). The import signal in rpL23a, the so-called beta-like import receptor binding (BIB) domain, contains 43 amino acids (human) and is extremely basic. According to distinct and non-overlapping binding sites for the M9 and BIB domain, Transportin can bind to these different import signals. In addition to Transportin, also Importinβ, Importin5 and Importin7 confer import of rpL23a [128].

The use of parallel import pathways applies also for its yeast homologue rpL25 which can choose between at least two transport factors, Yrb4p and Pse1p [131,132]. This redundancy in nuclear transport pathways of essential proteins (cargoes) explains for instance why the majority of nuclear transport receptors are not essential in yeast (*S. cerevisiae*). Observing redundant transport pathways often leaves the question open whether the same region/NLS is recognized by the individual import receptors or not. However, in the case of rpL23a it is known that Importinβ, Transportin, Importin5 and Importin7 bind to the same region. Thus, this region is referred to as beta-like import receptor binding (BIB) domain [128]. The four import receptors share less than 15 % sequence identity, which makes this functional conservation quite remarkable. Finally, the binding sites for cargoes in Importinβ correspond in general to the IBB domain binding site (HEAT 7-19, cargo binding site I) [95]. Recently, the crystal structure of a fragment of Importinβ bound to the ncNLS of the PTHrP revealed a second extended cargo binding site on Importinβ (HEAT 1-11, cargo binding site II) [97]. Since this second cargo binding site overlaps entirely with the RanGTP binding domain cargoes binding to this site must be released by RanGTP via a direct competition for the same binding site. In comparison, binding of RanGTP to Importinβ induces a conformational change that triggers the release of cargoes bound to the IBB domain binding site.

However, with the exception of a few cases (e.g. IBB, BIB, and M9) the cargo recognition sites (minimal NLSs) have not been mapped in detail. Thus, despite the growing list of identified cargoes for the individual import receptors knowledge about the nature of NLSs remains rather limited.

1.3.5.2. The Nuclear Export Sequences (NESs)

As mentioned above, nuclear export is as important as nuclear import since many highly abundant substrates such as mRNAs, tRNAs, transcription and translation factors, ribosomal subunits (small and big subunit) and import adaptors have to be exported from the nuclei [133]. So far, nuclear export receptors comprise the mRNA export factors [134] and seven Importinβ related transport receptors. In contrast to importins, most exportins seem to be specialized on a narrow group of cargoes or even a single export substrate. For instance, CAS/Exportin2 recycles Importinα adaptors to the cytoplasm [77], Exportin-t mediates export of tRNA [135], Exportin5 also exports tRNA and additionally the eukaryotic translation Elongation Factor 1A (eEF1A) [136] and short microRNA precursors (premiRNAs) [137], Exportin4 exports the translational factor eukaryotic Initiation Factor 5A (eIF5A) [138], and Exportin6 keeps actin cytoplasmic [80]. CRM1/Exportin1 has so far been the only exception [115], however, the recently identified Exportin7 [79] also appears to have a broad cargo specificity. Among the substrates recognized by CRM1 are several RNPs (ribosomes, SRP, U small-nuclear (sn)RNAs) and a large number of proteins with leucine-rich NESs. CRM1 mediated nuclear export of ribosomal subunits such as the large subunit (60S) however requires sometimes shuttling adaptor proteins (such as NMD3 for the 60S subunit). The identification of a canonical NES on nonsense-mediated mRNA decay protein 3 (NMD3) led the researchers to the finding that NMD3 acts as an adaptor for CRM1 within the 60S export [133]. Leucine-rich nuclear export sequences that mediate rapid export from the nucleus were originally identified in the viral protein HIV-1 Rev [74,139] and the cAMP-dependent Protein kinase inhibitor (PKI) [74,140]. Leptomycin B (LMB), an antifungal cytotoxin isolated from a *Streptomyces* strain [141,142], binds covalently to CRM1 and interferes with the formation of the heterotrimeric export complex [115]. Thus, it specifically inhibits the CRM1 export pathway by covalent modification at a cysteine residue in the central conserved region (CCR) of CRM1 [143]. The use of LMB has subsequently led to the identification of many CRM1 export substrates that carry leucine-rich nuclear export sequences such as in this work – Calcineurin as a new cargo protein for CRM1 [23]. By comparing several functional NESs and random mutagenesis studies, a consensus motif for leucine-rich NESs was defined [73,144]. However, this consensus motif does not allow a safe prediction of CRM1 cargoes based on their amino acid sequence alone. Examples show that even when a leucine-rich peptide sequence can direct export of a reporter protein and binds to CRM1 *in vitro* [145], no safe conclusion can be drawn regarding its export

function in the wildtype protein. In fact, the leucine-rich NES needs an appropriate protein context to fulfill its function, respectively to adopt a conformation that can be recognized by CRM1. To complicate matters even further, it recently was shown that nuclear export of 14-3-3σ (member of a larger protein family called the 14-3-3 proteins, that regulates diverse cellular processes) is mediated by Exportin7 and not by CRM1 as previously suggested [79]. Further, it is assumed that numerous other export events which are currently credited to CRM1, might in fact be mediated by export receptors such as Exportin7. The reason for their assumption is based, at least in part, on the use of LMB as sole assessment for defining nuclear export pathways. CRM1 is probably responsible for the cytoplasmic localization of RanGAP and RanBP1 [146]. Thus, a block of the CRM1 export pathway by LMB treatment impairs or at least disturbs the RanGTP gradient and therefore ultimately inhibits all nuclear transport pathways parallel to the CRM1 export pathway. The nuclear export signals recognized by Exportin7 can also not be compared with the leucine-rich NESs and Exportin7 binds to their cargoes probably through multiple low affinity interactions [79].

1.3.6. Regulation of Nuclear Protein Transport (Poon et al., 2005 [103])

A number of specific mechanisms regulate nuclear transport precisely, in response to a variety of signals such as hormones, cytokines and growth factors, cell-cycle signals, development signals, immune challenge and stress. Post-translational modification of signaling molecules through phosphorylation/dephosphorylation is the best understood mechanism to regulate nuclear transport and can be mediated by many different kinases/phosphatases. As kinases/phosphatases can be regulated by many different cellular signals, signal-responsive phosphorylation/dephosphorylation to modulate subcellular localization represents a direct link between extracellular signals/signals within the cell and response in terms of nuclear import or export of specific signaling molecules such as cell-cycle regulators, kinases and transcrption factors. Many of the latter proteins possess both NLS and NES, meaning that their nuclear concentration can be tightly regulated in response to different types of signals through the modulation of both nuclear import and export [103].

1.3.6.1. Intramolecular Masking of NLSs/NESs

A key step by which the efficiency of nuclear transport may be regulated is that of importin-NLS / exportin-NES interactions. Intramolecular or intermolecular masking of NLSs/NESs within cargo proteins to prevent importin/exportin recognition is one of the most common mechanisms to regulate the efficiency of nuclear transport. Intramolecular masking occurs when the accessibility of the NLS/NES is inhibited by the charge or conformation of the NLS/NES containing protein. The transcription factor Nuclear factor-kappa B (NFκB) p50 that regulates the expression of the κ light chain is an example, in that within the p105 precursor form, its Importinα/β_1-recognized NLS is masked and inaccessible. During an immune response, specific phosphorylation and degradation of the p105 C-terminus unmasks the NLS in the p50 form, enabling recognition by Importinα/β_1 and nuclear accumulation.
Intramolecular masking can also be effected by phosphorylation close to the targeting sequence to prevent importin/exportin binding. The Nuclear factor of activated T-cells 2 (NFAT2, NFATc1) contains two NLSs, both of which are masked by phosphorylation, preventing importin recognition and nuclear import, until dephosphorylation allows nuclear localization. Analogously phosphorylation at Ser^{152} near the NLS of the yeast transcription factor Pho4 by the Pho80-Pho85 cyclin-dependent kinase complex under high phosphate conditions prevents Importinβ_3 (Pse1) binding, inhibiting nuclear import. That similar mechanisms apply to nuclear export is indicated by observations for the budding yeast high osmolarity glycerol (HOG) pathway-signaling molecule HOG1p, where phosphorylation at Thr^{174} and Tyr^{176} masks the NES, preventing recognition by Exportin1 (Xpo1p) and inhibiting nuclear export.
Structural changes of proteins due to disulfide bond formation between cysteine residues can also lead to NES/NLS masking. The formation of an intramolecular disulfide linkage beween Cys^{598} and Cys^{620} within the cysteine rich region of yeast transcription factor Yap1p in response to oxidative stress, for example, renders the NES within this region inaccessible to Exportin1. The same mechanism probably applies to the yeast transcription factor Pap1 [103].

1.3.6.2. Intermolecular Masking of NLSs/NESs

Intermolecular masking occurs when the binding of a heterologous protein prevents importin-NLS or exportin-NES interactions. An example is the transcription factor NFAT4, where at

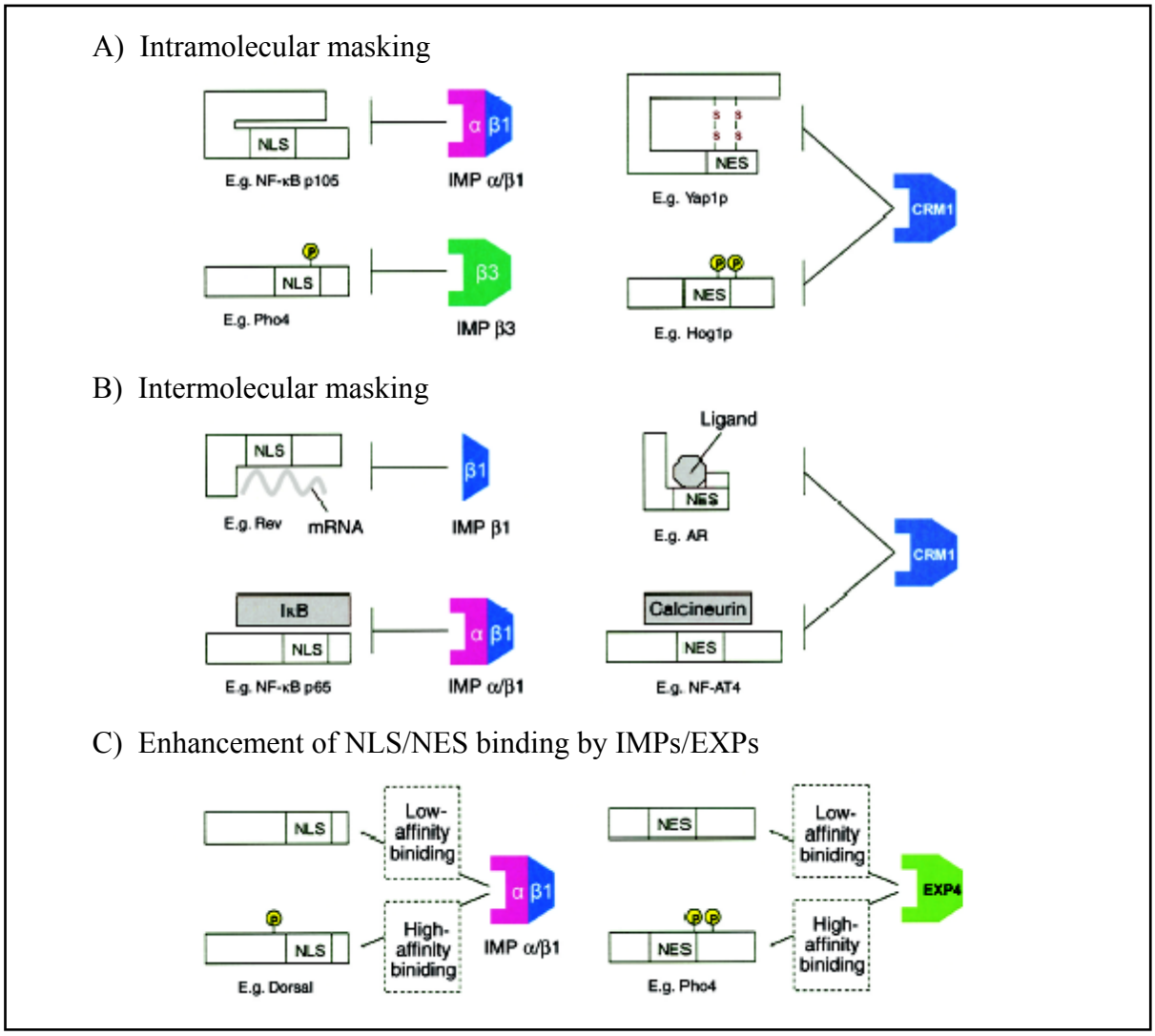

Figure 7. Mechanisms of regulation of nuclear transport. (Poon IKH, 2005)
A) Selected examples of intramolecular masking, where targeting signals are prevented from importin(IMP)/exportin(EXP) recognition by the conformation of the protein containing it. B) Selected examples of intermolecular masking, where targeting signals are protected from IMP/EXP recognition by binding of a heterologous molecule and finally C) selected examples of the enhancement of IMPs/EXPs binding to NLSs/NESs by phosphorylation.

high Ca^{2+} concentrations, the Ca^{2+}-responsive phosphatase Cn binds to and masks the NES of NFAT4, preventing CRM1 binding. At low Ca^{2+} concentrations, Cn disassociates from NFAT4 to unmask the NES and enables the nuclear export. That similar mechanisms apply to nuclear import is indicated by the example of NFκB p65, where, in the absence of immune challenge, the p65 NLS is masked from recognition by Importinα/β_1 due to binding of the specific inhibitor protein I-κB. Upon immune challenge, I-κB is phosphorylated, leading to its Ubiquitin dependent degradation by the proteosome, resulting in unmasking the NFκB p65 NLS and starting the NFκB p65 nuclear import.

Nuclear localization of the tumor-suppressor p53 is regulated by a number of mechanisms, one of which is tetramerization in the nucleus in response to DNA damage, resulting in masking of the C-terminal NES in the p53 tetramer. Dissociation of the tetramer is necessary to unmask the NES and allow nuclear export. Ligand binding can also mask NESs/NLSs, as shown for the NES of the Androgen receptor, which lies in the ligand binding domain of the molecule. In the presence of ligand (e.g. Androgen), the NES is masked and unable to be recognized by Exportin1. Re-localization of Androgen receptor to the cytoplasm can thus only occur when ligand dissociates from the Androgen receptor NES.

Intermolecular masking of targeting signals can also occur via RNA or DNA binding. In the case of the Human immunodeficiency virus 1 (HIV-1) Rev protein, whose role is to ferry unspliced nuclear HIV-1 mRNA to the cytoplasm, binding of mRNA masks its Importinβ_1 recognized NLS. This ensures mRNA release in the cytoplasm before another round of Rev nuclear import to ferry HIV-1 mRNA out to the nucleus; mRNA binding to Rev within the nucleus also facilitates its release from Importinβ_1 at the conclusion of Rev nuclear import. Both the yeast transcription factor GAL4 and the human Sex-determining region Y (SRY) have overlapping DNA binding domains and Importinβ_1 recognized NLSs, where DNA binding prevents Importinβ_1 binding and vice versa. The physiological role of this may be as an alternative mechanism to RanGTP mediated cargo release in the nucleus, i.e. DNA binding could well assist cargo release in the nucleus, under conditions of limiting RanGTP, or where Ran acitivity may be inhibited by cytosolic Ca^{2+} [103].

1.3.6.3. Modulation of Importin/Exportin Binding Affinity

In addition to NLS/NES masking, which prevents nuclear import or export, the affinity of importins/exportins for NLSs/NESs can be regulated positively by phosphorylation, where phosphorylation sites close to the targeting signal enhance importin/exportin binding. T-ag is an example where phosphorylation by protein kinase CK2 at $Ser^{111/112}$, flanking the NLS, enhances the affinity of Importinα/β_1 binding 100-fold, thereby increasing nuclear import 50-fold. Phosphorylation can similarly influence nuclear export, as indicated by the example of Pho4, where phosphorylation at Ser^{114} and Ser^{128} enhances recognition by Exportin4 (Msn5), and thereby nuclear export. Clearly, phosphorylation can enhance or inhibit nuclear import/export through a variety of mechanisms [103].

1.4. Cardiac Hypertrophy

Cardiomyocyte hypertrophy is the cellular response to an increase in biomechanical stress, be it extrinsic, such as in arterial hypertension or valvular heart disease, or intrinsic, as in familial hypertrophic cardiomyopathy. Cardiac hypertrophy eventually normalizes the increase in wall tension, thereby abrogating the initial stimulus. The defining features of hypertrophy are an increase in cardiomyocyte size, enhanced protein synthesis and a higher organization of the sarcomere. These changes in cellular phenotype are preceded and accompanied by the re-induction of the so-called fetal gene program [147]. In Figure 8 a mouse wiltype heart is faced to two hearts of hypertrophy transgenic mouse models. Both the phenotype of concentric and the phenotype of eccentric hypertrophy are shown.

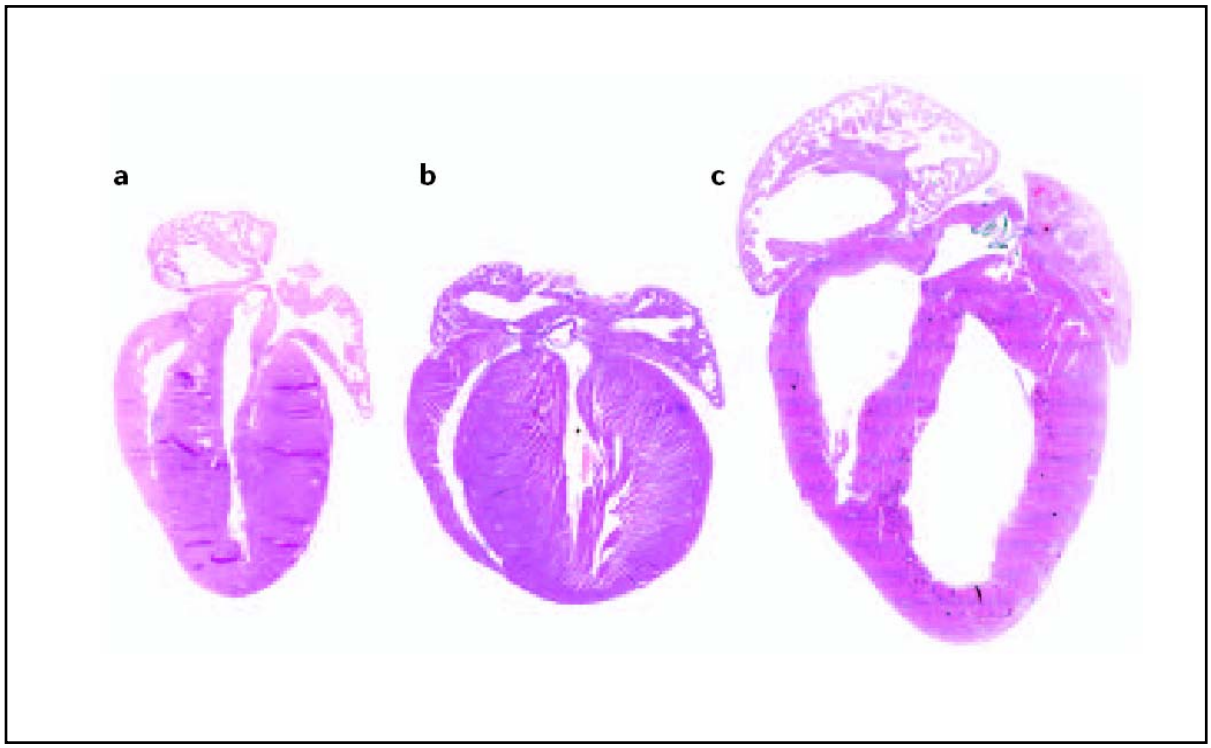

Figure 8. Different phenotypes of cardiac hypertrophy. (Heineke J, 2006)
Haematoxylin- and Eosin-stained histological cross sections of a) an adult wildtype mouse heart, b) an heart of transgenic cardiac-specific overexpression of activated Mitogen-activated protein kinase kinase-1 (MEK1, an upstream activator of the Mitogen-activated protein kinases (MAPKs)) and c) an heart of transgenic cardiac-specific overexpression of Calcineurin.
The MEK1 heart shows a so-called concentric hypertrophy, whereas the Calcineurin-overexpression results in a so-called eccentric hypertrophy and dilation.

Although hypertrophy in response to pathologic signaling has traditionally been considered an adaptive response required to sustain cardiac output in the face of stress, prolonged hypertrophy is associated with a significant increase in the risk for sudden death or progression to heart failure, independent of the underlying cause of hypertrophy, suggesting

that the hypertrophic process is not entirely beneficial. This notion is further supported by observations in clinical trials, such as the HOPE trial (Heart Outcomes Prevention Evaluation [148]), that inhibition or even regression of cardiac hypertrophy by certain drugs, such as Angiotensin-converting enzyme (ACE) inhibitors, lowers the risk for several endpoints, including death and progression to heart failure, whereas persistence of cardiac hypertrophy (despite similar blood pressure changes) predicts an adverse outcome [149]. These findings raise questions about whether stress-induced hypertrophy does any good or whether it may be initially adaptive and only leads to cardiac demise when prolonged. Equally important is the difference between physiological hypertrophy, as occurs during postnatal development and in response to exercise, and pathological hypertrophy. Strategies to stimulate the former and inhibit the latter would have obvious therapeutic value in the setting of heart failure.

If hypertrophy in response to stress were entirely maladaptive, a logical approach would be to identify the underlying molecular events and eventually develop strategies to prevent or reverse the hypertrophic phenotype to circumvent the subsequent development of heart failure at an early stage. Numerous cardiomyocyte autonomous and endocrine/paracrine pathways have been implicated in the heart's molecular response to increased wall stress and the development of hypertrophy. A large body of literature has emerged describing the intracellular signaling pathways that transduce hypertrophic stimulation into alterations in gene expression, which include the Mitogen-activated protein kinases (**MAPK**s), **PKC** and **Calcineurin-NFAT** signaling pathways [52,150-153].

1.4.1. Physiological Hypertrophy

Based on the fast increase of the whole body in neonatal organisms the myocardium have to reach a maximal level of pump capacity. Mammalian ventricular cardiomyocytes lose their capacity for cell division during the perinatal period, although the amitosis is still going on for a few days. Thus, the heart increases exclusively by ´physiological` hypertrophy – the volume increase of each cell. As a result, most of the cardiomyocytes become binuclear.

In adult myocardium chronic exercise training causes cardiac hypertrophy, which is defined as athletic heart [154,155]. The athletic heart is a physiological cardiac hypertrophy, which is an induced beneficial adaptive response of the cardiovascular system, i.e. decreased resting and

submaximal heart rates and increased filling time and venous return. Together, these adaptations can help the myocardium to satisfy the increased demands of exercise while maintaining or enhancing normal function. Although it has been considered that exercise training-induced cardiac hypertrophy is partly caused by the increase in mechanical load by repeated bouts of exercise, the precise mechanisms are not known. In contrast to the pathological hypertrophy, the physiological hypertrophy is reversible [154,156].

1.4.2. Pathological Hypertrophy

Cardiac hypertrophy is an adaptive response of the heart to a variety of intrinsic and extrinsic stimuli, including hypertension, valvular heart disease, aortic stenosis, myocardial infarction (extrinsic factors), endocrine disorders and mutations in sarcomeric proteins (intrinsic factors) that result in altered contractility [147,152]. Pathological cardiac hypertrophy is a compensatory adaptation to an increase in workload of the heart. Although hypertrophy is initially beneficial, permitting enhanced cardiac output, it can ultimately become deleterious and result in cardiomyopathy, heart failure, and sudden death. Thus, there are crucial differences in cardiac properties between pathological and physiological cardiac hypertrophy (athletic heart).

1.4.2.1. Extrinsic Factors

Pathological hypertrophy is beside the intrinsic factors caused by extracellular, so-called extrinsic factors, including hypertension, myocardial infarction or ischaemia associated with coronary disease, valvular heart disease and aortic stenosis, myocarditis due to an infectious agent, congenital malformations, familial hypertrophic and dilated cardiomyopathies, and diabetic cardiomyopathy. Most of these stimuli first induce a phase of cardiac hypertrophy in which individual myocytes grow in lenght and/or width as a means of increasing cardiac pump function and decreasing ventricular wall tension (inducing a state of ´compensated hypertrophy`). However, in the long term, myocardial hypertrophy predisposes individuals to heart failure, arrhythmia and sudden death [21].

1.4.2.2. Intrinsic Factors

Elucidation of the intracellular signal transduction systems and transcription factors that activate and maintain the hypertrophic program represents a major challenge. Recently, several mouse models that mimic aspects of hypertrophy and heart failure in humans have been described and new pathways for hypertrophic signaling have been uncovered [152,157].

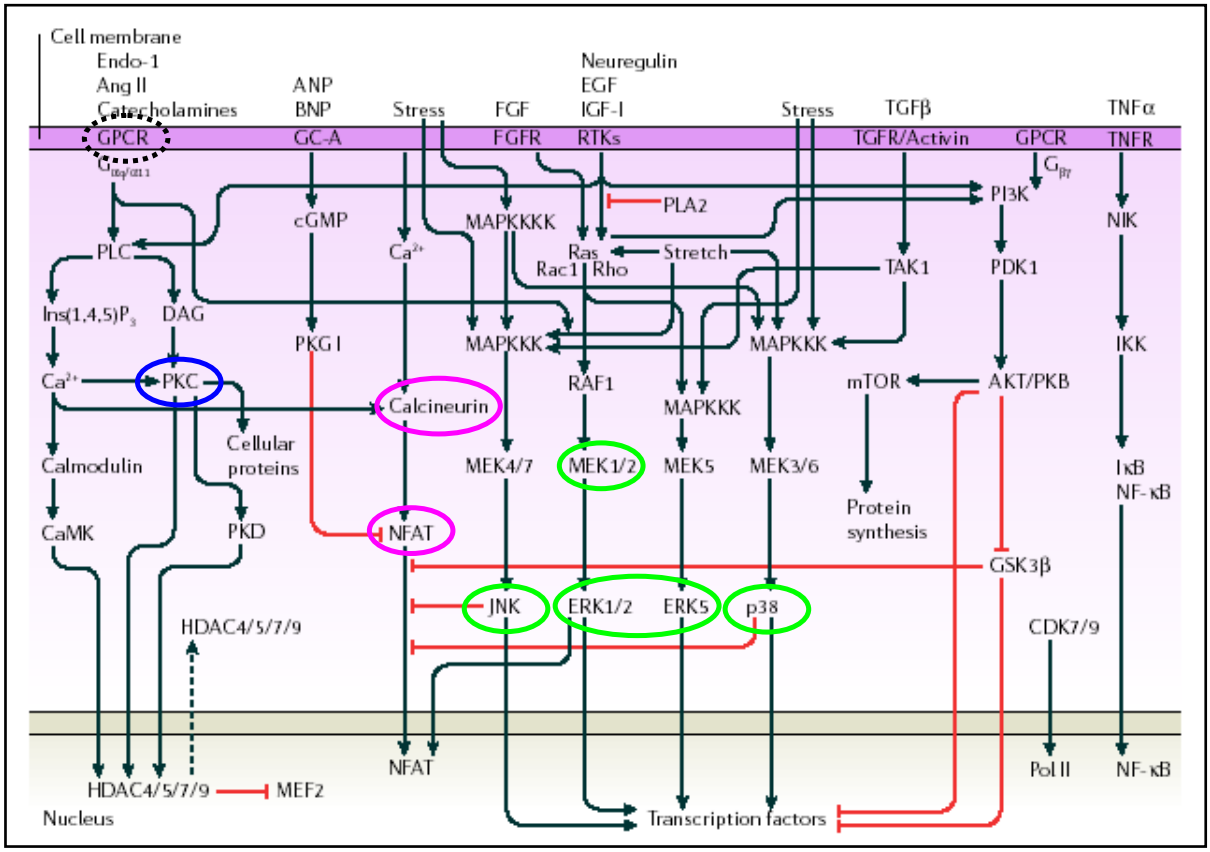

Figure 9. Integrated schematic of the more extensively characterized intracellular signal-transduction pathways that coordinate the cardiac hypertrophic response. (Heineke J, 2006)
Three pathways are explained more detailed in the text. Green framed: MAPKs pathway (JNK, ERKs, p38, MEK); blue framed: PKC pathway, pink framed: Calcineurin-NF-AT pathway; black coloured: G protein-coupled receptors (GPCRs)

The **MAPK** pathway (green framed in Figure 9) is one of the known pathways and provide an important link between external stimuli and the nucleus via phosphorylation and regulation of multiple transcription factors. On the basis of sequence homology, MAPKs can be divided into three major subfamilies: Extracellularly responsive kinases (ERKs), c-Jun N-terminal kinsases (JNKs) and p38 MAPKs [147]. Exposure of myocytes and whole hearts to G protein-coupled receptors (GPCRs, black framed in Figure 9) agonists leads to activation of ERKs, JNKs and p38 MAPKs. GPCR agonists, like Endothelin-1 (ET-1), Phenylephrine (PE) or Angiotension II (AngII), activate the small G protein Ras through a PKC dependent

mechanism and may also activate Rho subfamily small G proteins. Ras activates the ERK cascade and, eihter directly or indirectly, may activate JNKs and p38 MAPKs through a poorly understood mechanism. The acitvated MAPKs phosphorylate other kinases and transcriptions factors, which causes the transcription of hypertrophic genes [158]. The **PKC** (blue framed in Figure 9) is a ubiquitously expressed serine/threonine kinase, activated predominantely by GPCRs. Multiple studies implicate the various PKC isoforms in the pathogenesis of cardiac hypertrophy/failure and myocardial protection [147]. It has been difficult to establish particular roles for individual PKC isoforms due to the absence of isoformspecific agonists and antagonists. Targeted cardiac overexpression of PKC has been helpful in establishing possible effects of myocardial PKCβ signaling, but the potential for non-specific or non-physiological signaling of overexpressed enzymes warrants a cautious interpretation of resulting phenotypes [159]. Although the inhibition of PKCα, PKCβ and PKCε by gene targeting or blocking peptides has shown that they are not involved in the regulation of cardiac hypertrophy, the overexpression of these PKC isoforms can induce cardiac hypertrophy in transgenic mice. These findings indicate that these proteins might not be primary regulators of this process, or that gene redundancy is a significant issue *in vivo* [160]. Within the **Calcineurin-NFAT** signaling pathway (green framed in Figure 9) the Ca^{2+} dependent serine/threonine protein phosphatase Calcineurin (Cn) was identified as a central prohypertrophic signaling molecule in the myocardium by Molkentin J.D. In mammalian hearts only the isoforms CnAα, CnAβ and CnB1 are expressed. According to higher Ca^{2+} levels, Cn activates the transcription factor NFAT by dephosphorylation. As a result both the transcription factor NFAT and the phosphatase Cn are translocated into the nucleus. Both are responsible for activating the expression of prohypertrophic genes. Whereas the nuclear action of NFAT as a transcriptional co-activator within a heterocomplex binding to DNA promotors is relativley known, the nuclear function of Cn still remains unclear [21].

In this work more details about the function of Calcineurin within the Calcineurin-NFAT signaling cascade are given. Our working group demonstrate a new approach to prevent the development of myocardial hypertrophy.

2. Material

2.1. Equipment

autoclav	Sanoclav	KL-12-3
centrifuge	Sigma	2K15, Sigma 2-15
centrifuge	Hettich	Mikro 12-24
centrifuge	Beckmann	GPKR Centrifuge
centrifuge	Eppendorf	
centrifuge	Heraeus	Biofuge pico
confocal microscope	Nikon	EZ-C1
ELISA reader	Tecan	Tecan Spectra
fluroescence microscope	Zeiss	Axiovert 135
freezer (-20°C)	Liebherr	Economy
freezer (-20°C)	Bosch	economic
freezer (-80°C)	National Lab	Profi Star
fridge	Liebherr	glass line, Premium, comfort
gel dryer	Biotec Fischer	Phero Temp 60
heating block	Eppendorf	ThermoStat plus
heating block	Liebisch	
homogenizer	IKA Labortechnik	Eurostar digital
homogenizer	Janke/Kunkel	Ultra Turrax T25
incubator	Heraeus	Function line
incubator	Forma Scientific	Steri-Cult 200
light table	Uni Würzburg	
luminometer	Berthold Industries	Lumat LB9501
magnetic stirrer	IKA Labortechnik	RH basic2, Ikamag RET, Ikamag RCT
magnetic stirrer	Hartenstein	Hotplate Stirrer L81
microwave	Daewoo	KOR-6305BL
microscope	Leitz	Labovert
oven	MWG Biotech	Mini Oven
PCR machine	Eppendorf	Mastercycler
PCR machine	Perkin Elmer	DNA Thermocycler
photometer	Eppendorf	Bio-Photometer
power supply	Biometra	P25, PP4000
power supply	Hoefer	SX250
scale	Sartorius	BP61
scale	Kern	
sealing machine	Severin	Folio
shaker	Heidolph	Duomax 1030
shaker	Hartenstein	L40
shaker	Braun Biotech	Certomat R
spectrometer	Perkin Elmer	LS 50 B
supersonic bath	Julabo	USR05
turner	Heidolph	REAX 2
UV light	BioRad	Mini-Transluminator
vacuum pump	KNF	klein, mittel, groß
vortexer	Heidolph	REAX 1 D R
vortexer	Scientific Industries	Vortex-Genie2
water bath	Haake	Thermo C10
water bath	Inlabo	SW20C

2.2. Consumable Material

Common consumable material

The common consumable material, e.g. tubes and pipette tips, has been obtained from the University of Wuerzburg (Medical Department I; „Zentrallager“), Hartenstein or Noras (both Wuerzburg, Germany).

Chemicals

All chemicals have been received from the University of Wuerzburg (Medical Department I, Central pharmacy), Merck (Darmstadt, Germany), Roth (Karlsruhe, Germany) or Sigma-Aldrich (Munich, Germany).

Enzymes

The used enzymes have been ordered from Genaxxon (Biberach, Germany), Invitrogen (Karlsruhe, Germany), New England Biolabs (Ipswich, USA), MBI-Fermentas (St. Leon-Rot, Germany), Promega (Mannheim, Germany) or Stratagene (San Diego, USA).

2.3. Working Kits

BIOMOL	Cellular Calcineurin Assay Kit	Cat.No. #AK-816
BD Bioscience Clontech	BD Advantage™2 PCR Kit	Cat.No. #639207
Invitrogen Life Technologies	PCR Optimizer™ Kit	Cat.No. #K1220-01
Invitrogen Life Technologies	Lipofectamine™ Reagent	Cat.No. #18324-012
Macherey & Nagel GmbH & Co.KG	NucleoBond PC100	Cat.No. #740 573.100
Macherey & Nagel GmbH & Co.KG	NucleoBond PC500	Cat.No. #740 574.50
Macherey & Nagel GmbH & Co.KG	NucleoSpin Plasmid	Cat.No. #740 588.250
New England Biolabs Inc.	Quick Ligation Kit	Cat.No. #M2200S
Promega GmbH	Luciferase Assay System	Cat.No. #E1500
Promega GmbH	LigaFast™ Rapid DNALigationSystem	Cat.No. #M8221
PeqLab Biotechnologie GmbH	GenePorter™2 Transfection Reagent	Cat.No. #13-T202007
Qiagen	QIAquick PCR Purification Kit	Cat.No. #28104
Qiagen	QIAquick Gel Extraction Kit	Cat.No. #28704

2.4. Solutions and Buffers

2.4.1. DNA Electrophoresis

50x TAE Buffer (Tris-Acetate-EDTA):

component (MW [g/mol])	stock	weight/volume / l	final concentration
Tris [121.14]		242.0 g	2.0 mM
Acetic acid [60.05]		57.1 ml	1.0 mM
EDTA [292.25]	0.5 M pH 8.0	100.0 ml	0.05 mM
dH_2O		ad 1000 ml	

6x Loading Dye:

component	final concentration
Bromphenol blue	0.25 %
Xylene cyanol	0.25 %
Glycerol	30.0 – 60.0 %

2.4.2. Cardiomyocyte Preparation and Cell Culture

CBFHH (Calcium- and Bicarbonate-Free Hanks' solution with HEPES):

component (MW [g/mol]]	stock	volume / l CBFHH	final concentration
NaCl [58.44]	200.0 g/l	40.0 ml	137.0 mM
KCl [75.55]	40.0 g/l	10.0 ml	5.36 mM
$MgSO_4*7H_2O$ [246.48]	20.0 g/l	10.0 ml	0.81 mM
Dextrose [180.16]	100.0 g/l	10.0 ml	5.55 mM
KH_2PO_4 [136.09]	6.0 g/l	10.0 ml	0.44 mM
Na_2HPO_4 (water free) [141.96]	9.0 g/l	10.0 ml	0.34 mM
HEPES pH 7.4	47.66 g/l	100.0 ml	20.06 mM
dH_2O		ad 1000 ml (check pH)	

After filtration with a bottle top filter (Nunc; Wiesbaden, Germany) Penicillin G and Streptomycin were added.

component (MW [g/mol]]	stock	weight/volume / l CBFHH	final concentration
Penicillin G (1600 U/mg)	50000 U/ml	1.0 ml	50.0 U/ml
Streptomycin	50.0 mg/ml	1.0 ml	50.0 µg/ml

MEM (Minimal Essential Medium):

component (MW [g/mol])	stock	weight/volume /l MEM	final concentration
MEM HBS with NEAA (w/o L-Glutamine, Phenolred, $NaHCO_3$) (#1-33V12-K) (BioConcept, Switzerland)		10.5 g	
BrdU (Bromodeoxyuridine) [307.1]	20.0 mM 6.142 mg/ml	5.0 ml	0.1 mM 30.7 µg/ml
Penicillin G (1600 U/mg)	50000 U/ml	1.0 ml	50.0 U/ml
Streptomycin	50.0 mg/ml	1.0 ml	50.0 µg/ml
Vitamin B12	2.0 mg/ml	1.0 ml	2.0 µg/ml
L-Glutamine [146.15]		292.0 mg	2.0 mM
$NaHCO_3$ [84.01]		350.0 mg	4.2 mM
dH_2O		ad 1000 ml	

MEM/5: MEM, as described above containing 5.0 % foetal calf serum (FCS)

MEM/1: MEM, as described above containing 1.0 % foetal calf serum (FCS)

MEM/0.5: MEM, as described above containing 0.5 % foetal calf serum (FCS)

T & D (Trypsine and DNase):

component	stock	volume / 100 ml CBFHH	final concentration
DNase	2.0 mg/ml 0.15 M NaCl	1.0 ml (sterile filtrated)	0.02 mg/ml
Trypsine	1.5 mg/ml CBFHH	100.0 ml (sterile filtrated)	1.5 mg/ml

DMEM/10 (Dulbecco´s Modified Eagle´s Medium with 10 % FCS):

component	stock	volume	final concentration
DMEM (D6046; Invitrogen, Germany)		500.0 ml	
Penicillin	10000 U/ml	5.0 ml	100.0 U/ml
Streptomycin	10.0 mg/ml		0.1 mg/ml
FCS		50.0 ml	10.0 %

2.4.3. Immunohistochemistry

5x PBS (Phosphate Buffered Saline) pH 7.4:

component (MW [g/mol])	weight / 5 l	final concentration (5x)	final concentration (1x)
NaCl [58.44]	40.0 g	685.0 mM	137.0 mM
KCl [74.6]	1.0 g	13.4 mM	2.7 mM
$Na_2HPO_4*2H_2O$ [177.99]	7.2 g	40.5 mM	8.1 mM
KH_2PO_4 [136.09]	1.0 g	7.5 mM	1.5 mM
dH_2O (check pH 7.4)	ad 5000 ml		

0.1 % Triton / 1x PBS: addition of 100 µl Triton®X100 to 100.0 ml 1x PBS

4 % PFA / 1x PBS: addition of 4.0 g Paraformaldehyde (PFA) to 100.0 ml 1x PBS

2.4.4. Co-immunoprecipitation and Western blotting

RIPA (RadioImmunoPrecipitation Assay) Buffer:

component (MW [g/mol])	stock	volume/weight / 100 ml	final concentration
NaCl [58.44]	1.0 M	15.0 ml	150.0 mM
Tris [121.14]	1.0 M	5.0 ml	50.0 mM
PMSF	100.0 mM	1.0 ml	1.0 mM
IGEPAL CA-630		1.0 ml	1.0 %
Sodium deoxycholate (DOC)	10.0 %	5.0 ml	0.5 %
Sodium dodecyl sulfate (SDS)	10.0 %	1.0 ml	0.1 %
dH_2O		ad 100.0 ml	

Low Salt Buffer:

component (MW [g/mol])	stock	volume/weight / 100 ml	final concentration
Tris [121.14]	1.0 M	5.0 ml	50.0 mM
PMSF	100.0 mM	1.0 ml	1.0 mM
IGEPAL CA-630		1.0 ml	1.0 %
dH_2O		ad 100.0 ml	

1.5 M Tris pH 8.8:

component (MW [g/mol])	weight / 100 ml	final concentration
Tris [121.14]	18.15 g	1.5 M
dH_2O (check pH 8.8)	ad 100.0 ml	

0.5 M Tris pH 6.8:

component (MW [g/mol])	weight / 100 ml	final concentration
Tris [121.14]	6.0 g	0.5 M
dH_2O (check pH 6.8)	ad 100.0 ml	

10 % SDS (Sodium dodecyl sulfate):

component (MW [g/mol])	weight / 100 ml	final concentration
Sodium dodecyl sulfate (SDS)	10.0 g	10.0 %
dH_2O (check pH 8.0)	ad 100.0 ml	

5x PBS pH 7.4:

component (MW [g/mol])	weight / 5 l	final concentration (5x)	final concentration (1x)
NaCl [58.44]	20.0 g	342.0 mM	68.4 mM
$NaH_2PO_4*H_2O$ [137.99]	11.73 g	85.0 mM	17.0 mM
Na_2HPO_4 [141.96]	41.17 g	290.0 mM	58.0 mM
dH_2O (check pH 7.4)	ad 5000 ml		

5x Electrophoresis Buffer pH 8.3:

component (MW [g/mol])	weight / 5 l	final concentration (5x)	final concentration (1x)
Tris [121.14]	75.0 g	0.62 M	124.0 mM
Glycin [75.07]	360.0 g	4.8 M	960.0 mM
SDS	25.0 g	0.5 %	0.1 %
dH_2O (check pH 8.3)	ad 5000 ml		

Transfer Buffer pH 8.3:

component	stock	volume / 1 l	final concentration
5x Electrophoresis buffer	5x	200.0 ml	1x
Methanol		200.0 ml	20.0 %
dH_2O		ad 1000 ml	

Washing solution

component	stock	volume / 1 l	final concentration
5x PBS pH 7.4	5x	200.0 ml	1x
Tween20		0.5 ml	0.05 %
dH_2O		ad 1000 ml	

Blocking solution

component	stock	volume / 1l	final concentration
5x PBS pH 7.4	5x	20.0 ml	1x
nonfat dried milk powder		5.0 g	5.0 %
dH_2O		ad 100.0 ml	

SDS Gels:

Separating Gels:

component	5 %	7,5 %	10 %	12 %	15 %
dH_2O	11.39 ml	9.69 ml	8.02 ml	6.69 ml	4.69 ml
1,5 M Tris pH 8,8	5.0 ml	5.0 ml	5.0 ml	5.0 ml	5.0 ml
10 % SDS	0.2 ml	0.2 ml	0.2 ml	0.2 ml	0.2 ml
Acrylamide/Bis (30 % - Stock)	3.3 ml	5.0 ml	6.67 ml	8.0 ml	10.0 ml
10 % APS	0.1 ml	0.1 ml	0.1 ml	0.1 ml	0.1 ml
TEMED	0.01 ml	0.01 ml	0.01 ml	0.01 ml	0.01 ml

Stacking Gel (5 %):

component	2 Gels
H_2O_{dest}	5.65 ml
0,5 M Tris pH 6,8	2.5 ml
10 % SDS	0.1 ml
Acrylamide/Bis (30 % - Stock)	1.7 ml
10 % APS	0.05 ml
TEMED	0.01 ml

2.5. Vectors

pEGFP-C3

features:	cloning vector (4,7 kb), Neo^R, Kan^R; MCS 100 bp; expression vector in mammalian cells (P_{CMV}); N-terminal EGFP tag
origin:	BD Bioscience Clontech (Cat.No. #6082-1); GenBank Accession #U57607
use:	cloning of pEGFP-C3 – CnAβ(...) vectors

pEGFP-C3 - CnAβ(…)

features:	cloned vector (6 kb), Neo^R, Kan^R; MCS 100 bp; expression vector in mammalian cells (P_{CMV}); N-terminal EGFP tag; insertion of diverse human Calcineurin Aβ mutants; CnA(1-525), (1-505), (1-485), (1-465), (1-445), (1-425), (1-415), (Δ420-434), (Δ420-445), (171-190)
origin:	own work
use:	transfection of diverse cell lines

pEF-FLAG - hCnAα(2-173)

features:	cloned vector (5,5 kb), Amp^R; MCS 80 bp; expression vector in mammalian cells (P_{CMV}); N-terminal FLAG tag; insertion of human Calcineurin Aα (2-143)
origin:	Dr. M. H. Buch; Clinical Research Fellow, Division of Cardiology; The University of Manchester
use:	transfection of diverse cell lines

p3xFLAG-CMV7.1 - hCnAα(…)

features:	cloned vector (5 kb), Amp^R; MCS 70 bp; expression vector in mammalian cells (P_{CMV}); N-terminal FLAG tag; insertion of diverse human Calcineurin Aα mutants; CnAα(3-143), (3-97), (3-57)
origin:	Dr. M. H. Buch; Clinical Research Fellow, Division of Cardiology; The University of Manchester
use:	transfection of diverse cell lines

pNP1-luci

features:	cloned vector (6,5 kb), Amp^R; MCS 50 bp; pGL3-Basic Vector (Promega; Cat.No. #E1751) containing the eNOS promotor in wrong direction upstream of the luciferse gene (*luc*$^+$); NO expression of luciferase in transfected cells (control vector)
origin:	own laboratory
use:	transfection of diverse cell lines; especially for the luciferase assay

pNP3-luci

features:	cloned vector (6,5 kb), Amp^R; MCS 50 bp; pGL3-Basic Vector (Promega; Cat.No. #E1751) containing the eNOS promotor in right direction upstream of the luciferase gene (*luc*$^+$); expression of luciferase in transfected cells
origin:	own laboratory
use:	transfection of diverse cell lines; especially for the luciferase assay

2.6. Oligonucleotides

CN1855F-1	ATA CTC GAG TTT AAG CAG GAA TGT	CnAβ(171-190) (XhoI-site)
CN1914R-1	TAG GAT CCT CAA GCT TCC ATA CA	CnAβ(171-190) (BamHI site)
CN420R-1	TCC GGA TCC GAC TCT TGC CAT CTT	upstream fragment; CnAβ(Δ420-434/445) (BamHI site)
CN434F-1	ATA GGA TCC GGC CTG ACT CCC ACA	downstream fragment; CnAβ(Δ420-434) (BamHI site)
CN445F-1	CAG GGA TCC GTG TTA GCT GGA GGA	downstream fragment; CnAβ(Δ420-445) (BamHI site)
coCalci(full)R	TGC TCT AGA TGT TAT CAC TGG GCA GTA TGG	CnAβ(1-525) (XbaI site)
coCalci(Δ100)R	TCG TCT AGA TGT TAC TCC CTG AGA ACA GAG	CnAβ(1-425) (XbaI site)
coCalci(Δ110)R	TCG TCT AGA TGT TAC TTG CCA ATT GCT CGA	CnAβ(1-415) (XbaI site)
coCalci(Δ20)R	TCG TCT AGA TGT TAG AAA CCA TCT TGC TGT	CnAβ(1-505) (XbaI site)
coCalci(Δ40)R	TCG TCT AGA TGT TAA CCC TTT GCC TCT TCA	CnAβ(1-485) (XbaI site)
coCalci(Δ60)R	TCG TCT AGA TGT TAT TCA GCC TCA ATA GCC	CnAβ(1-465) (XbaI site)
coCalci(Δ80)R	TCG TCT AGA TGT TAT CCA CTA GGC AAC ATC	CnAβ(1-445) (XbaI site)
coCalciF	AAT ACT CGA GAT GGC CGC CCC GGA G	CnAβ(1-525 to 415) (XbaI site)
MCS1pEGFP	CAG TCC GCC CTG AGC AAA GA	MCS pEGFP-C3 (forward)
MCS2pEGFP	TCA GGT TCA GGG GGA GGT GT	MCS pEGFP-C3 (reverse)

2.7. Antibiotics and Proteins/Peptides

Antibiotics:

antibioticum	stock	final concentration	selection
Ampicillin	100 mg/ml in dH_2O	100 µg/ml	*E. coli*
Kanamycin	25 mg/ml in dH_2O	50 µg/ml	*E. coli*

Peptides: Import Blocking Peptide (IBP) and Control Peptide (ctr)

peptide	amino acid sequence	stock	final concentration
IBP	N - AAVALLPAVLLALLAKQECKIKYSERV - C	1.0 M	1.0 µM
ctr	N - AAVALLPAVLLALLAAQECAIAYSEAV - C	1.0 M	1.0 µM

2.8. Antibodies

Primary Antibodies:

antibody	species	company	Cat.No.
BNP	rabbit	Acris; Hiddenhausen, Germany	BP099
BNP	rabbit	Biotrend; Köln, Germany	1505-0639
BNP	mouse	Abcam; Cambrigde, UK	ab20984
BNP	mouse	HyTest; Turku, Finland	4BNP2
Calcineurin A	rabbit	Stressgen; Ann Arbor, USA	SPA-610
cJun	rabbit	Biomol; Hamburg, Germany	1254-1
ERK1-2	rabbit	Chemicon; Hampshire, UK	AB3053
FLAG	rabbit	Acris; Hiddenhausen, Germany	DP3002
GAPDH	mouse	Chemicon; Hampshire, UK	MAB374
GATA4	rabbit	Chemicon; Hampshire, UK	AB4132
GFP	goat	Abcam; Cambrigde, UK	ab5450
Histon H1	rabbit	Santa Cruz; Santa Cruz, USA	sc10806
Histon H1	sheep	Abcam; Cambrigde, UK	ab1938
Karyopherinβ	mouse	Sigma-Genosys; St. Louis, USA	I2534
MEF2A	rabbit	Abcam; Cambrigde, UK	ab32866
NFAT1	mouse	Abcam; Cambrigde, UK	ab2722
NFAT2	mouse	Santa Cruz; Santa Cruz, USA	sc7294
NFAT2	mouse	Abcam; Cambrigde, UK	ab25916
NFAT2	mouse	Abcam; Cambrigde, UK	ab2796
NFAT3	goat	Santa Cruz; Santa Cruz, USA	sc1153
NFAT3	rabbit	Oncogene; Cambrigde, USA	PC625
NFAT3	rabbit	Santa Cruz; Santa Cruz, USA	sc13036
NFAT4	rabbit	Santa Cruz; Santa Cruz, USA	sc8321
NFκB	rabbit	Abcam; Cambrigde, UK	ab16502
Troponin I	goat	Santa Cruz; Santa Cruz, USA	sc8118
Troponin I	rabbit	Santa Cruz; Santa Cruz, USA	ab15368

Secondary Antibodies:

antibody	label	species	company	Cat.No.
goat	Alexa Fluor 488nm	donkey	Molecular Probes; Leiden, Netherlands	A-11055
goat	Alexa Fluor 546nm	donkey	Molecular Probes; Leiden, Netherlands	A-11056
goat	Alexa Fluor 594nm	donkey	Molecular Probes; Leiden, Netherlands	A-11058
goat	Alexa Fluor 633nm	donkey	Molecular Probes; Leiden, Netherlands	A-21082
mouse	Alexa Fluor 488nm	goat	Molecular Probes; Leiden, Netherlands	A-11001
mouse	Alexa Fluor 546nm	goat	Molecular Probes; Leiden, Netherlands	A-11003
mouse	Alexa Fluor 594nm	goat	Molecular Probes; Leiden, Netherlands	A-11005
mouse	Alexa Fluor 633nm	goat	Molecular Probes; Leiden, Netherlands	A-21050
rabbit	Cy3 (Carbocyanin 3)	goat	Jackson Immunoresearch; Suffolk, UK	111-165-003
rabbit	Alexa Fluor 488nm	goat	Molecular Probes; Leiden, Netherlands	A-11008
rabbit	Alexa Fluor 546nm	goat	Molecular Probes; Leiden, Netherlands	A-11010
rabbit	Alexa Fluor 594nm	goat	Molecular Probes; Leiden, Netherlands	A-11012
rabbit	Alexa Fluor 633nm	goat	Molecular Probes; Leiden, Netherlands	A-21070
sheep	Cy3 (Carbocyanin 3)	donkey	Jackson Immunoresearch; Suffolk, UK	713-165-147
sheep	HRP (Horseradish Peroxidase)	donkey	Abcam; Campbrigde, UK	ab6900
rabbit	HRP (Horseradish Peroxidase)	donkey	GE Healthcare; Munich, Germany	NA9340V
mouse	HRP (Horseradish Peroxidase)	sheep	GE Healthcare; Munich, Germany	NA9310V

2.9. Components for Bacteria and Cell Culture

Bacteria Culture:

All media and agar plates (10.0 mm dishes) have been prepared according to the following prescription and autoclaved (20 minutes at 120°C). After cooling down to 50°C, additives, e.g. antibiotics (diverse concentrations), have been completed and plates have been spilled.

LB medium:	Bacto-Pepton	10.0 g
	Yeast extrakt	5.0 g
	NaCl	10.0 g
	ad 1000 ml dH_2O	
LB agar:	Addition of 15.0 g agar to 1000 ml LB-Medium	

Cell Culture:

The cell culture components, e.g. DMEM, Trypsin and other additives, like Penicillin G and Streptomycin, have been received from Invitrogen (Karlsruhe, Germany), Sigma Aldrich (Munich, Germany), Nunc (Wiesbaden, Germany) and PAA Laboratories GmbH (Pasching, Austria).

2.10. Bacteria Strains

Escherichia coli

K12 AB1157: F$^-$ *thr-1 araC14 leuB6*(Am)Δ *(gpt-proA)62 lacY1 tsx-33supE44*(AS) *galK2*(Oc) *hisG4*(Oc) *rfbD1 mgl-51 rpoS396*(Am) *rpsL31*(Str^R) *kdgK51 xylA5 mtl-1 argE3*(Oc) *thi-1*

origin: DSMZ; Braunschweig, Germany
E. coli K12 AB1157 (Cat. No. #4509)

K12 DH5α: F$^-$ φ80*d lacZ*Δ*M*15 Δ(*lac*ZYA-*arg*F)U169 *rec*A1 *end*A1 *hsd*R17 (*rk*$^-$mk$^-$) *pho*A *sup*E44 *thi*-1 *gyr*A96 *rel*A1 λ$^-$

origin: Invitrogen; Karlsruhe, Germany
Library Efficiency DH5α; Competent Cells (Cat. No. #18263-012)

XL10-Gold: Tet^R Δ*(mcrA)183* Δ*(mcrCB-hsdSMR-mrr)173 endA1 supE44 thi-1 recA1 gyrA96 relA1 lacHte* [F′ *proAB laclZΔM15 Tn10* (Tet^R) Amy CamR]

origin: Stratagene; San Diego, USA
XL-10-Gold Ultracompetent Cells (Cat. No. #200314)

2.11. Cell Lines

HEK293 *Homo sapiens*
human embryonic kidney
origin: own store; commercial: ATCC, USA (Cat. No. #CRL-1573)

HeLa *Homo sapiens*
human cervix
(Henrietta Lacks)
origin: own store; commercial: ATCC, USA (Cat. No. #CCL-2)

NRCM *Rattus norvegicus*
Wistar rats (HsdCpb:WU)
(Hsd (Harlan Sprague Dawley Inc.); origin;
Cpd: Central Institute for Breeding of Laboratory Animals; breeding place (Netherlands);
WU: Wistar Unilever Company; Vlaardingen, Netherlands)
neonatal rat cardiomyocytes
origin: own preparation

2.12. Animals

Rattus norvegicus	outbred rats	HsdCpb:WU	(Harlan-Winkelmann; Borchen, Germany)
Mus musculus		FVB/HanHsd	(Harlan-Winkelmann; Borchen, Germany)

3. Methods

3.1. Generation of Expression Constructs

Epitope tagged derivatives of Calcineurin Aβ, containing N-terminal EGFP, were generated using the mammalian expression vector pEGFP-C3 (BD Bioscience Clontech). For cloning different Calcineurin mutants the mammalian expression vector pCMV-Sport6 containing the directionally cloned cDNA of human Calcineurin Aβ was used (Invitrogen). The following C-terminal truncated mutants have been amplified by PCR. The truncation was done step by step starting at the C-terminal end. Full length Calcineurin Aβ, CnAβ(1-525) was amplified by coCalciF and coCalci(full)R. The mutants CnAβ(1-505), (1-485), CnAβ(1-465), CnAβ(1-445), CnAβ(1-425) and CnAβ(1-415) were amplified with the same forward primer coCalciF. The reverse primer was specific for each mutant: coCalci(Δ20)R for CnAβ(1-505), coCalci(Δ40)R for CnAβ(1-485), coCalci(Δ60)R for CnAβ(1-465), coCalci(Δ80)R for CnAβ(1-445), coCalci(Δ100)R for CnAβ(1-425) and coCalci(Δ110)R for CnAβ(1-415). The mutant coding only for the NLS region of Cn, amino acid region 171 to 190, was amplified by CN1855F-1 and CN1914R-1. All PCR fragments were digested with XbaI and XhoI in singular registriction steps (each one hour at 37°C) and afterwards purified with the PCR Purification Kit (Qiagen).

The two internal mutants CnAβ(Δ420-434) and CnAβ(Δ420-445) were cloned into the XbaI and XhoI sites of pEGFP-C3 by a two step strategy. For deleting the short area from amino acid 420 to 434 and from 420 to 445 two fragments were amplified by PCR. The upstream fragment (upstream of the deleting region (420 – 434/445)) was identical and was amplified by coCalciF and CN420R-1, whereas the two different downstream fragments (downstream of the deleting region) were amplifed by CN434F-1 and CN445F-1 respectively and coCalci(full)R. The upstream fragment was digested with XbaI and BamHI, whereas the downstream fragments were digested with BamHI and XhoI. After BamHI ligation the whole fragment was ligated to the XbaI and XhoI site of the digested pEGFP-C3 like all the other PCR fragments of all mutants. Resulted vectors were transformed into *E. coli* DH5α and screened for positive clones by PCR reaction. Positive clones have been isolated and kryoconserved.

Generation of FLAG-tagged Calcineurin derivatives has been described previously [161].

3.2. Cell Culture

3.2.1. Isolation of Neonatal Rat Cardiomyocytes (NRCMs)

Cardiac myocytes were isolated and cultured from neonatal rat hearts based on the method reported previously [162]. Experiments were performed according to ´Institutional Animal Care and Use Committee` and ´National Institute of Health (NIH)` guide lines. After decapitation the hearts were removed from 1- to 2-day old neonatal wistar rats, cut into small pieces and digested in T&D (Trypsine). To digest the heart pieces a magnetic stirrer at the lowest speed (100-140 rpm) were used at room temperature (22°C). After five minutes of incubation the supernatant was transferred to a 50 ml falcon tube containing 7.5 ml foetal calf serum (FCS), whereby 12.5 ml T&D [CBFHH (Calcium- and Bicarbonate-Free Hanks' with HEPES: containing 137 mM NaCl, 5.36 mM KCl, 0.81 mM $MgSO_4$*7 H_2O, 5.5 mM Dextrose, 0.44 mM KH_2PO_4, 0.34 mM Na_2HPO_4, 20.06 mM HEPES (pH 7.4), 50.0 U/ml Penicillin G, 50 µg/ml Streptomycin) containing 10 mg/ml DNase and 1.5 mg/ml Trypsin] was added to the remaining tissue pellet. This step was repeated until the whole tissue was digested. The collected supernatants were pelleted by ten minutes of centrifugation at 700 *g* and resuspended in MEM/5 (10.5 g MEM HBS with NEAA (BioConcept, Switzeland) ad 1 l dH_2O, containing 0.1 mM BrdU, 50 U/ml Penicillin G, 50 µg/ml Streptomycin, 2 µg/ml Vitamin B12, 2.0 mM L-Glutamine, 4.2 mM $NaHCO_3$ and 5 % FCS). After filtering through a metal sieve most of the non-cardiomyocytes were removed by preplating for one hour at 37°C in the CO_2 incubator (0.9 %). After preplating, the supernatant, approximately 90 % were cardiomyocytes, was saved and cells were counted in a Fuchs-Rosenthal chamber and plated in MEM/5 on 6-well plates at a density of 0.7 million cells/well (low-density culture) (for 100 mm dishes: 5.0 million cells/dish; for chamber slides (2 and 4 wells): 200.000 cells/well). After twenty-four hours the cells were washed with MEM and incubated for additionally twenty-four hours in MEM/5. After forty-eight hours of preparation the treatment of cells was specific for each experiment. Non-myocyte contamination of primary cultures forty-eigth hours after isolation consisted of approximately 5 % of the total cell population. Myocardial cells were morphologically distinguished by a coarse, granular cytoplasm containing small, dense nuclei, whereas non-myocytes were readily distinguished by a phase-lucent cytoplasm. Contamination of cardiomyocyte cultures with non-myocytes was determined by immuno-histochemical stainings for Troponin I.

3.2.2. Handling of HeLa and HEK 293 Cells

HeLa (human epithelial cells from a fatal cervical carcinoma; Henrietta Lacks, 1951) and HEK 293 cells (human embryonic kidney cells) were cultered in Dulbecco´s modified Eagle´s medium (DMEM) with 10 % FCS, 100 U/ml Penicillin and 100 µg/ml Streptomycin. For experiments cells were plated on 100 mm dishes, 6-well plates or chamber slides.

3.2.3. Transfection of Cell Lines and Cell Treatment

NRCMs were transfected with Lipofectamine (Invitrogen Life Technologies; Karlsruhe, Germany) forty-eight hours after preparation, on 6-well plates at a density of 1 x 10^6 cells per well or on chamber slides at a density of 700000 cells per well. The transfection was performed as described by the manufacturers with the following plasmids: pEGFP-C3 – CnAβ(full), (1-505), (1-485), (1-465), (1-445), (1-425), (1-415), (171-190), (Δ420-434), (Δ420-445); pEf-FLAG – CnAα(2-173), p3xFlag-CMV7.1 – CnAα(3-143), (3-97), (3-57); pNP1-luci and pNP3-luci. After incubation for three hours at 37°C in the CO_2-incubator (0,9 %) following a medium change to MEM/1, cells were treated according to the respective experiments with the following chemicals: Angiotensin II (Ang II; 10 µM), Phenylephrine (PE; 10 µM), Calpeptin (10 µM), Leptomycin B (LMB; 1 µM) and IBP or ctr peptide (1 µM). All cells were harvested twenty-four hours after stimulation and peptide treatment with low salt buffer (1 % IGEPAL CA-630, 50 mM Tris (pH 8.0), 1 mM PMSF) or visualized by confocal microscopy.

HeLa cells were transfected twenty-fours hours after trypsinization with GenePorter2 (PeqLab Biotechnologie GmbH; Erlangen, Germany) on 100 mm dishes, 6-well plates or chamber slides at a confluency of 70 – 80 %. The performance was done according to the manufacturer´s manual. After three hours of incubation at 37°C in the CO_2-incubator (5 %) the booster 2 reagent was added at a concentration of 1 : 100 and incubated in turn for twenty-four hours. Finally, cells were harvested with low salt buffer or visualized by confocal microscopy.

3.3. Co-immunoprecipitation and Western Blotting

Proteins were extracted from tissue or cultured cells by lysis of cells in RIPA buffer, low salt buffer (Western blotting during the co-immunoprecipitation) or specific lysis buffer (CnA Kit, Biomol; see manufacturer's protocol). Detergent soluble fractions were prepared from the supernatant after a centrifugation step at 14000 g for ten minutes at 4°C to remove nuclei and the insoluble fraction. Afterwards the samples were stored at -80°C. The protein concentrations were determined by the Bradford Protein Assay using a BSA standard curve.

For Co-IP experiments HeLa cells were used (because of the higher transfection efficiency compared to cardiomyocytes) according to a standard protocol (Immunoprecipitation Starter Pack; GE Healthcare, Amersham; Munich, Germany). Cells of two 100 mm dishes, transfected with diverse EGFP-tagged CnAβ mutants, were harvested in 1.0 ml low salt buffer (1 % IGEPAL CA-630, 50.0 mM Tris (pH 8.0), 1.0 mM PMSF). After an initial pre-clearing step of one hour at 4°C (500 µl of whole cell lysate with ever 25.0 µl protein G / A sepharose beads), antigens were coupled overnight at 4°C to 2.5 µg purified antibody anti-Importinβ_1 (Sigma-Genosys, #I2534). Protein - antibody complexes were precipitated with a mix of 25 µl protein A and protein G sepharose beads for one hour at 4°C. The saved beads were washed three times with low salt buffer and suspended in 50.0 µl Laemmli buffer (Laemmli sample buffer containing 2-Mercaptoethanol). After denaturation for 5 minutes at 95°C and a following centrifugation step the supernatant was analysed by a SDS-PAGE (8 and 12 % gels). For detecting the CnA fragments, an anti-GFP (1 : 500; Abcam, ab5450) antibody was used. The species-specific second antibody was HRP-conjugated. For visualizing the ECL kit (enhanced chemiluminescence) was used (GE Healthcare, Amersham; Munich, Germany).

For Western blotting, Laemmli buffer was added to each sample (v/v 1:1) and boiled at 95°C for ten minutes to denaturate the proteins. Protein samples were separated on 7.5 - 15 % SDS polyacrylamide gels, depending on the size of each target protein, and electrophoretically transferred to nitrocellulose membranes. After transfer membranes were blocked for one hour using blocking solution (5 % nonfat dried milk powder in PBS/Tween20), following incubation with the primary antibody (diverse incubation times; regularly one to two hours at room temperature). After washing with 1x PBS (six times á five minutes) membranes were incubated with species specific horseradish peroxidase labelled secondary antibodies in PBS/Tween20 buffer for one hour at room temperature. Visualization was done by ECL kit accordining to the manufacturer's manual (GE Healthcare, Amersham; Munich, Germany).

3.4. Immunohistochemistry

3.4.1. Immunohistochemistry with Frozen Mouse Heart Tissue

Fresh frozen mice or human heart (left ventricular) tissue sections (4 µm) were mounted on object slides. After fixation in 4 % Paraformaldehyde/PBS for twenty minutes the tissues were permeabilized in 1 % Triton X-100/PBS for twenty minutes. Afterwards, the sections were washed (six times á five minutes with 1x PBS), blocked with 1x PBS containing 10 % serum (species specific respecting to the second antibody) and incubated overnight with the primary antibodies versus diverse target proteins, e.g. Calcineurin A, at diverse dilutions (normally 1 : 500). Next day, sections were washed (six times á five minutes with washing solution (see Material)) and incubated with diverse fluorescence-labeled secondary antibodies (species specific to the first antibody). Antibodies were diluted in 1x PBS containing 5 % serum (species specific respecting to the second antibody). For counter staining the nucleus, the fluorescent stain DAPI at a dilution of 1 : 5.000 was used. Negative controls were processed using only the primary, secondary or none antibody. The samples were visualized by using a confocal or fluorescent microscope and specific software.

3.4.2. Immunohistochemistry with Isolated NRCMs

Isolated NRCMs were fixed in 4 % Paraformaldehyde/PBS for 20 minutes and permeabilized in 1 % Triton X-100/1x PBS for twenty minutes. Afterwards, the sections were washed (six times á five minutes with 1x PBS), blocked with 1x PBS containing 10 % serum (species specific respecting to the second antibody) and incubated overnigth with primary antibodies versus diverse target proteins, at diverse dilutions (normally 1:500). Next day, sections were washed (six times á five minutes with washing solution (see Material)) and incubated with diverse fluorescence-labeled secondary antibodies (species specific to the first antibody). Antibodies were diluted in 1x PBS containing 5 % serum (species specific respecting to the second antibody). For counter staining the nucleus, the fluorescent stain DAPI at a dilution of 1 : 5000 was used. Negative controls were processed using only the primary, secondary or none antibody. Samples were visualized by using a confocal or fluorescent microscope and specific software.

3.5. Synthesis of Import Blocking Peptide (IBP) and Control Peptide (ctr)

The Import Blocking Peptide (IBP) and the control peptide (ctr peptide) were synthesized by Genosphere Biotechnologies (Paris, France). To improve import into cells, a hydrophobic membrane permable sequence (MPS) [163] was attached at the N-terminus (small letters in the sequences below). The IBP mimicked the amino acid sequence of Calcineuin Aβ from amino acid 172 to 183 (bold and underlined letters in the IBP sequence below) whereas the amino acid sequence of the control peptide is modified (underlined letters in the sequence below (ctr peptide)). The positive charged amino acid (position 172, 176, 178 and 182) are replaced by uncharged amino acids (alanin and tyrosine). During the experiments the final concentration of these peptides was 1.0 µM.

The amino acid sequences are:

IBP: AAVALLPAVLLALLA**KQECKIKYSERV**

ctr peptide: AAVALLPAVLLALLAAQECAIAYSEYV

3.6. Measurement of Transcriptional Activity: NFAT Reporterassay

The activity of Calcineurin was determined using a luciferase assay according to the manufacturer's protocol (Promega; Mannheim, Germany). The NFAT reporter plasmid pNP3-luci was used. It contains the Il-2 promotor in forward direction whereas the promotor in a control plasmid, pNP1-luci, is in reverse direction. The plasmids were transfected to cardiomyocytes as described above on 6-well plates. After cell treatment for twenty-four hours cells were harvested with 1 x luciferase cell culture lysis reagent (25 mM Tris phosphate (pH 7.8), 2.0 mM DTT, 2.0 mM 1,2-Diamino-cyclohexane-N,N,N´,N´-tetraacetic acid, 10 % Glycerol, 1 % Triton®X-100). After rocking the 6-well plates for ten minutes cells were harvested and centrifuged for five minutes at 8000 g. The luciferase activity was measured for ten seconds using a luminometer by adding 20.0 µl cell lysate to 100.0 µl of pre-warmed (37°C) 1 x luciferase assay reagent. During the measuring time relative light units (RLU) were measured and transformed to relative values (rel. %).

3.7. Measurement of Translational Activity: [^{3}H]-Leucine Incorporation

NRCMs were prepared as described above. On day 3, the MEM/1 was replaced by a medium containing growth stimulus Angiotensin II (AngII, 10 µmol/l) and IBP or ctr (1 µmol/l). Cells were incubated for twenty-four hours. Four hours before ending of incubation period, [^{3}H]-leucine at an activity of 2.5 µCi/ml was added. After incubation, cells were washed two times with 1x PBS, lysed with 1 % SDS and harvested. A small amount of the cell lysate (20.0 µl) was used to determine DNA concentration using the Hoechst 33258 dye. The protein was precipitated by icecold 10 % TCA (500.0 µl) for thirty minutes. After centrifugation for ten minutes at 13000 g supernatant was discarded and the remaining pellet resolved in 500.0 µl 1 % SDS. After incubation for thirty minutes at room temperature, 5.0 ml scintillation fluid was added and the amount of the incorporated [^{3}H]-marked leucine was measured in counts/ml/min (c.p.m./CPM) using a β-counter. The CPM : DNA concentration ratio was calculated for each sample. The change in protein synthesis is expressed as a percentage of the CPM : DNA concentration ration in unstimulated cells which was taken as 100 %.

3.8. Enzymatic Activity of Calcineurin A

3.8.1. Commercial CnA Kit Assay

For determination of CnA phosphatase activity, a commercial kit (CnA kit assay; Biomol; Hamburg, Germany) was used as described previously with minor modifications [164]. The RII-phosphopeptide (Biomol) was used as a specific substrate for Calcineurin (PP2B). Nonetheless the phospho group is cleaved by other competing phosphatases. Thus a few condititons have been preserved to discriminate between contributions of other phophateses. PP2B requires Ca^{2+} for its activity. For this reason "EGTA buffer" sample represents total phosphatase activity apart from PP2B. Okadaic acid ("OA") inhibits protein phosphatases 1 and 2A (PP1, PP2A) but not PP2B and PP2C. Finally, "OA + EGTA buffer" inhibits PP1, PP2A and PP2B, but not PP2C. The detection of free phosphate released from RII by Calcineurin was based on the Malachite green dye reaction at OD_{620nm}. For valuating the data, "background" was substracted from each sample and Calcineurin activity was determined as phosphate released from RII in the presence of "OA" minus phosphate released in the

presence of "OA + EGTA buffer". For a detailed description, please read user's manual (CnA Kit Assay, Biomol Cat.No. #AK-816).

3.8.2. State of Phosphorylation of NFATc2

To confirm CnA activity, the state of phosphorylation of NFAT was measured. The method was described earlier [164]. The antibody was directed against NFATc2 (Abcam; Cambrigde, UK; #ab2722).

3.9. Animal Experiments

3.9.1. Hypertrophy in Mice induced by Myocardial Infarction (Model)

3.9.1.1. Experimental Design

The protocol for left coronary artery ligation has been described previously [165]and is routinely performed in our laboratory. Mice were sacrificed two days (2 d), seven days (7 d), and one month (1 m) post infarction to analyze immediate responses. Therefore hearts were excised and the infarct size was calculated as a percentage of left ventricular surface area. Animals with less than 30 % of infarct size will be excluded from the studies, as they generally do not show typical left ventricular remodeling. Ventricles were isolated and snap frozen in liquid nitrogen using for immunohistochemistry.

3.9.1.2. Execution of Operation

After an adequate depth of anesthesia the mouse was fixed in a supine position with tape. A 5-0 ligature was placed behind the front upper incisors and pulled taut so that the neck is slightly extended. The tongue was retracted, held with forceps and a 20-G i/v catheter was inserted into the trachea. Afterwards, the catheter was attached to the mouse ventilator via the Y-shaped connector. Ventilation was performed with a tidal volume of 200.0 µl and a respiratory rate of 133 per minute. 100 % oxygen was provided to the inflow of the ventilator.

Prior to the incision, chest was disinfected with Betadine solution and 70 % ethyl alcohol. The chest cavity was opened by an incision of the left fourth intercostal space, whereby the chest retractor was applied to facilitate the view. The heart was exposed, the pericardial sac was opened and pulled apart, and the left anterior descending (LAD) artery was excavated. Ligation was proceeded with a 7-0 silk suture passed with a tapered needle underneath the LAD artery about 1-2 mm lower than the tip of the left auricle (Figure 10A). Occlusion was confirmed by pallor of the anterior wall of the left ventricle. A drop of 1 % Lidocaine was placed on the apex of the heart to prevent arrhythmia. Finally, lungs were overinflated and the chest cavity, muscles and skin were closed.

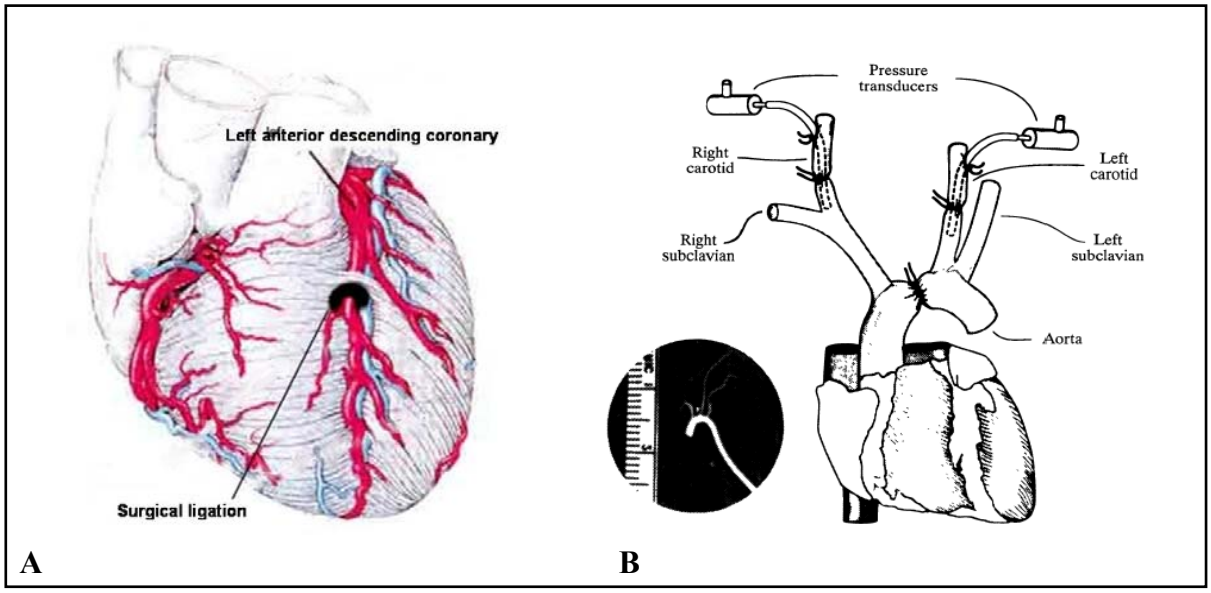

Figure 10. Induction of myocardial infarction.
Myocardial infarction (MI) was induced by surgical ligation of proximal left anterior descending coronary artery. Sham operated animals underwent the same procedure except that no ligation was performed (A) . Left ventricular pressure-overload hypertrophy in mice was induced by partial banding of the aorta. As control, a thoracotomy was performed on the sham operated mice without hemodynamic interventions (B).

3.9.2. Hypertrophy in Mice induced by Pressure Overload (Model)

Chronic pressure-overload LV hypertrophy was induced by aortic banding (AB) in wildtype (WT) mice. Aortic banding was maintained for two days, seven days and one month. Mice were anesthetized with Tribromoethanol/Amylene hydrate (Avertin; 2.5 % wt/vol, 6.0 µl/g body weight, intra peritoneal (i.p.)). A topical depilatory agent was applied to the neck and chest. Surrounding area was cleaned with Betadine and alcohol. Mice were placed supine and a horizontal skin incision 0.5-1.0 cm in length was made at the level of the suprasternal notch.

The thyroid was retracted and a 2-3 mm longitudinal cut was made in the proximal portion of the sternum. This allowed visualization of the aortic arch under low-power magnification. A wire with a snare on the end was passed under the aorta between the origin of the right innominate and left common carotid arteries. A 6-0 silk suture was snared with the wire and pulled back around the aorta. Afterwards a bent 27-gauge needle was placed next to the aortic arch and the suture was snugly tied around the needle and the aorta. After ligation, the needle was quickly removed, the skin was closed and mice were allowed to recover on a warming pad until they were fully awake. The sham procedure was identical except the aorta was not ligated (Figure 10B).

3.10. Statistics

All data are presented as mean ± SEM. Statistical analyses are performed using the Student´s *t*-Test. Significances are assigned for a value of $p < 0.05$ as (*) and for $p < 0.01$ as (**). Non-significant differences are expressed as n.s.

4. Results

4.1. Calcineurin Mutants

After targeted proteolysis of Calcineurin by Calpain it was seen that this constitutive active form was not able to leave the nucleus, regardless of which pathway – by passive or active transport or even by itself. The phosphatase remained nuclear. According to this observations an important sequence in the truncated C-terminal region, which remained cytosolic after proteolysis, was presumed. Sequences responsible for nuclear export (so-called nuclear export sequences or signals (NESs)) are recognized by so-called exportins. Based on this knowledge five mutants lacking parts of the C-terminus were generated. The truncation was started at the C-terminus bit by bit (around twenty amino acids) to the cleavage site of Calpain at amino acid 423 of CnA. First transfection studies with these mutants demonstrated, that only the mutatnts CnAβ(1-425) and (1-415) were contineously nuclear. On that account two internal CnAβ mutants were generated (CnAβ(Δ420-434) and (Δ420-445). Additionally, a NES database was used for predicting a potential NES. This results are shown in 4.5.
Following these results, also a nuclear localization sequence/signal (NLS) was presumed in Calcineurin. It was known, that only activated Calcineurin was localized nuclear. Based on this information, the NLS was assumed to be localized next to the phosphatase pattern. This pattern is masked by the autoinhibitory domain. After activation, regardless of which activation pathway, the pattern is demasked and the nuclar import is possible. To identify the specific NLS for CnA, a NLS motif research by using known NLSs of diverse proteins was done. Additionally, diverse FLAG-tagged mutants, lacking the potential NLS region, were used for transfection experiments. Finally, a mutant consisting only of the potential NLS region downstream of the EGFP-tag, was generated.

4.1.1. EGFP-tagged Calcineurin Aβ Mutants

Based on the strategy as described in 3.1. the following Calcineurin Aβ mutants were generated, whereby each mutant contains a N-terminal EGFP-tag. The mutants are: CnAβ(1-525), (1-505), (1-485), (1-465), (1-445), (1-425), (1-415), (171-190), (Δ420-434) and (Δ420-445) (Figure 11).

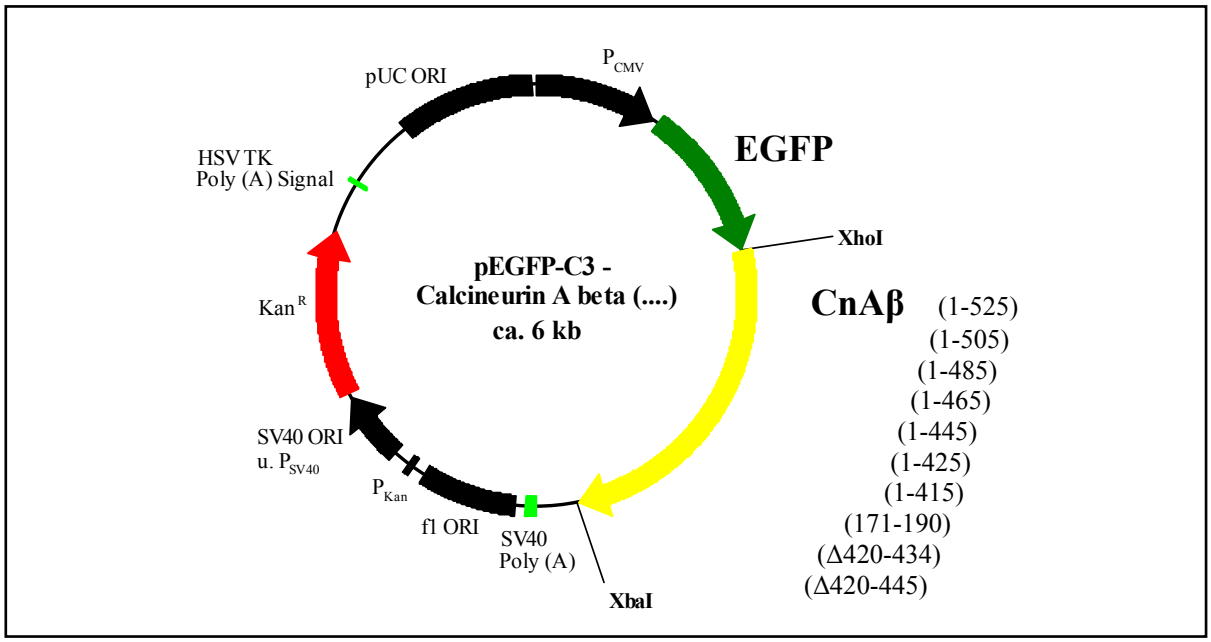

Figure 11. Generation of Calcineurin Aβ mutants.
All mutants were cloned into the XhoI and XbaI sites of pEGFP-C3 (BD Bioscience). In that way the EGFP-tag is localized N-terminal of each construct. All potential clones were tested by PCR with the MCS primer of pEGFP-C3 (MCS1pEGFP and MCS2pEGFP).

4.1.2. FLAG-tagged Calcineurin Aα Mutants

The four FLAG-tagged Calcineurin Aα mutants were kindly provided by Mamta H. Buch (Division of Cardiology, The University of Manchester; Manchester, UK).

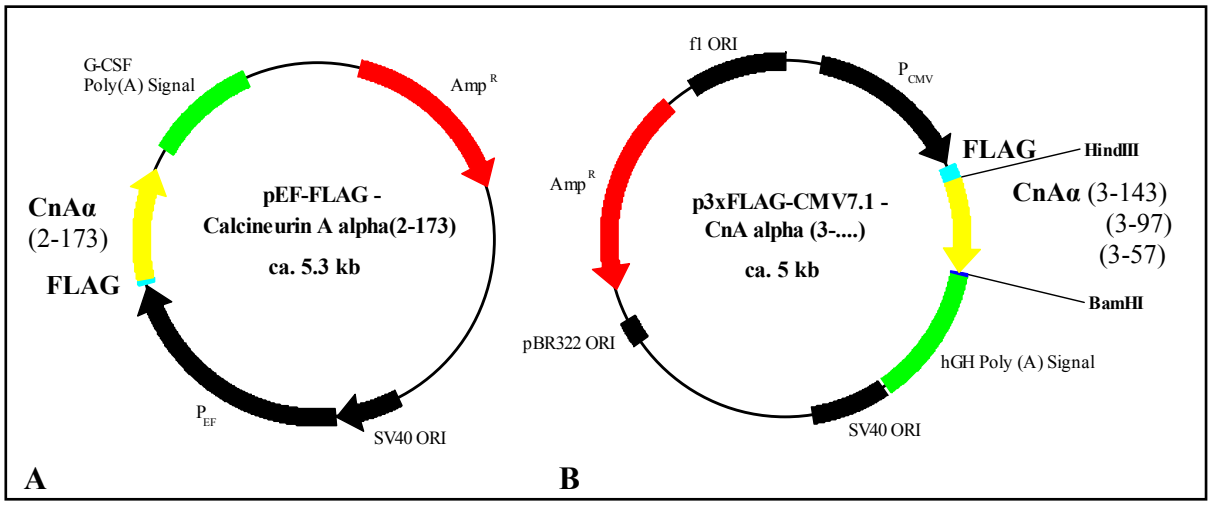

Figure 12. Generation of Calcineurin Aα mutants.
FLAG-tagged CnAα(2-173) (A) and FLAG-tagged CnAα(3-143), (3-97) and (3-57) (B) were kindly provided by Mamta H. Buch (Division of Cardiology, The University of Manchester; Manchester, UK).

4.1.3. Linear Demonstration of all Calcineurin Mutants

For better understanding all Calcineurin mutants are demonstrated linear. All characteristic domains are marked in colour. In Figure 13A the CnAβ mutants are drawn, whereas the CnAα mutants are illustrated in Figure 13B.

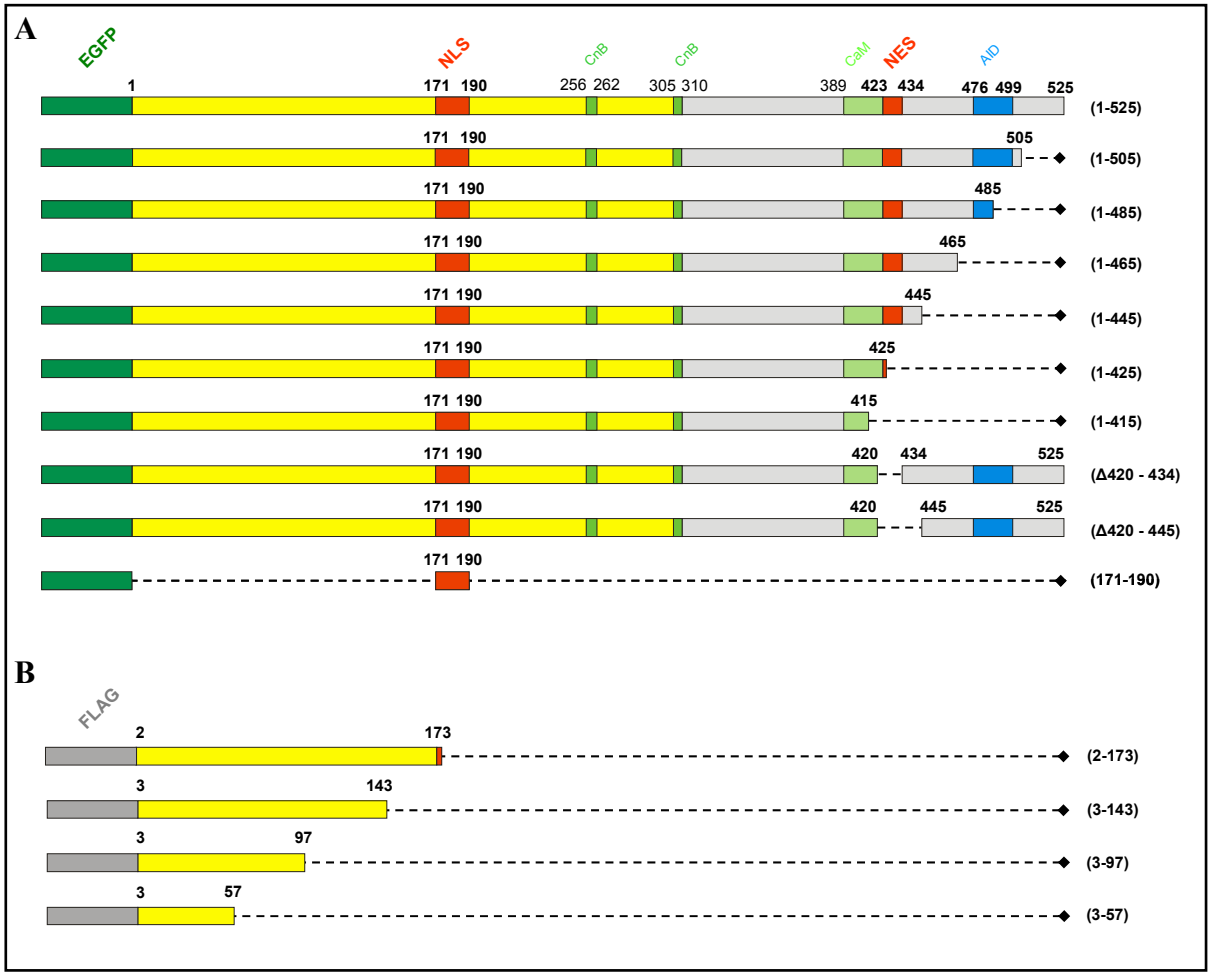

Figure 13. Linear drawing of Calcineurin A mutants.
EGFP- (A) and FLAG-tagged (B) Calcineurin A mutants. Important domains are marked in colour and clearly localized by amino acid positions. The potential NLS and NES are red coloured for better orientation.

EGFP: enhanced green fluorescent protein; NLS: nuclear localization sequence; NES: nuclear export sequence; CnB: CnB binding site; CaM: CaM binding site; AID: autoinhibitory domain

4.2. Nuclear Translocation of Calcineurin (*in vivo*)

Recently it could be identified that posttranslational modification, specifically proteolysis of the autoinhibitory domain (AID), leads to activation of Calcineurin and its strong nuclear translocation. The Calpain-mediated cleavage of the C-terminal AID and the causative link to myocardial tissue. In this work, the nuclear translocation of Calcineurin is demonstrated both in rodent (Figure 14) and in human myocardium (Figure 15).

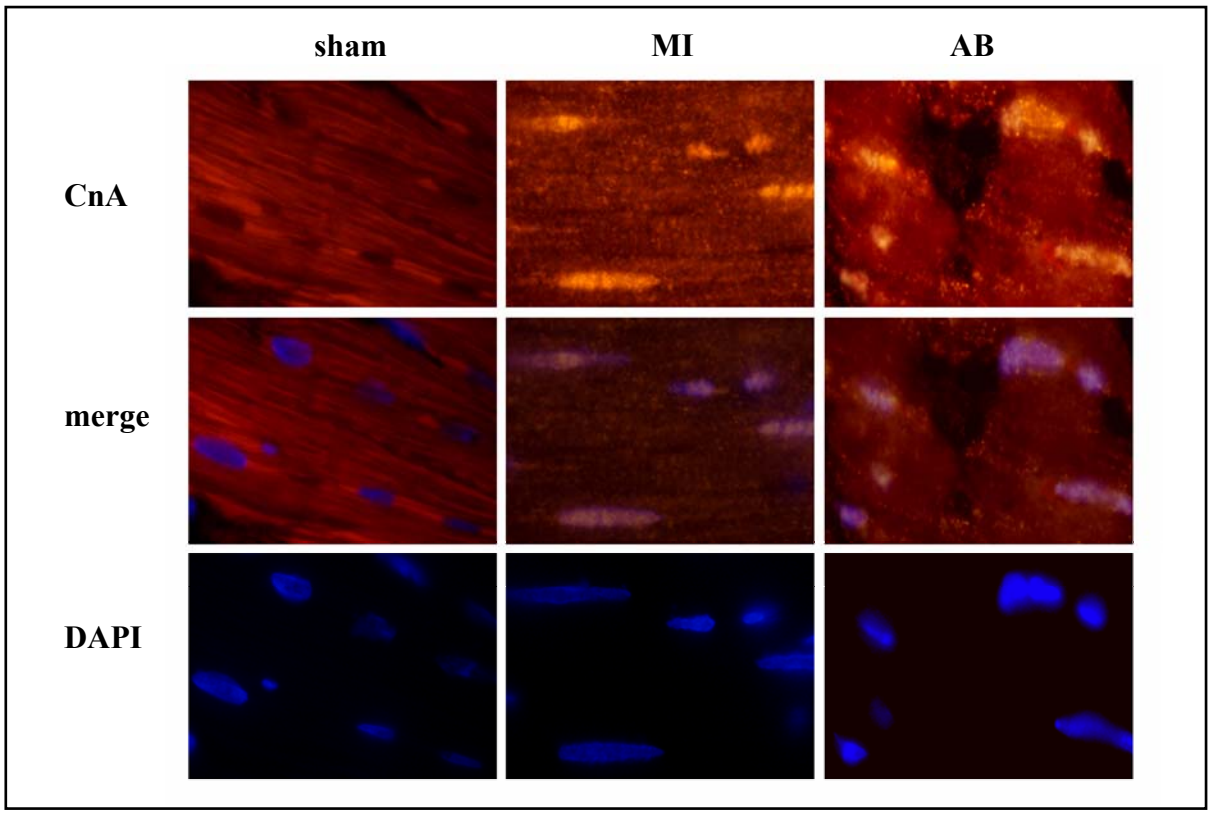

Figure 14. Nuclear translocation of Calcineurin A in the myocardium of different animal models of myocardial disease. (Hallhuber M, 2006.)
Myocardial hypertrophy was induced by subjecting rats to myocardial infarction (MI) or aortic banding (AB). Four weeks post procedure, a predominantely nuclear localization of Calcineurin A was observed in both models of cardiac stress compared to sham operated rats. Antibodies were directed against catalytic domain of CnA. Merged pictures indicate overlay of nuclear (DAPI (binds specific DNA)) and Calcineurin staining.

In sham operated wildtype rats (sham), there was a predominant cytosolic distribution of CnA, whereas in rats which underwent aortic banding (AB) or myocardial infarction (MI) a strong nuclear localization of CnA was observed (Figure 14). After four weeks the nuclear localization in the hypertrophied myocardium is distinct. But already after two days similar changes within the subcellular distribution was seen. The nuclear accumulation of Calcineurin was observed in 82 ± 13 % ($p < 0.01$) of cardiomyocytes in pathological myocardial

hypertrophy. In contrast, nuclear Calcineurin was not observed in normal myocardium. For evaluation, more than one hundred cells of six animals per group were counted.

Furthermore, also the subcellular CnA localization on histological sections of human normal hearts (n=4) and diseased human myocardium from patients with coronary artery disease (CAD; n=3), hypertrophic cardiomyopathy (HCM; n=9), and aortic stenosis (AS; n=7) were investigated. Patients with HCM and AS had maintained systolic function but marked left ventricular hypertrophy with diastolic dysfunction. Patients with CAD had systolic heart failure. In normal heart, there was homogeneous cytosolic distribution of CnA. In all patient groups, there was a marked increase in nuclear localization of CnA, whereby only the sections of CAD are shown (Figure 15). About 70 % of cardiomyocytes in diseased heart displayed an increase in nuclear CnA with no difference between the AS, HCM or CAD group.

Hearts were a great gift from Prof. Dr. P. E. Lange (Deutsches Herzzentrum Berlin (DHZB); Berlin, Germany; normal heart and coronary artery disease (CAD)) and from Prof. Dr. H.Schulte (Uniklinikum Düsseldorf; Düsseldorf, Germany; aortic stenosis (AS) and hypertrophic cardiomyopathy (HCM)).

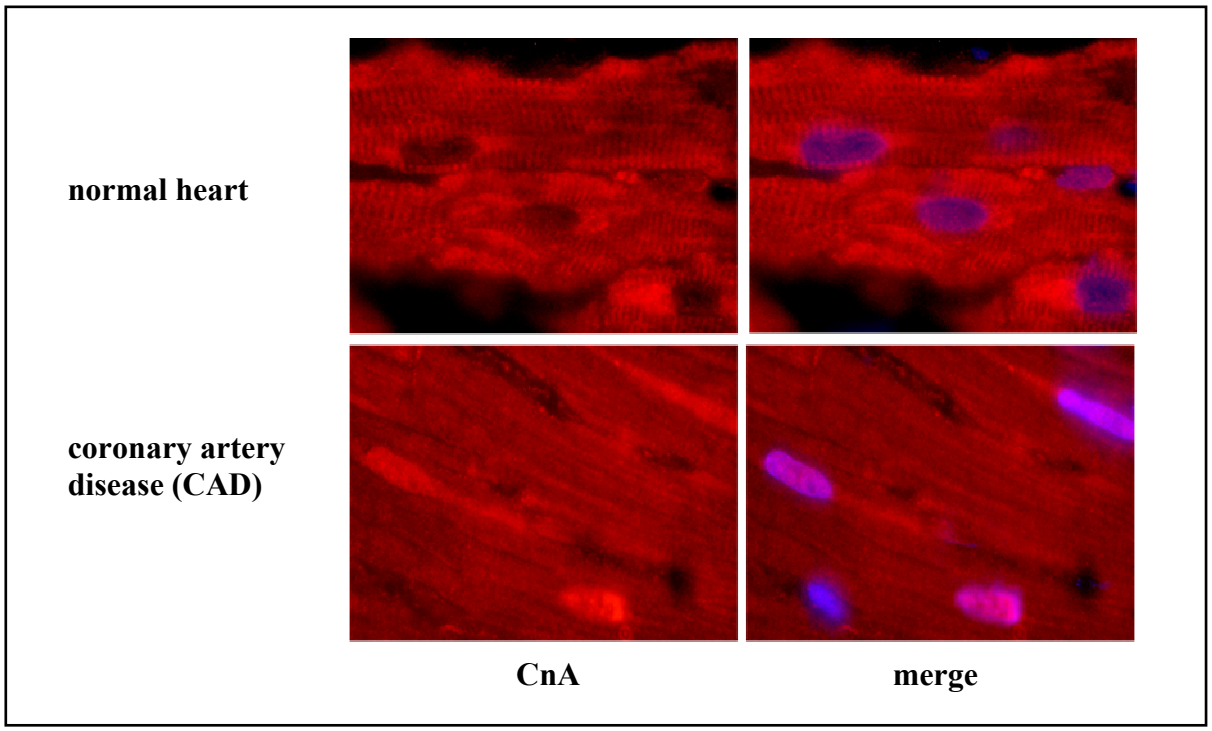

Figure 15. Nuclear translocation of Calcineurin A in human myocardium with coronary artery disease. Representative immunohistochemical staining of cardiomyocytes from normal human heart and failing human myocardium (from underlying coronary artery disease). In normal heart, no CnA could be detected in the nucleus. In human myocardium with coronary artery disease (CAD), nuclear enrichment of CnA was clearly demonstrated. Antibodies were directed against catalytic domain of CnA. Merged pictures show superposition of CnA staining and nuclear staining (DAPI).

4.3. Subcellular Localization of EGFP-tagged Calcineurin Aβ(1-525) during Angiotensin II Stimulation in NRCMs

To assess whether CnA import into the nucleus is a chronic phenomenon or an acute response to a myocardial insult, the time course of CnA shuttling was investigated. A plasmid encoding EGFP-tagged full-length CnAβ (CnAβ(1-525)) was transfected into neonatal rat cardiomyocytes (NRCMs). Cells were stimulated with Angiotensin II (AngII, 10.0 µM). Confocal microscopy revealed onset of nuclear translocation of Calcineurin after two hours. After four hours of AngII stimulation, CnA was predominantly nuclear. After six hours, maximum of intensity of the EGFP-Calcineurin signal was seen in the nucleus (Figure 16A). A nuclear accumulation of Calcineurin was observed in over 90 % of transfected cardiomyocytes. Similarly, two hours after removal of AngII from the medium, CnA was homogenously distributed in the cytosol and the nucleus, whereby after four hours CnA was localized in the perinuclear region. Six hours after removal of the stimulus, CnA was localized completely in the cytosol again (Figure 16B).

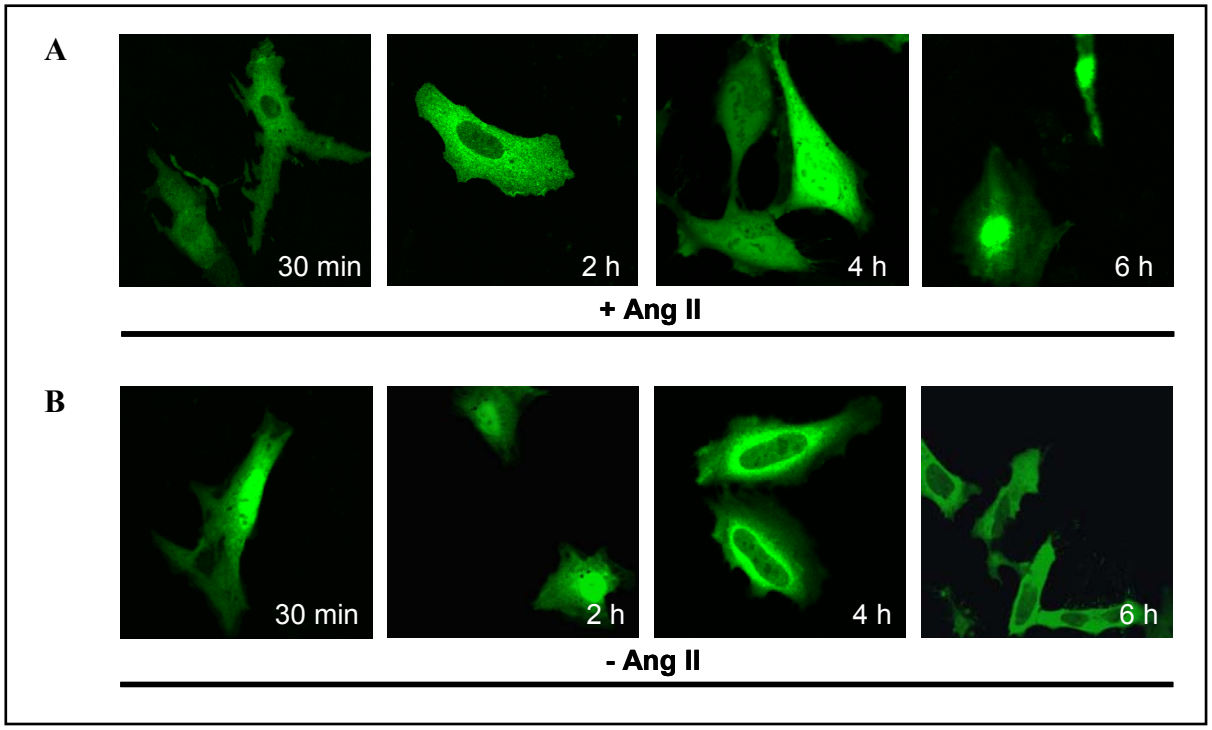

Figure 16. Time course of EGFP-CnA import and export in Angiotensin II stimulated NRCMs.
Cardiomyocytes were transfected with EGFP-tagged CnAβ(1-525) and stimulated with Angiotensin II (AngII, 10.0 µM). After four hours of stimulation, there was predominantly nuclear localization of CnA in approximately 90 % of transfected cells (A). After removal of the stimulus, CnA moved back to cytosol within four hours. All experiments were performed in the presence of the Calpain inhibitor Calpeptin (10.0 µM) to prevent proteolysis of the CnA autoinhibitory domain, which would leave CnA constitutively nuclear.

To protect CnA from Calpain-mediated proteolysis, which would cause a constitutive activation of CnA and therefore a persistent nuclear translocation, all experiments were performed in the presence of the membrane permeable Calpain inhibitor Calpeptin (10.0 μM).

4.4. Identification of a Nuclear Localization Sequence and the Corresponding Importin

To define the regions of Calcineurin that are required for nuclear import different EGFP- and FLAG-tagged Calcineurin mutants (see Figure 13) were screened to assess for those that entered the nucleus and those that remained cytosolic. In general, deletion of the auto-inhibitory domain (AID) led to nuclear translocation and deletion of the region starting with amino acid 171 (within the putative NLS) prevented Calcineurin from entering the nucleus.

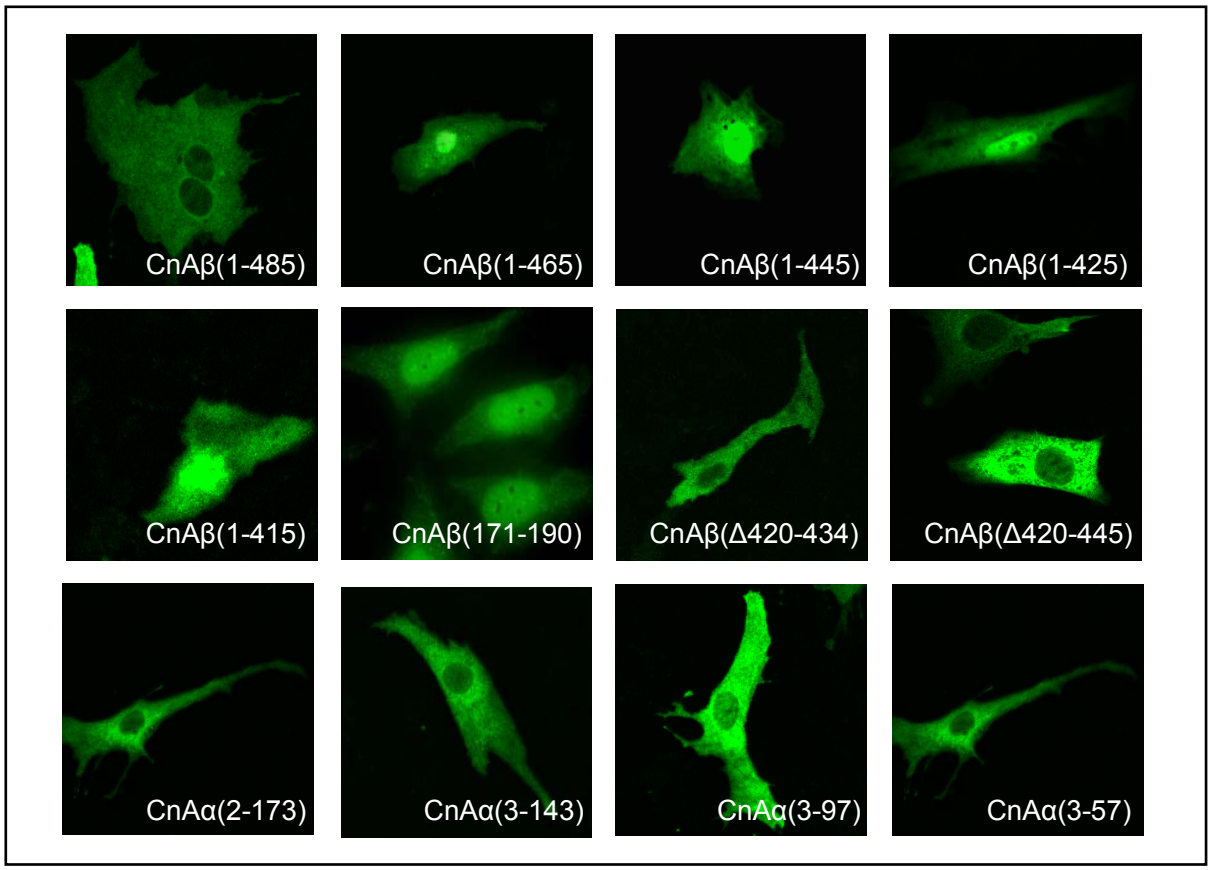

Figure 17. Subcellular localization of Calcineurin mutants in NRCMs.
Deletion of the autoinhibitory domain and presence of a putative NLS were crucial for nuclear import. Fusion of the NLS (amino acid 171 to 190 of CnAβ) to EGFP demonstrated the capability of this region for entrance to the nucleus.

Sequence comparisons with known NLSs of diverse proteins enabeled further delineation of the putative NLS region to the sequence from amino acid 171 to 190 of CnAβ. Fusion of this fragment, amino acid 171 to 190, to the EGFP backbone resulted in translocation of the EGFP-NLS fusion protein (CnAβ(171-190)) into the nucleus, whereas the pure EGFP backbone (pEGFP-C3) remained cytosolic. Although full-length CnA (CnAβ(1-525)) resided in the cytosol, it was translocated into the nucleus after AngII stimulation attributable to uncovering of the catalytic subunit and probably of the putative NLS. In contrast, CnAα(2-173) and CnAα(3-143), both lacking the putative NLS, remained exclusively cytosolic despite AngII stimulation (Figure 18). The same subcellular localization was seen for the mutants CnAα(3-97) and CnAα(3-57) (data not shown).

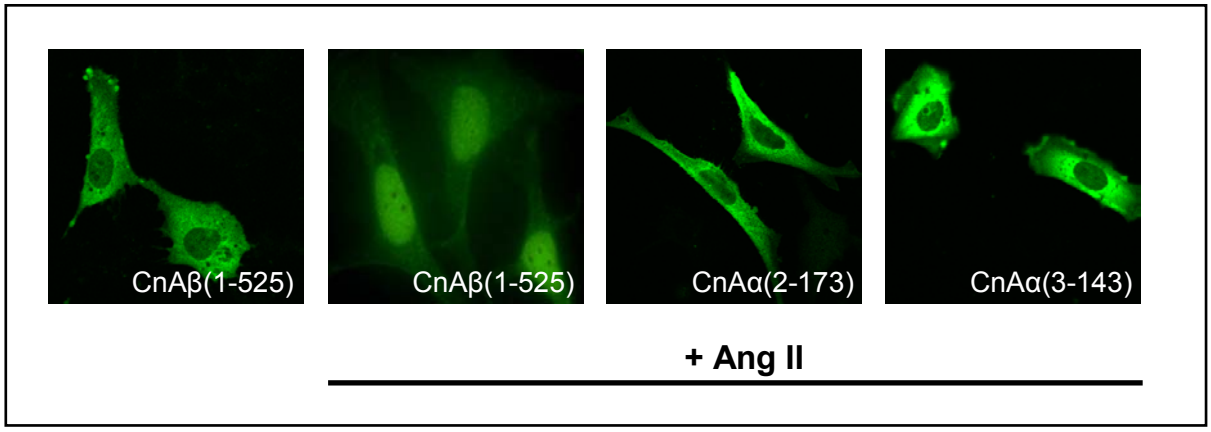

Figure 18. Subcellular localization of Calcineurin mutants, lacking the potential NLS, in Angiotensin II stimulated NRCMs.
After Angiotensin II (AngII, 10.0 µM) stimulation of cardiomyocytes, transfected with CnAβ(1-525), Calcineurin was translocated into the nucleus, whereas deletion mutants lacking the potential NLS (region of amino acid from 171 to 190) were not able to enter the nucleus despite stimulation. Subcellular distribuation of CnAα(2-173) and CnAα(3-143), representing NLS deletion mutants, is shown.

Importinβ$_1$ has been shown to bind the nonclassical NLS of different cargo proteins [93]. Interactions between the CnA mutants and Importinβ$_1$ were therefore assessed to determine whether the functionally defined NLS physically interacts with Importinβ$_1$. As demonstrated by co-immunoprecipitations, Importinβ$_1$ binds to full-length Calcineurin (CnAβ(1-525)). Furthermore, this importin also binds to Calcineurin mutants CnAβ(1-415) and CnAβ(1-445) respectively. During the co-immunoprecipitation an antibody against Importinβ$_1$ was used for precipitation, whereas the antibody versus EGFP was used during Western blotting (Figure 19). To demonstrate further that the identified NLS in Calcineurin is essential for the nuclear import of Calcineurin, a peptide competition assay was used to prevent the CnA/Importinβ$_1$ interaction. A peptide containing the putative NLS sequence of Calcineurin (AAVALLPAVLAALAA **KQECKIKYSERV**) was synthesized and added to the medium. In

control experiments, a nonsense peptide (control peptide, ctr) (AAVALLPAVLAALAA AQECAIAYSEYV) was used. Noninvasive cellular import of synthetic peptides can be accomplished by incorporating a hydrophobic, membrane permeable sequence (MPS). In this case the MPS was added to each functional peptide by stepwise synthesis, thus creating cell permeable peptides with hydrophobic (small letters in the shown sequence of the used peptides) and functional (underlined letters in the shown sequence) sequences linked by a normal peptide bond. The used hydrophobic sequence derived from the signal sequences of Kaposi´s fibroblast growth factor and was used in other groups successfully [163,166]. Addition of the synthetic peptide IBP (1.0 μM) saturated the binding domain of Importinβ$_1$ for CnA and thereby prevented CnA binding to Importinβ$_1$.

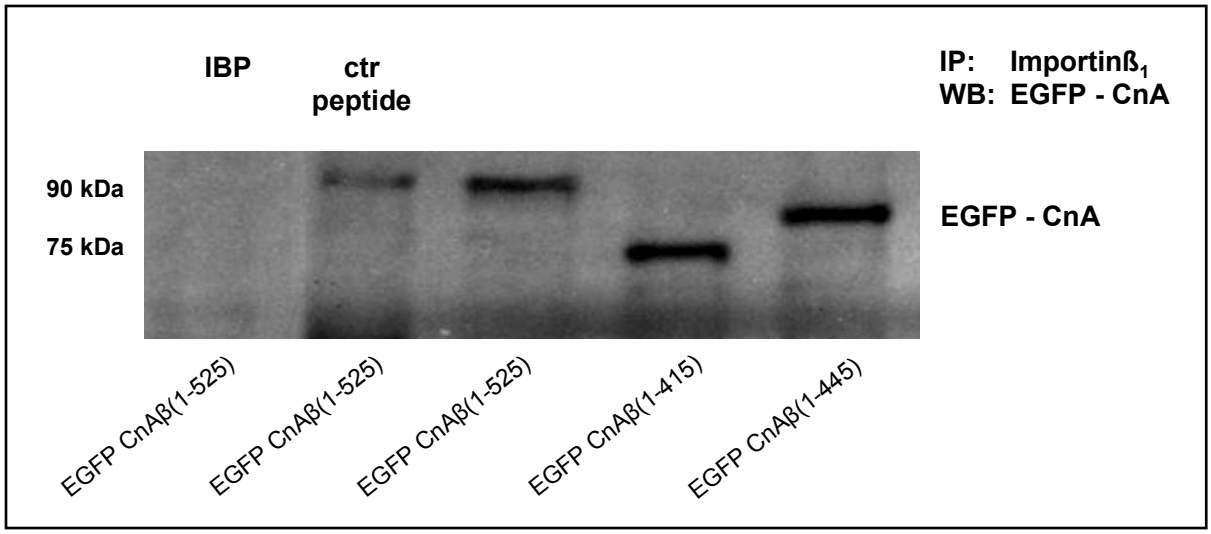

Figure 19. Co-immunoprecipitation: Interaction of Calcineurin A with Importinβ$_1$.
To investigate the interaction of Calcineurin A with Importinβ$_1$, HeLa cells were transfected with EGFP-tagged CnA mutants CnAβ(1-525), CnAβ(1-415) and CnAβ(1-445). Immunoprecipitation of CnA/Importin complexes was performed with an anti-Importinβ$_1$ antibody, whereas the detection of EGFP-tagged Calcineurin mutants was done by using an antibody versus GFP-tag. The full length CnA (CnAβ(1-525)) interacted with Importinβ$_1$, as evidenced by their Co-IP. Addition of the synthetic peptide IBP (1.0 μM) abrogated the interaction between CnA and its importin. The control peptide (ctr peptide) did not impair this interaction. Additionally the Co-IP was repeated with two other CnA mutants. Like full length CnA, both showed interaction with Importinβ$_1$.
IBP: Import Blocking Peptide; ctr peptide: Control peptide; IP: Immunoprecipitation; WB: Western blotting

Specifically, the interaction domain was mapped to the region of amino acid 171 to 190 as evidenced by the ability of the blocking peptide IBP to abbolish the interaction between CnA and Importinβ$_1$ completely. These data indicate that the NLS identified by functional analyses also mediates physical interactions between CnA and Importinβ$_1$ (Figure 19). Inhibition of this interaction suppressed nuclear import of a constitutively active CnA mutant (CnAβ(1-525)). The noninhibitory peptide (ctr peptide; (1.0 μM)) did not interfere with the CnA/Importinβ$_1$ interaction.

To confirm the results of co-immunoprecipitations the inhibitory effect of IBP was observed in NRCMs by analyzing the subcellular distribution of EGFP-tagged Calcineurin. After transfection with full-length Calcineurin (CnAβ(1-525)), cells were stimulated with AngII (10.0 µM) or with the α-adrenergic receptor agonist Phenylephrine (PE, 10.0 µM). Additionally, stimulated cells were treated either with IBP (1.0 µM) or control peptide (ctr peptide, 1.0 µM). Compared to only AngII stimulated cells without any peptide, cells treated with IBP showed no nuclear localization of EGFP-tagged CnAβ(1-525). The import was prevented. This effect was not seen in AngII stimulated cells treated with ctr peptide (Figure 20).

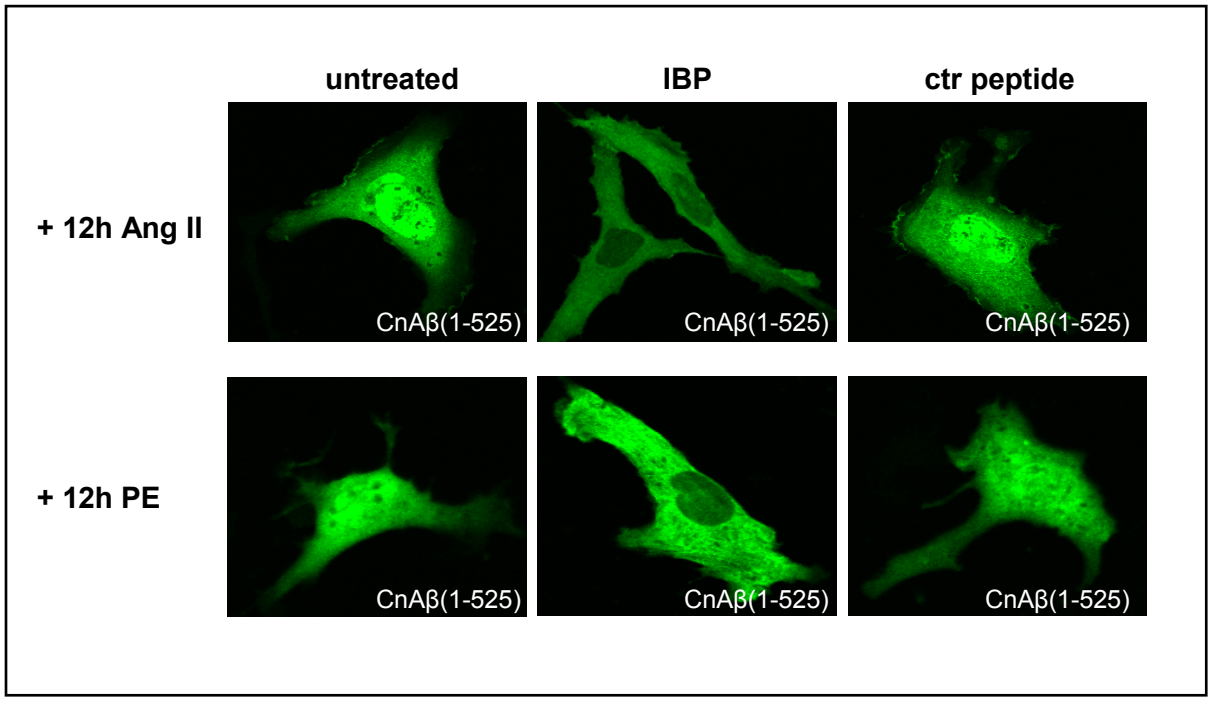

Figure 20. Subcellular localization of CnAβ(1-525): the inhibitory effect of IBP.
Inhibition of CnA/importin interaction prevented nuclear import of Calcineurin in NRCMs. A synthetic peptide corresponding to the putative NLS of Calcineurin was added to the medium (1.0 µM) to saturate the importin binding sites for CnA. This saturation resulted in inhibition of nuclear import of CnA(1-525). In contrast, treatment with the noninhibitory control peptide (1.0 µM) did not affect nuclear import of CnA(1-525). NRCMs were stimulated either with AngII (10.0 µM) or PE (10.0 µM).

IBP: Import Blocking Peptide; ctr peptide: control peptide; AngII: Angiotensin II; PE: Phenylephrine

Neonatal rat cardiomyocytes were also transfected with other Calcineurin mutants. Mutants containing the NLS showed identical subcellular localization. IBP showed no effect on mutants lacking the NLS (data not shown).

4.5. Detection of a Nuclear Export Sequence and the Corresponding Exportin

To screen the Calcineurin sequence for potential nuclear export sequences the NetNES 1.1 server was used. The NES predictor (Net NES) is made available for general use at (http://www.cbs.dtu.dk/). The creators employed both neural networks and hidden Markov models in the prediction algorithm and verify the method on the most recently discovered NESs [167-169]. This programm predicts leucine-rich NESs in eukaryotic proteins. The CnAβ sequence form amino acid 411 to 525 was used as input. Within this C-terminal region of CnAβ, a typical NES was predicted between the amino acids 420 and 445. The exact position was localized from amino acid 423 to 433. Two internal CnAβ mutants, lacking the potential NES, were generated, because it was not definitely clear, if the leucine residues upstream amino acid 433 play an important role within the nuclear export, although it was not predicted to be part of the NES.

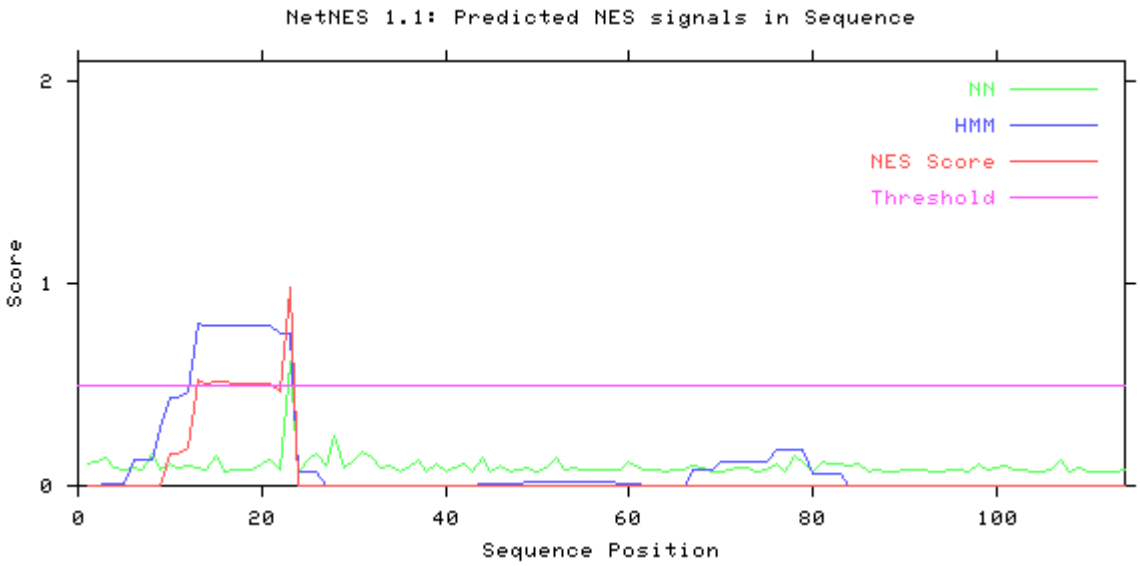

predicted leucine rich NES: from 423 to 433 (**red** coloured)

input: sequence of CnAβ (amino acid 411-525; signed as 1-115)

RAIGKMARVFSV**LREESESVLTL**KGLTPTGMLPSGVLAG
GRQTLQSATVEAIEAEKAIRGFSPPHRICSFEEAKGLDRINE
RMPPRKDAVQQDGFNSLNTAHATENHGTGNHTAQ*

Figure 21. Prediction of a nuclear export sequence (NES) within the Calcineurin sequence.
Using the sequence from amino acid 411 to 525 of Calcineurin Aβ as input for the NetNES 1.1 server, a leucine rich nuclear export sequence was predicted from amino acid 423 to 433. This sequence could be responsible for the nuclear export of Calcineurin.

To exactly identify the sequence in CnA that controls nuclear export, serial carboxy-terminally truncated CnA mutants with an N-terminal EGFP-tag were genereated (Figure 13) and examined by confocal microscopy (Figure 22).

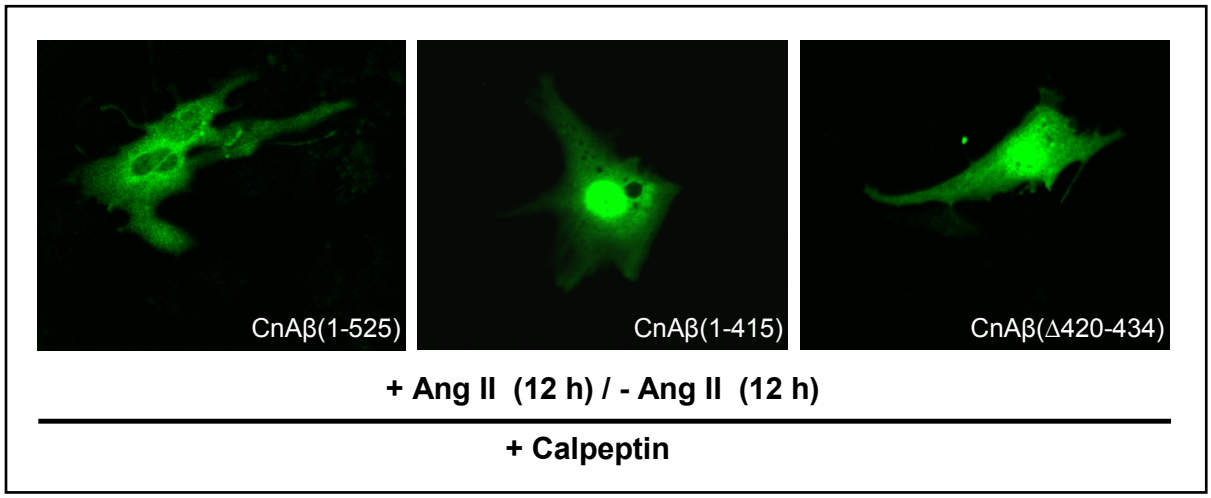

Figure 22. Nuclear export sequence (NES) within the Calcineurin sequence.
NRCMs were transfected with different EGFP-tagged CnA mutants (see Figure 13). After stimulating cells (Angiotensin II (AngII) 10.0 µM) for twelve hours (to promote nuclear import), stimulus was subsequently removed for twelve hours. Throughout Calpeptin was present to prevent proteolysis of the AID. A truncated deletion mutant lacking the C-terminal part of CnA (CnAβ(1-415)) was not able to leave the nucleus. The mutant with targeted disruption of the NES showed identical subcellular localization - export was impossible.

Experiments were performed in the presence of a specific Calpain inhibitor, called Calpeptin, to prevent Calpain-induced cleavage of the autoinhibitory domain (AID) and to ensure fractional integrity of Calcineurin. Cells were stimulated with AngII for twelve hours to achieve nuclear entry of CnA, followed by removal of the stimulus to promote nuclear export. Full-length CnA (CnAβ(1-525)) was re-localized exclusively to the cytosol of transfected cardiomyocytes after removal of the stimulus. An extended deletion mutant (CnAβ(1-415)) was not able to leave the nucleus any more (Figure 22). These results suggest that sequences in the region downstream of amino acid 415 regulate nuclear export. Consistent with these findings and sequence comparisons with known NES sites, two internal deletion CnA mutants were generated – CnAβ(Δ420-434) and CnAβ(Δ420-445). Both were lacking the region 423 to 433 and both remained exclusively nuclear after removal of the stimulus. Inhibition of Calpain did not influence this result as the Calpain cleavage site (at aa 424) was deleted in these mutation variants (Figure 22). Two internal deletion CnA mutants were generated for analyzing the importance of the flanking region downstream the sequence KGLTPTGMLPS, containing a similar pattern to the predicted NES. Transfection of both mutants showed no difference. According to these experiments it was clear, that the NES is localized at 423 to 433 and the flanking region is not essential for nuclear export.

To address whether CnA nuclear export is mediated by the export protein CRM1, experiments using the CRM1-specific inhibitor, Leptomycin B (LMB), were performed. Agonist-dependent nuclear import of full-lenght CnA was achieved by AngII stimulation. Calpeptin was added to prevent proteolysis of CnA. The addition of LMB, to prevent CRM1-mediated export, suppressed nuclear export of CnA. Interestingly, LMB alone resulted in nuclear accumulation of Calcineurin after forty-eight hours. There is, of course, a continous shuttling of Calcineurin across the nuclear membrane even under basal conditions. This support the hypothesis that nucleocytoplasmic shuttling of CnA is coupled to an NES localized within the region containing amino acid 423 to 434 and is mediated by CRM1 (Figure 23).

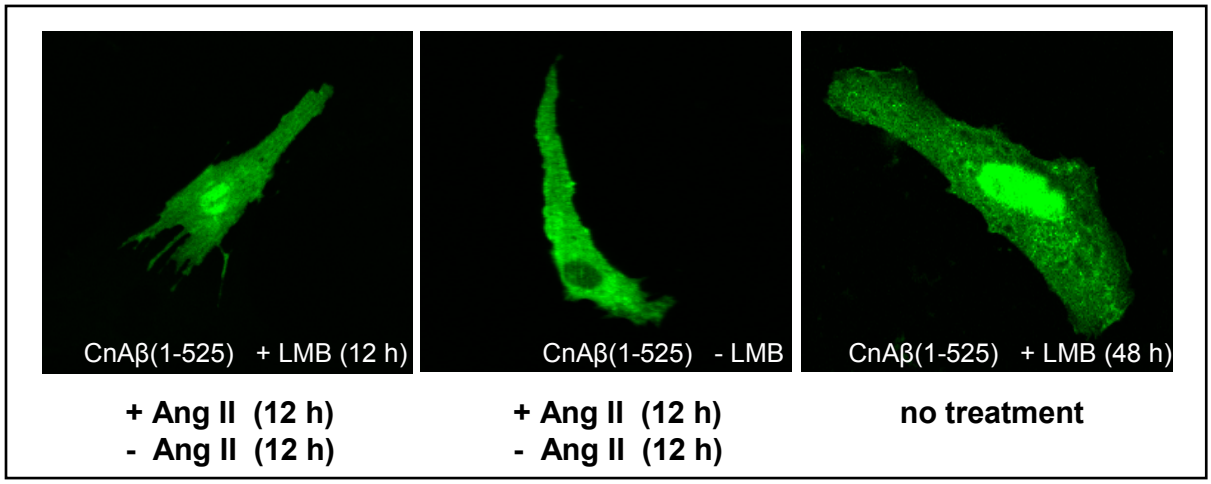

Figure 23. CRM1 mediated export of Calcineurin.
CRM1 mediates nuclear export of CnA. EGFP-tagged CnAβ(1-525) remained nuclear even when the hypertrophic stimulus (Angiotensin II (AngII), 10.0 μM) was removed. Without additional treatment, Leptomycin B (LMB) alone caused nuclear accumulation of CnA after forty-eight hours, indicating permanent shuttling of CnA across the nuclear membrane.

In vivo studies of pathological myocardial hypertrophy showed that proteolysis of the Calcineurin autoinhibitory domain at amino acid 424 results in a constitutively active Calcineurin mutant lacking both the AID (amino acid from 468 to 490) and the NES (amino acid from 423 to 433). To determine whether loss of the AID or disruption of the NES is responsible for strong nuclear accumulation of CnA, the nuclear import and export qualities of an EGFP-tagged CnA mutant with the deletion of the NES, CnAβ(Δ420-434), was investigated. In this case Calcineurin resided in the cytosol. Stimulation of transfected cells with AngII resulted in subsequent translocation of CnA into the nucleus. Based on these results, it is concluded that the AID not only blocks the catalytic activity of CnA but also masks the NLS. Removal of the AID via a conformational change in Calcineurin following Ca^{2+} activation or by proteolysis of the AID leads to exposure of the NLS and resultant

nuclear translocation of CnA. Subsequent removal of the stimulus resulted in a nuclear localization of the CnA(Δ420-434) mutant, as the lack of the NES made it possible for CRM1 to interact with CnA and to transport it back to the cytosol (Figure 24). Loss of the C-terminal part of CnA would, therefore, appear to regulate nuclear shuttling of CnA at the level of both nuclear import and export. Deprivation of the AID promotes import via Importinβ$_1$ and loss of the NES hinders nuclear export via CRM1 mediated mechanism.

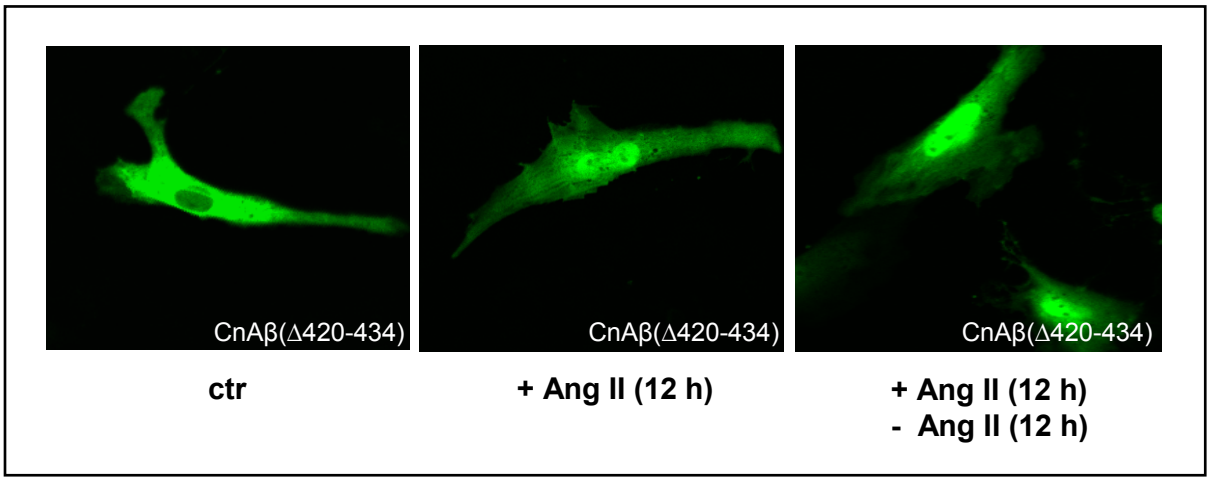

Figure 24. Relative importance of the NES for nuclear export of Calcineurin.
To investigate the relative importance of the NES for nuclear export, an EGFP-tagged CnA mutant with targeted disruption of the NES region was transfected into NRCMs. In resting conditions, the deletion mutant resided in the cytosol. Stimulation (Angiotensin II (AngII), 10.0 µM) resulted in nuclear translocation. After removal of the stimulus CnAβ(Δ420-434) remained nuclear, confirming the necessity of the NES for Calcineurin export.

4.6. Inhibition of Myocardial Hypertrophy by IBP (Import Blocking Peptide)

To analyze the effect of the Import Blocking Peptide (IBP), the phosphatase activity of CnA, transcriptional activity, translational activity (protein synthesis), cell size and markers of myocardial hypertrophy in response to the peptide-related inhibition of CnA nuclear import was examined. Additionally, concentration-related dependence and the toxicity of IBP was analyzed.

Phosphatase activity was assessed using a specific substrate (RII) for CnA [164]. NRCMs were stimulated with AngII (10.0 µM) and the CnA phosphatase activity was measured in the presence of IBP (1.0 µM) or a control peptide (ctr peptide; 1.0 µM). Total CnA phosphatase activity was not affected by inhibition of the access of Importinβ$_1$ to the CnA NLS (298 ± 9 % versus 270 ± 11 %; n = 8; p = n.s.; Figure 25A). Additionally, NFATc2 phosphorylation

status was assessed, because NFAT is the physiological substrate for Calcineurin. In cells that were stimulated with AngII (10.0 µM) there was an increase in dephosphorylated NFATc2 (120 kDa) compared to control cells. Addition of IBP had no significant effect on NFATc2 dephosphorylation. This indicates that IBP had no impact on phosphatase activity of Calcineurin (Figure 25B).

In contrast to unaffected phosphatase activity of CnA, transcriptional activity of the CnA/NFAT signaling pathway was decreased significantly by IBP in cardiomyocytes stimulated with AngII (10.0 µM) (227 ± 11 % versus 133 ± 8 %; n = 8; $p < 0.05$) or with PE (10.0 µM) (189 ± 10 % versus 91 ± 7 %; n = 8; $P < 0.05$). To analyze the transcriptional activity the so-called NFAT reporterassay was used (Figure 26A). Similarly, myocardial hypertrophy, as evidenced by protein synthesis (translational activity), was suppressed by the blocking peptide IBP (159 ± 9 % versus 111 ± 11 %; n = 8; $p < 0.05$; Figure 26B).

To further investigate the inhibitory effect of IBP, the cell size of cardiomyocytes and the expression of Brain natriuretic peptide (BNP), as a molecular marker of myocardial hypertrophy was measured. The cell size of stimulated cardiomyocytes was suppressed by using IBP (1.0 µM) (1180 ± 91 μm^2 versus 744 ± 65 μm^2; n = 25; $p < 0.05$), whereas the cell growth could not be reduced by the control peptide (1.0 µM) (Figure 27A). In cardiomyocytes, stimulated with AngII (10.0 µM) to induce myocardial hypertrophy, the IBP significantly reduced the expression of BNP (163 ± 11 % versus 88 ± 8 %; n = 8; $p < 0.05$) (Figure 27B). Finally, the dose-dependence of IBP and the toxicity was analyzed. For analyzing dose-dependence, the transcriptional activity was measured for AngII (10.0 µM) stimulated cardiomyocytes at different concentrations of IBP. Stimulated NRCMs showed first significant inhibitory effects at a concentration of 1.0 µM IBP. The differences at concentrations of 500.0 and 750.0 nM were not significant. The best inhibitory effect was assumed for 10.0 µM, whereas the effect at 50.0 µM could not be related clearly to the inhibitory effect of IBP (Figure 28A). According to the [^{3}H]-leucine incorporation for AngII stimulated NRCMs there were no signals for protein synthesis level at a concentration of 100.0 µM of each IBP and ctr peptide (Figure 28B). This concentration was toxic for cells. Thus, the great inhibitory effect at 50.0 µM is assumed to be a toxic effect.

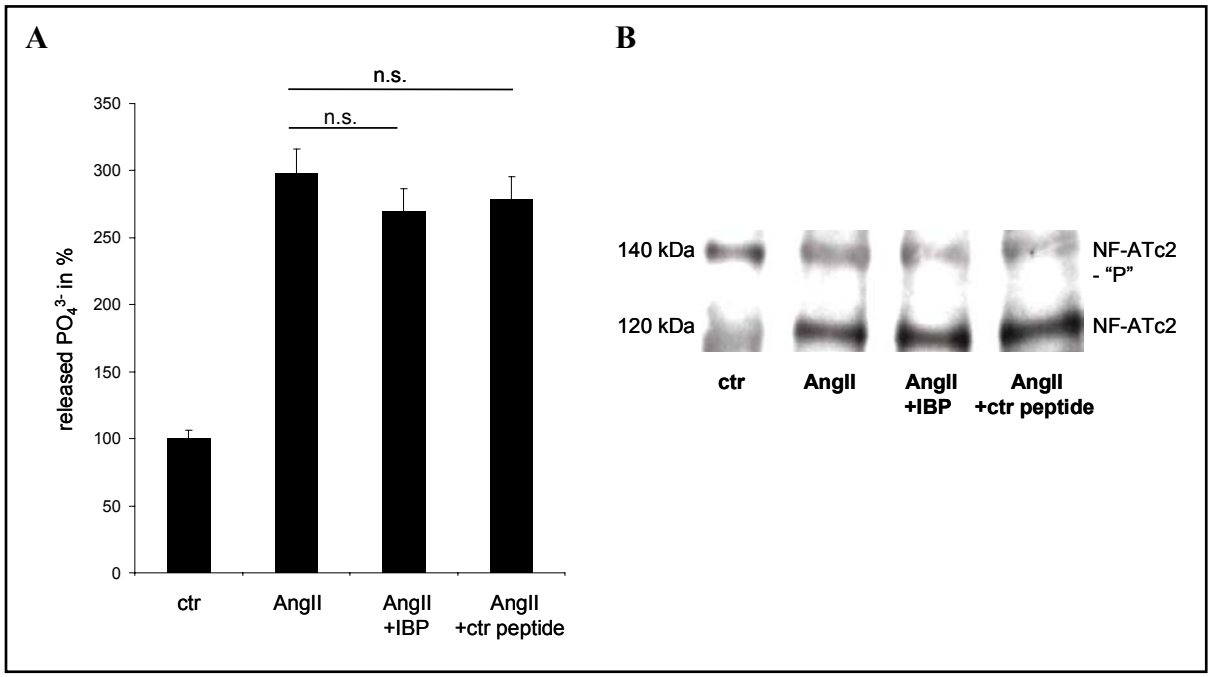

Figure 25. IBP had no effect on the phosphatase activity of CnA in Angiotensin II stimulated NRCMs.
To analyze the effect of IBP on the phosphatase activity of CnA during Angiotensin II (AngII) stimulation (10.0 µM) in NRCMs two methods were used. On the one side, a commercial kit was used (A; *Biomol*). On the other side, the phosphorylation status of NFATc2 was examined (B). Independent of which method was done, the phosphatase activity was not affected by the blocking peptide IBP. There are no significant differences compared to the use of control peptide or the use of no peptide.

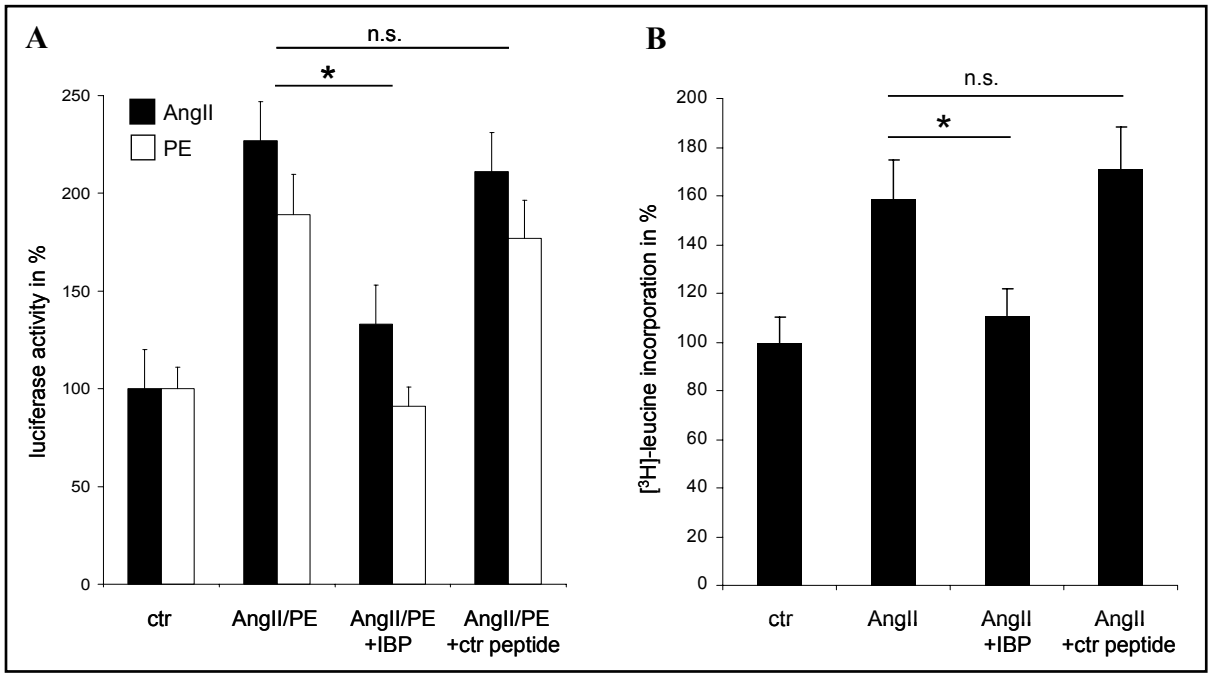

Figure 26. IBP suppressed transcriptional / translational activity in Angiotensin II stimulated NRCMs.
In contrast to unaffected phosphatase activity of CnA during Angiotensin II (AngII) stimulation (10.0 µM) in NRCMs, both the transcriptional and the translational activity were suppressed by IBP. Transcriptional activity was measured by the NF-AT reporterassay (A), whereas translational activity was examined by [^{3}H]-leucine incorporation (B). There was no significant effect of the control peptide (ctr peptide).

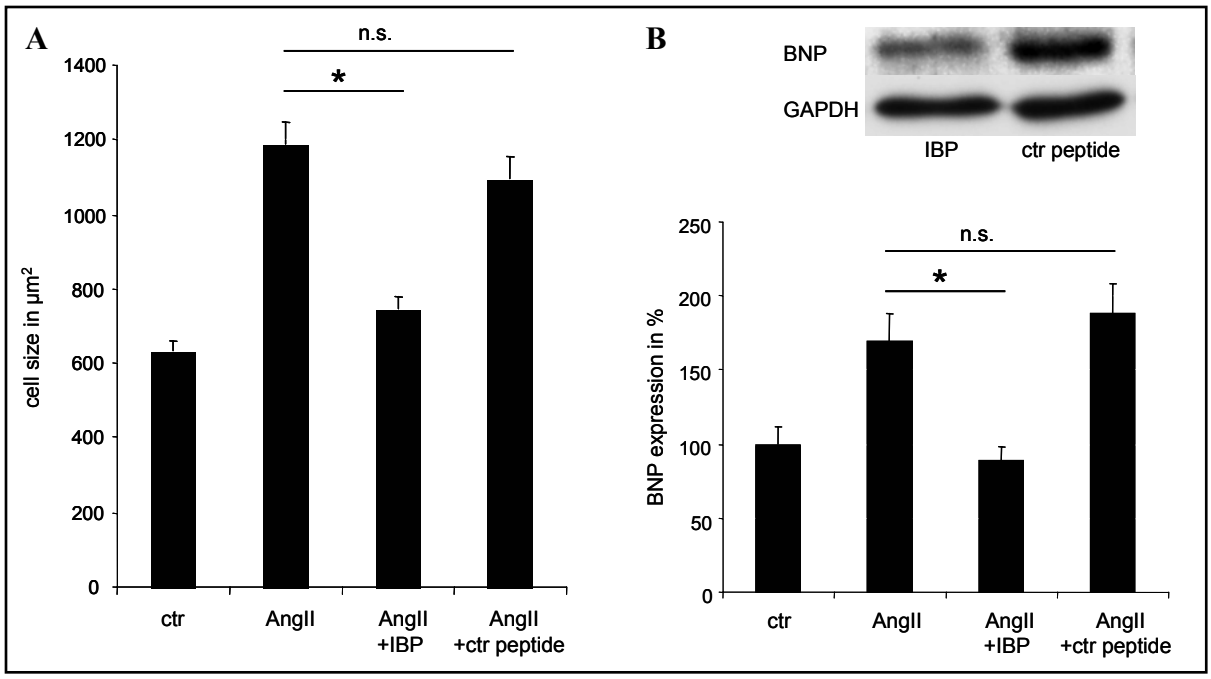

Figure 27. IBP suppressed cell size and BNP expression in Angiotensin II stimulated NRCMs.
In Angiotensin II (AngII, 10.0 µM) stimulated NRCMs the cell size was reduced by IBP compared to control peptide (ctr peptide). IBP treated cells showed sizes similarly to control cells (A). Expression of the Brain natriuretic peptide (BNP) was measured as a marker for myocardial hypertrophy (B). Top, representative BNP Western blot of cardiomyocyte lysate stimulated with AngII and treated with IBP or ctr peptide. Bottom, relative expression levels of GAPDH (loading control). Western Blot was calculated graphically.

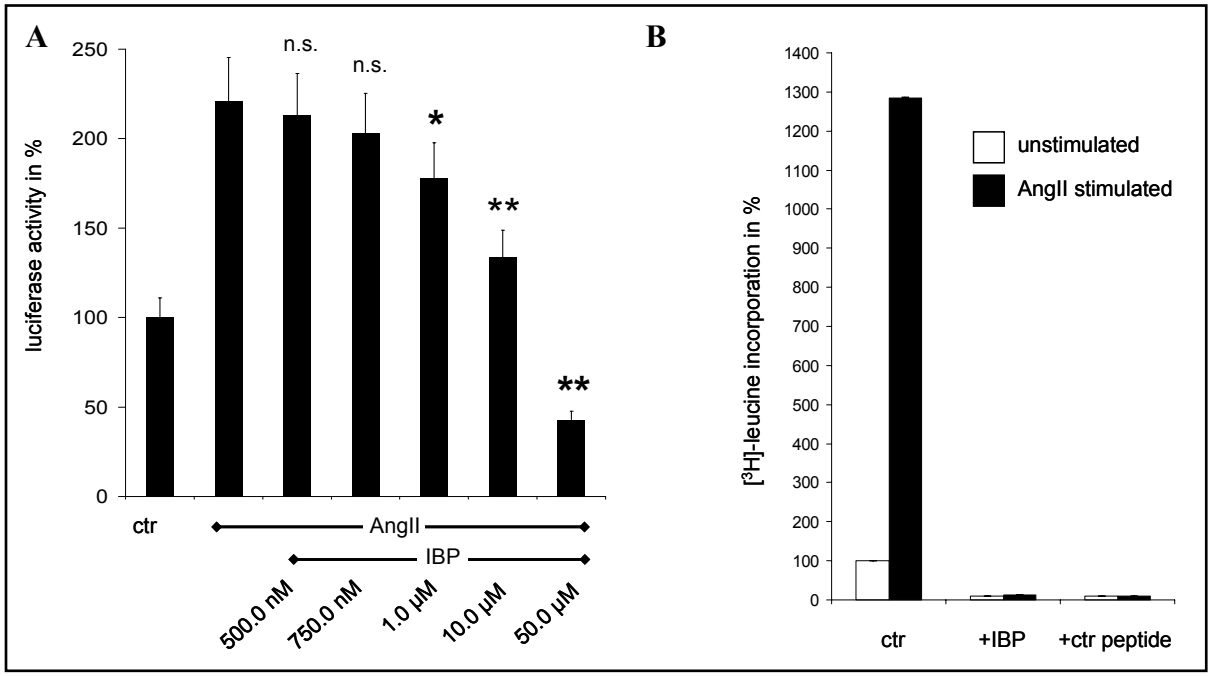

Figure 28. Dose-dependence and toxicity of IBP.
In Angiotensin II (AngII, 10.0 µM) stimulated NRCMs the transcriptional activity was measured for different concentration of IBP. The first significant difference to AngII stimulated cells could be detected at 1.0 µM. The best inhibitory effect was presumed for 10.0 µM, whereby 50.0 µM could be toxic already (A). This presumption is confirmed by analysis the protein synthesis during AngII (10.0 µM) stimulation for 100.0 µM IBP or control peptide. This concentration was definitely toxic for NRCMs. Cells showed no protein synthesis.

5. Discussion

The Calcineurin/NFAT signaling cascade is crucial for T-cell activation and for the development of myocardial hypertrophy. After activation, nuclear localization of NFAT is directly induced by Calcineurin-mediated dephosphorylation of multiple conserved serine residues in the N-terminus of these proteins, revealing a nuclear localization sequence [170]. Once dephosphorylated, NFAT is translocated into the nucleus by its importin, Importinβ_1, and the transcriptional processes begin.

The biological activity of transcription factors is in part regulated by their intracellular localization. According to the Calcineurin/NFAT signaling cascade this means, inactive (hyperphosphorylated) NFAT resides in the cytosol and activated (dephosphorylated) NFAT resides in the nucleus. However, it has also been demonstrated by our group and others that full transcriptional activity of the Calcineurin/NFAT pathway is achieved only when Calcineurin is also translocated into the nucleus. The nuclear half-life of NFAT alone is very short. In the absence of active Calcineurin, the transcription factor is rapidly transported back into the cytoplasm within minutes [171].

In this study, the exact mechanisms and their components leading to nuclear import and export of Calcineurin were investigated. The active transport of proteins into the nucleus requires an array of proteins including nuclear cargo or carrier proteins (so-called importins or karyopherins), which in many instances make the primary contact with the classical nuclear localization sequence (NLS) of the imported protein [75]. Classical NLSs consist of 5-11 amino acids. When Importinα binds to the target protein that contains the classical NLS, the complex interacts with accessory proteins such as Importinβ and the small GTP binding protein, Ran. This complex binds to the nuclear pore complex and is then transported through it in an energy-dependent manner. Nonclassical NLSs can bind directly to Importinβ_1 initiating nuclear transport through the nuclear pore complex [108]. Similary,nuclear export sequences (NESs) are responsible for binding to export proteins, so-called exportins. Exportins transport their target proteins across the nuclear envelop back into the cytosol. A number of proteins that shuttle across the nuclear membrane by using CRM1 as the export shuttle have been identified (e.g. NFAT). Mainly CRM1 recognizes leucine rich NESs, binds these proteins and shuttles them out the nucleus. The processes of import and export are controlled by the regulator Ran. The GTPase Ran acts as the energy source and the directional cue is controlled by two additional regulators: Ran guanosine nucleotide exchange factor (RanGEF) and Ran-

specific GTPase-activating protein (RanGAP). RanGEF loads Ran with GTP in the nucleus, whereas RanGAP is found predominantly in the cytoplasm. In this work a NLS and a NES in the sequence of Calcineurin have been identified. The NLS is located in the region of amino acid 172 to 183 of CnAβ, whereas the NES is defined from amino acid 423 to 433. Additionally, respective carrier proteins for Calcineurin shuttling across the nuclear membrane have been characterized. Importinβ_1 is responsible for the nuclear import and recognizes the NLS of Calcineurin, whereas the export protein CRM1 is required for nuclear export and realizes the NES.

These findings identify a potentially novel therapeutic strategy to inhibit myocardial hypertrophy. Inhibition of the Calcineurin/Importinβ_1 interaction would prevent nuclear translocation of Calcineurin and therefore disrupt the Calcineurin/NFAT signaling cascade. Similar approaches, such as inhibition of the NF-κB/importin interaction [172,173] and Calcineurin/NFAT interaction by competitive peptides have already been successfully proven. A known blocking peptide is the cell-permeable NFAT inhibitor VIVIT. This molecule consists of 16 amino acids according to the sequence of the Calcineurin docking site of the NFAT family. This high-affinity Calcineurin-binding peptide inhibits the Calcineurin/NFAT1 (NFATc2) interaction by saturating Calcineurin. NFAT1 cannot bind to the phosphatase any longer [174]. Without dephosphorylating the transcriptional factor NFAT1 remains cytosolic, whereby the transcriptional activity remains low. Using VIVIT as a specific blocking peptide the nuclear import of NFAT1 is blocked in an indirect manner. In contrast, using this strategy, a polypeptide comprising 12 amino acids was synthesized. This so-called ´Import Blocking Peptide` (IBP) mimicked the NLS sequence of Calcineurin Aβ and blocks the nuclear import of Calcineurin directly by saturating the specific importin (Importinβ_1). To increase membrane permeability for this blocking peptide, a N-terminal peptide extension of additional 15 amino acids was added. This N-terminal sequence is very hydrophob and guarantees uptake into cells. By using the blocking peptide IBP it was able to suppress Calcineurin/Importinβ_1 interaction, which subsequently prevented nuclear import of Calcineurin. The physiological result was blunting of NFAT transcriptional activity and inhibition of the development of myocardial hypertrophy. In contrast, Calcineurin phosphatase activity was unaffected although assessment of Calcineurin phosphatase activity *in vivo* is often imprecise. As a surrogate, the blocking peptide IBP had no impact on NFATc2 dephosphorylation. It is known that four isoforms of NFAT, NFATc1, NFATc2, NFATc3 and NFATc4, are expressed in myocardium. But there exist different opinions about the most

important isoform. In this work, the focus of NFAT isoforms was concentrated on NFATc2, according to de Windt L. (unpublished data).
These results demonstrated that inhibition of the Calcineurin/importin interaction by interfering peptides is an effective tool to suppress Calcineurin signaling. However, the question, what is the precise role of Calcineurin in the nucleus, is still unanswered.

The transcriptional effector of the Calcineurin/NFAT system is NFAT through its DNA binding domain. NFAT isoforms share an imperfect Rel homology domain that is only capable of weak DNA binding in the monomeric or dimeric state. In order to strengthen NFAT–DNA interactions, these factors prefer to interact co-operatively with other nuclear transcription factors such as AP-1 (c-Jun/c-Fos), GATA-4 and MEF-2 [175]. Therefore, Calcineurin may act as a transcriptional co-activator. According to this presumption the sequence of Calcineurin have to be checked for any DNA binding domain or any binding domain for proteins. Additionally, DNA binding assays and co-immunoprecipitations should be done. Competition by Calcineurin with the Glycogen synthase kinase 3β (GSK3β) to ensure further dephosphorylation of NFAT in the nucleus or at least to prevent rephosphorylation is however unlikely to be the major task of nuclear Calcineurin as CnA mutants devoid of phosphatase function also increase transcriptional activity of the CnA/NFAT signaling pathway when translocated to the nucleus [176]. Also, multiple other kinases beside GSK-3β such as c-Jun N terminal kinase (JNK) and p38 MAP kinases, Casein kinase I (CK1), Protein kinase A (PKA), and Mitogen-activated protein kinase kinase 1 (MEKK1) (indirectly) all promote rephosphorylation of the serine-rich N-terminus of NFAT isoforms enabling CRM1-mediated nuclear export [177-180]. Another model of competition between Calcineurin and CRM1 for the nuclear export sequence of NFAT has also been proposed. It has previously been demonstrated that the nuclear export protein CRM1 is capable of transporting NFAT out of the nucleus. A constitutive nuclear Calcineurin will shift CRM1 off the NES of NFAT and leave the Calcineurin/NFAT complex nuclear, thereby enhancing transcriptional output [176,181]. These data show that CRM1 not only exports NFAT, but also Calcineurin from the nucleus. To interrupt transcriptional activity of the Calcineurin/NFAT signaling cascade, CRM1 is first required to export Calcineurin, so that in a second round CRM1 can access the NES of NFAT and subsequently proceed with its nuclear export. This mechanism may be prevented in myocardial hypertrophy by the proteolysis of Calcineurin by Calpain at amino acid 424, resulting in a loss of the

autoinhibitory domain including the NES. In this scenario, Calcineurin remains nuclear because it is inaccessible to the export protein CRM1. These observations suggest that Calcineurin function in the nucleus is largely driven via its anti-CRM1 as opposed to anti-GSK3β effects. As import always precedes export, the inhibition of CnA nuclear import by peptide competition for the binding of the nuclear import protein Importinβ_1 presents a sophisticated approach to abolishing the deleterious effects of exaggerated NFAT transcriptional activity. Nevertheless, it is obligate to assess the specific action of IBP on the Calcineurin/NFAT interaction prior to further experiments *in vivo*.

A completely different point of view would be the acting of Calcineurin as a nuclear phosphatase. There exist two models of dephosphorylation of NFAT. The first one, described in this work, depends on a complete dephosphorylation within the cytosol by Calcineurin. NFAT is translocated completely dephosphorylated into the nucleus. But there is a second model conception. The difference depends on the translocation of partial dephosphorylated NFAT. Not until arrived in the nucleus, NFAT is dephosphorylated completely by diverse phosphatases, like Calcineurin. In this case, Calcineurin would work as a cytosolic and a nuclear phosphatase. For analyzing, nuclear and cytosolic specific, respectively, phosphatase deficient Calcineurin mutants have to be transfected, to check the transcriptional and translational activity for stimulated cardiomyocytes.

Future perspective

The demonstrated data resulted from *in vitro* experiments on neonatal rat cardiomyocytes. In further work the *in vitro* data should be confirmed by *in vivo* studies with mice. Therefore, three groups á five to eight animals, should be investigated. To simulate Angiotensin II stimulated neonatal rat cardiomyocytes osmotic minipumps (Alzet; Charles River, Germany) will be used. Osmotic pumps will be filled with Angiotensin II (5.0 mg/kg/d) and with NaCl (0,9 %) as control respectively. After implantation of minipumps, mice will be kept under control for three to four weeks. The first group is treated with the blocking peptide IBP (25.0 mg/kg/d; daily i.p.), the second group is stimulated with the AngII pumps without any peptide treatment, whereas the third group is treated only with NaCl as control. After three to four weeks, the mice will be despatched, ratio of body weight to heart weight and expression

of ANP, BNP and β-MHC will be measured. Additionally, immunohistochemistry of frozen heart sections will be analyzed according to the subcellular localization of Calcineurin.
In cooperation with PD Dr. rer. nat. Christoph Otto (Experimentelle Transplantations-Immunologie (ETI), Chirurgische Universitätsklinik I, Zentrum für Operative Medizin (ZOM); Universität Würzburg), similar experiments will be done on T-cells. First experiments showed inhibitory effects on stimulated T-cells at a concentration at 1.0 μM. These studies are still going on and will be expanded to heterotopic heart transplantation. To prevent graft rejection the common pharmacological agent Cyclosporin A should be used for one group. The second group is treated with the blocking peptide IBP, whereas the control group is kept without any treatment. The scientists hope for a inhibition of graft rejection by IBP.
Another important point of IBP is the specificity. The effect of IBP have aleady been tested for diverse transcriptional factors in AngII stimulated NRCMs. NFATc2, NF-κB, GATA4, cJun and ERK1/2 showed no effect in their subcellular localization compared to control experiments. Without any treatment, all transcriptionsfactors were predominantely localized in the nucleus. This nuclear localization could also been seen for AngII stimulated cells, for AngII stimulated cells treated with IBP and also for AngII stimulated cells treated with control peptide. In conclusion, a first step to demonstrate the specificity of IBP, was done, but it have to extended. For example, a IBP-specific antibody has been genereated to detect IBP *in vivo*. Additionally, a functional test to detect IBP concentrations in serum will be in the future focus.

Taken all together, the Import Blocking Peptide IBP, is a new approach to prevent the interaction of Calcineurin and its Importinβ_1. Therefore, the development of myocardial hypertrophy is prevented *in vitro*. These results have to be confirmed in further studies - especially *in vivo* studies. Additionally, the specificity of IBP have to be demonstrated and a method to detect the pharmacological reagent *in vivo* have to be established. This new approach has already been patented.

6. References

1. Wang JH, Desai R. A brain protein and its effect on the Ca2+-and protein modulator-activated cyclic nucleotide phosphodiesterase. *Biochem Biophys Res Commun*. 1976;72:926-32.
2. Liu J, Farmer JD, Jr., Lane WS, Friedman J, Weissman I, Schreiber SL. Calcineurin is a common target of cyclophilin-cyclosporin A and FKBP-FK506 complexes. *Cell*. 1991;66:807-15.
3. Griffith JP, Kim JL, Kim EE, Sintchak MD, Thomson JA, Fitzgibbon MJ, Fleming MA, Caron PR, Hsiao K, Navia MA. X-ray structure of calcineurin inhibited by the immunophilin-immunosuppressant FKBP12-FK506 complex. *Cell*. 1995;82:507-22.
4. Kissinger CR, Parge HE, Knighton DR, Lewis CT, Pelletier LA, Tempczyk A, Kalish VJ, Tucker KD, Showalter RE, Moomaw EW, et al. Crystal structures of human calcineurin and the human FKBP12-FK506-calcineurin complex. *Nature*. 1995;378:641-4.
5. Martin BL, Graves DJ. Mechanistic aspects of the low-molecular-weight phosphatase activity of the calmodulin-activated phosphatase, calcineurin. *J Biol Chem*. 1986;261:14545-50.
6. Yu L, Golbeck J, Yao J, Rusnak F. Spectroscopic and enzymatic characterization of the active site dinuclear metal center of calcineurin: implications for a mechanistic role. *Biochemistry*. 1997;36:10727-34.
7. Rusnak F, Mertz P. Calcineurin: form and function. *Physiol Rev*. 2000;80:1483-521.
8. Anthony FA, Winkler MA, Edwards HH, Cheung WY. Quantitative subcellular localization of calmodulin-dependent phosphatase in chick forebrain. *J Neurosci*. 1988;8:1245-53.
9. Jiang H, Xiong F, Kong S, Ogawa T, Kobayashi M, Liu JO. Distinct tissue and cellular distribution of two major isoforms of calcineurin. *Mol Immunol*. 1997;34:663-9.
10. Kuno T, Mukai H, Ito A, Chang CD, Kishima K, Saito N, Tanaka C. Distinct cellular expression of calcineurin A alpha and A beta in rat brain. *J Neurochem*. 1992;58:1643-51.
11. Reiter TA, Abraham RT, Choi M, Rusnak F. Redox regulation of calcineurin in T-lymphocytes. *J Biol Inorg Chem*. 1999;4:632-44.
12. Coghlan VM, Perrino BA, Howard M, Langeberg LK, Hicks JB, Gallatin WM, Scott JD. Association of protein kinase A and protein phosphatase 2B with a common anchoring protein. *Science*. 1995;267:108-11.
13. Liu JO. Endogenous protein inhibitors of calcineurin. *Biochem Biophys Res Commun*. 2003;311:1103-9.
14. Sun L, Youn HD, Loh C, Stolow M, He W, Liu JO. Cabin 1, a negative regulator for calcineurin signaling in T lymphocytes. *Immunity*. 1998;8:703-11.
15. Dodge KL, Scott JD. Calcineurin anchoring and cell signaling. *Biochem Biophys Res Commun*. 2003;311:1111-5.
16. Rothermel B, Vega RB, Yang J, Wu H, Bassel-Duby R, Williams RS. A protein encoded within the Down syndrome critical region is enriched in striated muscles and inhibits calcineurin signaling. *J Biol Chem*. 2000;275:8719-25.
17. Fuentes JJ, Genesca L, Kingsbury TJ, Cunningham KW, Perez-Riba M, Estivill X, de la Luna S. DSCR1, overexpressed in Down syndrome, is an inhibitor of calcineurin-mediated signaling pathways. *Hum Mol Genet*. 2000;9:1681-90.

18. Lai MM, Burnett PE, Wolosker H, Blackshaw S, Snyder SH. Cain, a novel physiologic protein inhibitor of calcineurin. *J Biol Chem*. 1998;273:18325-31.
19. Lai MM, Luo HR, Burnett PE, Hong JJ, Snyder SH. The calcineurin-binding protein cain is a negative regulator of synaptic vesicle endocytosis. *J Biol Chem*. 2000;275:34017-20.
20. Fiedler B, Wollert KC. Interference of antihypertrophic molecules and signaling pathways with the Ca2+-calcineurin-NFAT cascade in cardiac myocytes. *Cardiovasc Res*. 2004;63:450-7.
21. Molkentin JD, Lu JR, Antos CL, Markham B, Richardson J, Robbins J, Grant SR, Olson EN. A calcineurin-dependent transcriptional pathway for cardiac hypertrophy. *Cell*. 1998;93:215-28.
22. Burkard N, Becher J, Heindl C, Neyses L, Schuh K, Ritter O. Targeted proteolysis sustains calcineurin activation. *Circulation*. 2005;111:1045-53.
23. Hallhuber M, Burkard N, Wu R, Buch MH, Engelhardt S, Hein L, Neyses L, Schuh K, Ritter O. Inhibition of nuclear import of calcineurin prevents myocardial hypertrophy. *Circ Res*. 2006;99:626-35.
24. Klee CB, Crouch TH, Krinks MH. Calcineurin: a calcium- and calmodulin-binding protein of the nervous system. *Proc Natl Acad Sci U S A*. 1979;76:6270-3.
25. Stewart AA, Ingebritsen TS, Manalan A, Klee CB, Cohen P. Discovery of a Ca2+- and calmodulin-dependent protein phosphatase: probable identity with calcineurin (CaM-BP80). *FEBS Lett*. 1982;137:80-4.
26. Klee CB, Krinks MH, Manalan AS, Cohen P, Stewart AA. Isolation and characterization of bovine brain calcineurin: a calmodulin-stimulated protein phosphatase. *Methods Enzymol*. 1983;102:227-44.
27. Barford D. Molecular mechanisms of the protein serine/threonine phosphatases. *Trends Biochem Sci*. 1996;21:407-12.
28. Barford D, Das AK, Egloff MP. The structure and mechanism of protein phosphatases: insights into catalysis and regulation. *Annu Rev Biophys Biomol Struct*. 1998;27:133-64.
29. Bollen M, Stalmans W. The structure, role, and regulation of type 1 protein phosphatases. *Crit Rev Biochem Mol Biol*. 1992;27:227-81.
30. Cohen P. The structure and regulation of protein phosphatases. *Annu Rev Biochem*. 1989;58:453-508.
31. Shenolikar S, Nairn AC. Protein phosphatases: recent progress. *Adv Second Messenger Phosphoprotein Res*. 1991;23:1-121.
32. Axton JM, Dombradi V, Cohen PT, Glover DM. One of the protein phosphatase 1 isoenzymes in Drosophila is essential for mitosis. *Cell*. 1990;63:33-46.
33. Ceulemans H, Bollen M. Functional diversity of protein phosphatase-1, a cellular economizer and reset button. *Physiol Rev*. 2004;84:1-39.
34. Dombradi V, Axton JM, Barker HM, Cohen PT. Protein phosphatase 1 activity in Drosophila mutants with abnormalities in mitosis and chromosome condensation. *FEBS Lett*. 1990;275:39-43.
35. Wera S, Hemmings BA. Serine/threonine protein phosphatases. *Biochem J*. 1995;311 (Pt 1):17-29.
36. Nasmyth K. How might cohesin hold sister chromatids together? *Philos Trans R Soc Lond B Biol Sci*. 2005;360:483-96.
37. Trinkle-Mulcahy L, Lamond AI. Mitotic phosphatases: no longer silent partners. *Curr Opin Cell Biol*. 2006.

38. Tang Z, Shu H, Qi W, Mahmood NA, Mumby MC, Yu H. PP2A is required for centromeric localization of Sgo1 and proper chromosome segregation. *Dev Cell*. 2006;10:575-85.
39. Moore F, Weekes J, Hardie DG. Evidence that AMP triggers phosphorylation as well as direct allosteric activation of rat liver AMP-activated protein kinase. A sensitive mechanism to protect the cell against ATP depletion. *Eur J Biochem*. 1991;199:691-7.
40. Maeda T, Wurgler-Murphy SM, Saito H. A two-component system that regulates an osmosensing MAP kinase cascade in yeast. *Nature*. 1994;369:242-5.
41. Muramatsu T, Kincaid RL. Molecular cloning and chromosomal mapping of the human gene for the testis-specific catalytic subunit of calmodulin-dependent protein phosphatase (calcineurin A). *Biochem Biophys Res Commun*. 1992;188:265-71.
42. Politino M, King MM. Calcium- and calmodulin-sensitive interactions of calcineurin with phospholipids. *J Biol Chem*. 1987;262:10109-13.
43. Moriya M, Fujinaga K, Yazawa M, Katagiri C. Immunohistochemical localization of the calcium/calmodulin-dependent protein phosphatase, calcineurin, in the mouse testis: its unique accumulation in spermatid nuclei. *Cell Tissue Res*. 1995;281:273-81.
44. Shibasaki F, Kondo E, Akagi T, McKeon F. Suppression of signalling through transcription factor NF-AT by interactions between calcineurin and Bcl-2. *Nature*. 1997;386:728-31.
45. Lohse DL, Denu JM, Dixon JE. Insights derived from the structures of the Ser/Thr phosphatases calcineurin and protein phosphatase 1. *Structure*. 1995;3:987-90.
46. Klee CB, Ren H, Wang X. Regulation of the calmodulin-stimulated protein phosphatase, calcineurin. *J Biol Chem*. 1998;273:13367-70.
47. Bueno OF, van Rooij E, Molkentin JD, Doevendans PA, De Windt LJ. Calcineurin and hypertrophic heart disease: novel insights and remaining questions. *Cardiovasc Res*. 2002;53:806-21.
48. De Windt LJ, Lim HW, Bueno OF, Liang Q, Delling U, Braz JC, Glascock BJ, Kimball TF, del Monte F, Hajjar RJ, Molkentin JD. Targeted inhibition of calcineurin attenuates cardiac hypertrophy in vivo. *Proc Natl Acad Sci U S A*. 2001;98:3322-7.
49. Taigen T, De Windt LJ, Lim HW, Molkentin JD. Targeted inhibition of calcineurin prevents agonist-induced cardiomyocyte hypertrophy. *Proc Natl Acad Sci U S A*. 2000;97:1196-201.
50. Yang J, Rothermel B, Vega RB, Frey N, McKinsey TA, Olson EN, Bassel-Duby R, Williams RS. Independent signals control expression of the calcineurin inhibitory proteins MCIP1 and MCIP2 in striated muscles. *Circ Res*. 2000;87:E61-8.
51. Rothermel BA, McKinsey TA, Vega RB, Nicol RL, Mammen P, Yang J, Antos CL, Shelton JM, Bassel-Duby R, Olson EN, Williams RS. Myocyte-enriched calcineurin-interacting protein, MCIP1, inhibits cardiac hypertrophy in vivo. *Proc Natl Acad Sci U S A*. 2001;98:3328-33.
52. Wilkins BJ, Molkentin JD. Calcineurin and cardiac hypertrophy: where have we been? Where are we going? *J Physiol*. 2002;541:1-8.
53. Crabtree GR, Clipstone NA. Signal transmission between the plasma membrane and nucleus of T lymphocytes. *Annu Rev Biochem*. 1994;63:1045-83.
54. Rao A, Luo C, Hogan PG. Transcription factors of the NFAT family: regulation and function. *Annu Rev Immunol*. 1997;15:707-47.
55. Tanida I, Hasegawa A, Iida H, Ohya Y, Anraku Y. Cooperation of calcineurin and vacuolar H(+)-ATPase in intracellular Ca2+ homeostasis of yeast cells. *J Biol Chem*. 1995;270:10113-9.

56. Yoshida T, Toda T, Yanagida M. A calcineurin-like gene ppb1+ in fission yeast: mutant defects in cytokinesis, cell polarity, mating and spindle pole body positioning. *J Cell Sci*. 1994;107 (Pt 7):1725-35.
57. Stathopoulos AM, Cyert MS. Calcineurin acts through the CRZ1/TCN1-encoded transcription factor to regulate gene expression in yeast. *Genes Dev*. 1997;11:3432-44.
58. Periasamy M. Calcineurin and the heartbeat, an evolving story. *J Mol Cell Cardiol*. 2002;34:259-62.
59. Lin Q, Schwarz J, Bucana C, Olson EN. Control of mouse cardiac morphogenesis and myogenesis by transcription factor MEF2C. *Science*. 1997;276:1404-7.
60. Kumai M, Nishii K, Nakamura K, Takeda N, Suzuki M, Shibata Y. Loss of connexin45 causes a cushion defect in early cardiogenesis. *Development*. 2000;127:3501-12.
61. Mesaeli N, Nakamura K, Zvaritch E, Dickie P, Dziak E, Krause KH, Opas M, MacLennan DH, Michalak M. Calreticulin is essential for cardiac development. *J Cell Biol*. 1999;144:857-68.
62. de la Pompa JL, Timmerman LA, Takimoto H, Yoshida H, Elia AJ, Samper E, Potter J, Wakeham A, Marengere L, Langille BL, Crabtree GR, Mak TW. Role of the NF-ATc transcription factor in morphogenesis of cardiac valves and septum. *Nature*. 1998;392:182-6.
63. Wilkins BJ, De Windt LJ, Bueno OF, Braz JC, Glascock BJ, Kimball TF, Molkentin JD. Targeted disruption of NFATc3, but not NFATc4, reveals an intrinsic defect in calcineurin-mediated cardiac hypertrophic growth. *Mol Cell Biol*. 2002;22:7603-13.
64. Frank K, Kranias EG. Phospholamban and cardiac contractility. *Ann Med*. 2000;32:572-8.
65. Munch G, Bolck B, Karczewski P, Schwinger RH. Evidence for calcineurin-mediated regulation of SERCA 2a activity in human myocardium. *J Mol Cell Cardiol*. 2002;34:321-34.
66. Yatani A, Honda R, Tymitz KM, Lalli MJ, Molkentin JD. Enhanced Ca2+ channel currents in cardiac hypertrophy induced by activation of calcineurin-dependent pathway. *J Mol Cell Cardiol*. 2001;33:249-59.
67. Klee CB, Draetta GF, Hubbard MJ. Calcineurin. *Adv Enzymol Relat Areas Mol Biol*. 1988;61:149-200.
68. Stemmer PM, Klee CB. Dual calcium ion regulation of calcineurin by calmodulin and calcineurin B. *Biochemistry*. 1994;33:6859-66.
69. Wu HY, Tomizawa K, Oda Y, Wei FY, Lu YF, Matsushita M, Li ST, Moriwaki A, Matsui H. Critical role of calpain-mediated cleavage of calcineurin in excitotoxic neurodegeneration. *J Biol Chem*. 2004;279:4929-40.
70. Lund E, Dahlberg JE. Proofreading and aminoacylation of tRNAs before export from the nucleus. *Science*. 1998;282:2082-5.
71. Fried H, Kutay U. Nucleocytoplasmic transport: taking an inventory. *Cell Mol Life Sci*. 2003;60:1659-88.
72. Rout MP, Aitchison JD. The nuclear pore complex as a transport machine. *J Biol Chem*. 2001;276:16593-6.
73. Gorlich D, Mattaj IW. Nucleocytoplasmic transport. *Science*. 1996;271:1513-8.
74. Gorlich D, Kutay U. Transport between the cell nucleus and the cytoplasm. *Annu Rev Cell Dev Biol*. 1999;15:607-60.
75. Weis K. Nucleocytoplasmic transport: cargo trafficking across the border. *Curr Opin Cell Biol*. 2002;14:328-35.
76. Mattaj IW, Conti E. Cell biology. Snail mail to the nucleus. *Nature*. 1999;399:208-10.

77. Kutay U, Bischoff FR, Kostka S, Kraft R, Gorlich D. Export of importin alpha from the nucleus is mediated by a specific nuclear transport factor. *Cell*. 1997;90:1061-71.
78. Schuller C, Ruis H. Regulated nuclear transport. *Results Probl Cell Differ*. 2002;35:169-89.
79. Mingot JM, Bohnsack MT, Jakle U, Gorlich D. Exportin 7 defines a novel general nuclear export pathway. *Embo J*. 2004;23:3227-36.
80. Stuven T, Hartmann E, Gorlich D. Exportin 6: a novel nuclear export receptor that is specific for profilin.actin complexes. *Embo J*. 2003;22:5928-40.
81. Fornerod M, Ohno M. Exportin-mediated nuclear export of proteins and ribonucleoproteins. *Results Probl Cell Differ*. 2002;35:67-91.
82. Yang Q, Rout MP, Akey CW. Three-dimensional architecture of the isolated yeast nuclear pore complex: functional and evolutionary implications. *Mol Cell*. 1998;1:223-34.
83. Stoffler D, Feja B, Fahrenkrog B, Walz J, Typke D, Aebi U. Cryo-electron tomography provides novel insights into nuclear pore architecture: implications for nucleocytoplasmic transport. *J Mol Biol*. 2003;328:119-30.
84. Fahrenkrog B, Stoffler D, Aebi U. Nuclear pore complex architecture and functional dynamics. *Curr Top Microbiol Immunol*. 2001;259:95-117.
85. Fahrenkrog B, Aebi U. The nuclear pore complex: nucleocytoplasmic transport and beyond. *Nat Rev Mol Cell Biol*. 2003;4:757-66.
86. Fahrenkrog B, Koser J, Aebi U. The nuclear pore complex: a jack of all trades? *Trends Biochem Sci*. 2004;29:175-82.
87. Rout MP, Aitchison JD, Magnasco MO, Chait BT. Virtual gating and nuclear transport: the hole picture. *Trends Cell Biol*. 2003;13:622-8.
88. Cronshaw JM, Krutchinsky AN, Zhang W, Chait BT, Matunis MJ. Proteomic analysis of the mammalian nuclear pore complex. *J Cell Biol*. 2002;158:915-27.
89. Rout MP, Aitchison JD, Suprapto A, Hjertaas K, Zhao Y, Chait BT. The yeast nuclear pore complex: composition, architecture, and transport mechanism. *J Cell Biol*. 2000;148:635-51.
90. Macara IG. Transport into and out of the nucleus. *Microbiol Mol Biol Rev*. 2001;65:570-94, table of contents.
91. Ribbeck K, Gorlich D. Kinetic analysis of translocation through nuclear pore complexes. *Embo J*. 2001;20:1320-30.
92. Jans DA, Xiao CY, Lam MH. Nuclear targeting signal recognition: a key control point in nuclear transport? *Bioessays*. 2000;22:532-44.
93. Pemberton LF, Paschal BM. Mechanisms of receptor-mediated nuclear import and nuclear export. *Traffic*. 2005;6:187-98.
94. Gorlich D, Dabrowski M, Bischoff FR, Kutay U, Bork P, Hartmann E, Prehn S, Izaurralde E. A novel class of RanGTP binding proteins. *J Cell Biol*. 1997;138:65-80.
95. Cingolani G, Petosa C, Weis K, Muller CW. Structure of importin-beta bound to the IBB domain of importin-alpha. *Nature*. 1999;399:221-9.
96. Bayliss R, Littlewood T, Stewart M. Structural basis for the interaction between FxFG nucleoporin repeats and importin-beta in nuclear trafficking. *Cell*. 2000;102:99-108.
97. Cingolani G, Bednenko J, Gillespie MT, Gerace L. Molecular basis for the recognition of a nonclassical nuclear localization signal by importin beta. *Mol Cell*. 2002;10:1345-53.
98. Vetter IR, Arndt A, Kutay U, Gorlich D, Wittinghofer A. Structural view of the Ran-Importin beta interaction at 2.3 A resolution. *Cell*. 1999;97:635-46.
99. Stewart M. Structural biology. Nuclear trafficking. *Science*. 2003;302:1513-4.

100. Matsuura Y, Stewart M. Structural basis for the assembly of a nuclear export complex. *Nature*. 2004;432:872-7.
101. Petosa C, Schoehn G, Askjaer P, Bauer U, Moulin M, Steuerwald U, Soler-Lopez M, Baudin F, Mattaj IW, Muller CW. Architecture of CRM1/Exportin1 suggests how cooperativity is achieved during formation of a nuclear export complex. *Mol Cell*. 2004;16:761-75.
102. Kutay U, Guttinger S. Leucine-rich nuclear-export signals: born to be weak. *Trends Cell Biol*. 2005;15:121-4.
103. Poon IK, Jans DA. Regulation of nuclear transport: central role in development and transformation? *Traffic*. 2005;6:173-86.
104. Conti E, Uy M, Leighton L, Blobel G, Kuriyan J. Crystallographic analysis of the recognition of a nuclear localization signal by the nuclear import factor karyopherin alpha. *Cell*. 1998;94:193-204.
105. Nigg EA. Nucleocytoplasmic transport: signals, mechanisms and regulation. *Nature*. 1997;386:779-87.
106. Kobe B. Autoinhibition by an internal nuclear localization signal revealed by the crystal structure of mammalian importin alpha. *Nat Struct Biol*. 1999;6:388-97.
107. Gorlich D, Henklein P, Laskey RA, Hartmann E. A 41 amino acid motif in importin-alpha confers binding to importin-beta and hence transit into the nucleus. *Embo J*. 1996;15:1810-7.
108. Chook YM, Blobel G. Karyopherins and nuclear import. *Curr Opin Struct Biol*. 2001;11:703-15.
109. Conti E. Structures of importins. *Results Probl Cell Differ*. 2002;35:93-113.
110. Kalab P, Weis K, Heald R. Visualization of a Ran-GTP gradient in interphase and mitotic Xenopus egg extracts. *Science*. 2002;295:2452-6.
111. Gorlich D, Pante N, Kutay U, Aebi U, Bischoff FR. Identification of different roles for RanGDP and RanGTP in nuclear protein import. *Embo J*. 1996;15:5584-94.
112. Rexach M, Blobel G. Protein import into nuclei: association and dissociation reactions involving transport substrate, transport factors, and nucleoporins. *Cell*. 1995;83:683-92.
113. Ossareh-Nazari B, Gwizdek C, Dargemont C. Protein export from the nucleus. *Traffic*. 2001;2:684-9.
114. Kutay U, Izaurralde E, Bischoff FR, Mattaj IW, Gorlich D. Dominant-negative mutants of importin-beta block multiple pathways of import and export through the nuclear pore complex. *Embo J*. 1997;16:1153-63.
115. Fornerod M, Ohno M, Yoshida M, Mattaj IW. CRM1 is an export receptor for leucine-rich nuclear export signals. *Cell*. 1997;90:1051-60.
116. Gorlich D, Seewald MJ, Ribbeck K. Characterization of Ran-driven cargo transport and the RanGTPase system by kinetic measurements and computer simulation. *Embo J*. 2003;22:1088-100.
117. Mingot JM, Kostka S, Kraft R, Hartmann E, Gorlich D. Importin 13: a novel mediator of nuclear import and export. *Embo J*. 2001;20:3685-94.
118. Yoshida K, Blobel G. The karyopherin Kap142p/Msn5p mediates nuclear import and nuclear export of different cargo proteins. *J Cell Biol*. 2001;152:729-40.
119. Mattaj IW, Englmeier L. Nucleocytoplasmic transport: the soluble phase. *Annu Rev Biochem*. 1998;67:265-306.
120. Lanford RE, Butel JS. Construction and characterization of an SV40 mutant defective in nuclear transport of T antigen. *Cell*. 1984;37:801-13.

121. Lanford RE, Kanda P, Kennedy RC. Induction of nuclear transport with a synthetic peptide homologous to the SV40 T antigen transport signal. *Cell*. 1986;46:575-82.
122. Dingwall C, Sharnick SV, Laskey RA. A polypeptide domain that specifies migration of nucleoplasmin into the nucleus. *Cell*. 1982;30:449-58.
123. Christophe D, Christophe-Hobertus C, Pichon B. Nuclear targeting of proteins: how many different signals? *Cell Signal*. 2000;12:337-41.
124. Strom AC, Weis K. Importin-beta-like nuclear transport receptors. *Genome Biol*. 2001;2:REVIEWS3008.
125. Forwood JK, Lam MH, Jans DA. Nuclear import of Creb and AP-1 transcription factors requires importin-beta 1 and Ran but is independent of importin-alpha. *Biochemistry*. 2001;40:5208-17.
126. Xiao Z, Liu X, Lodish HF. Importin beta mediates nuclear translocation of Smad 3. *J Biol Chem*. 2000;275:23425-8.
127. Truant R, Cullen BR. The arginine-rich domains present in human immunodeficiency virus type 1 Tat and Rev function as direct importin beta-dependent nuclear localization signals. *Mol Cell Biol*. 1999;19:1210-7.
128. Jakel S, Gorlich D. Importin beta, transportin, RanBP5 and RanBP7 mediate nuclear import of ribosomal proteins in mammalian cells. *Embo J*. 1998;17:4491-502.
129. Lam MH, Briggs LJ, Hu W, Martin TJ, Gillespie MT, Jans DA. Importin beta recognizes parathyroid hormone-related protein with high affinity and mediates its nuclear import in the absence of importin alpha. *J Biol Chem*. 1999;274:7391-8.
130. Pollard VW, Michael WM, Nakielny S, Siomi MC, Wang F, Dreyfuss G. A novel receptor-mediated nuclear protein import pathway. *Cell*. 1996;86:985-94.
131. Rout MP, Blobel G, Aitchison JD. A distinct nuclear import pathway used by ribosomal proteins. *Cell*. 1997;89:715-25.
132. Schlenstedt G, Smirnova E, Deane R, Solsbacher J, Kutay U, Gorlich D, Ponstingl H, Bischoff FR. Yrb4p, a yeast ran-GTP-binding protein involved in import of ribosomal protein L25 into the nucleus. *Embo J*. 1997;16:6237-49.
133. Lei EP, Silver PA. Protein and RNA export from the nucleus. *Dev Cell*. 2002;2:261-72.
134. Izaurralde E. Nuclear export of messenger RNA. *Results Probl Cell Differ*. 2002;35:133-50.
135. Kutay U, Lipowsky G, Izaurralde E, Bischoff FR, Schwarzmaier P, Hartmann E, Gorlich D. Identification of a tRNA-specific nuclear export receptor. *Mol Cell*. 1998;1:359-69.
136. Bohnsack MT, Regener K, Schwappach B, Saffrich R, Paraskeva E, Hartmann E, Gorlich D. Exp5 exports eEF1A via tRNA from nuclei and synergizes with other transport pathways to confine translation to the cytoplasm. *Embo J*. 2002;21:6205-15.
137. Lund E, Guttinger S, Calado A, Dahlberg JE, Kutay U. Nuclear export of microRNA precursors. *Science*. 2004;303:95-8.
138. Lipowsky G, Bischoff FR, Schwarzmaier P, Kraft R, Kostka S, Hartmann E, Kutay U, Gorlich D. Exportin 4: a mediator of a novel nuclear export pathway in higher eukaryotes. *Embo J*. 2000;19:4362-71.
139. Fischer U, Huber J, Boelens WC, Mattaj IW, Luhrmann R. The HIV-1 Rev activation domain is a nuclear export signal that accesses an export pathway used by specific cellular RNAs. *Cell*. 1995;82:475-83.
140. Wen W, Meinkoth JL, Tsien RY, Taylor SS. Identification of a signal for rapid export of proteins from the nucleus. *Cell*. 1995;82:463-73.

141. Hamamoto T, Gunji S, Tsuji H, Beppu T. Leptomycins A and B, new antifungal antibiotics. I. Taxonomy of the producing strain and their fermentation, purification and characterization. *J Antibiot (Tokyo)*. 1983;36:639-45.
142. Hamamoto T, Seto H, Beppu T. Leptomycins A and B, new antifungal antibiotics. II. Structure elucidation. *J Antibiot (Tokyo)*. 1983;36:646-50.
143. Kudo N, Matsumori N, Taoka H, Fujiwara D, Schreiner EP, Wolff B, Yoshida M, Horinouchi S. Leptomycin B inactivates CRM1/exportin 1 by covalent modification at a cysteine residue in the central conserved region. *Proc Natl Acad Sci U S A*. 1999;96:9112-7.
144. Bogerd HP, Fridell RA, Benson RE, Hua J, Cullen BR. Protein sequence requirements for function of the human T-cell leukemia virus type 1 Rex nuclear export signal delineated by a novel in vivo randomization-selection assay. *Mol Cell Biol*. 1996;16:4207-14.
145. Ossareh-Nazari B, Bachelerie F, Dargemont C. Evidence for a role of CRM1 in signal-mediated nuclear protein export. *Science*. 1997;278:141-4.
146. Richards SA, Lounsbury KM, Carey KL, Macara IG. A nuclear export signal is essential for the cytosolic localization of the Ran binding protein, RanBP1. *J Cell Biol*. 1996;134:1157-68.
147. Frey N, Olson EN. Cardiac hypertrophy: the good, the bad, and the ugly. *Annu Rev Physiol*. 2003;65:45-79.
148. Yusuf S, Sleight P, Pogue J, Bosch J, Davies R, Dagenais G. Effects of an angiotensin-converting-enzyme inhibitor, ramipril, on cardiovascular events in high-risk patients. The Heart Outcomes Prevention Evaluation Study Investigators. *N Engl J Med*. 2000;342:145-53.
149. Mathew J, Sleight P, Lonn E, Johnstone D, Pogue J, Yi Q, Bosch J, Sussex B, Probstfield J, Yusuf S. Reduction of cardiovascular risk by regression of electrocardiographic markers of left ventricular hypertrophy by the angiotensin-converting enzyme inhibitor ramipril. *Circulation*. 2001;104:1615-21.
150. Wilkins BJ, Molkentin JD. Calcium-calcineurin signaling in the regulation of cardiac hypertrophy. *Biochem Biophys Res Commun*. 2004;322:1178-91.
151. Chien KR. Stress pathways and heart failure. *Cell*. 1999;98:555-8.
152. McKinsey TA, Olson EN. Cardiac hypertrophy: sorting out the circuitry. *Curr Opin Genet Dev*. 1999;9:267-74.
153. Molkentin JD, Dorn IG, 2nd. Cytoplasmic signaling pathways that regulate cardiac hypertrophy. *Annu Rev Physiol*. 2001;63:391-426.
154. Iemitsu M, Miyauchi T, Maeda S, Sakai S, Kobayashi T, Fujii N, Miyazaki H, Matsuda M, Yamaguchi I. Physiological and pathological cardiac hypertrophy induce different molecular phenotypes in the rat. *Am J Physiol Regul Integr Comp Physiol*. 2001;281:R2029-36.
155. Fagard RH. Impact of different sports and training on cardiac structure and function. *Cardiol Clin*. 1997;15:397-412.
156. Richey PA, Brown SP. Pathological versus physiological left ventricular hypertrophy: a review. *J Sports Sci*. 1998;16:129-41.
157. Steinberg SF. Many pathways to cardiac hypertrophy. *J Mol Cell Cardiol*. 2000;32:1381-4.
158. Sugden PH. Signaling in myocardial hypertrophy: life after calcineurin? *Circ Res*. 1999;84:633-46.

159. Wu G, Toyokawa T, Hahn H, Dorn GW, 2nd. Epsilon protein kinase C in pathological myocardial hypertrophy. Analysis by combined transgenic expression of translocation modifiers and Galphaq. *J Biol Chem*. 2000;275:29927-30.
160. Heineke J, Molkentin JD. Regulation of cardiac hypertrophy by intracellular signalling pathways. *Nat Rev Mol Cell Biol*. 2006;7:589-600.
161. Buch MH, Pickard A, Rodriguez A, Gillies S, Maass AH, Emerson M, Cartwright EJ, Williams JC, Oceandy D, Redondo JM, Neyses L, Armesilla AL. The sarcolemmal calcium pump inhibits the calcineurin/nuclear factor of activated T-cell pathway via interaction with the calcineurin A catalytic subunit. *J Biol Chem*. 2005;280:29479-87.
162. Ritter O, Schuh K, Brede M, Rothlein N, Burkard N, Hein L, Neyses L. AT2 receptor activation regulates myocardial eNOS expression via the calcineurin-NF-AT pathway. *Faseb J*. 2003;17:283-5.
163. Zhang L, Torgerson TR, Liu XY, Timmons S, Colosia AD, Hawiger J, Tam JP. Preparation of functionally active cell-permeable peptides by single-step ligation of two peptide modules. *Proc Natl Acad Sci U S A*. 1998;95:9184-9.
164. Ritter O, Hack S, Schuh K, Rothlein N, Perrot A, Osterziel KJ, Schulte HD, Neyses L. Calcineurin in human heart hypertrophy. *Circulation*. 2002;105:2265-9.
165. Li J, Brown LF, Laham RJ, Volk R, Simons M. Macrophage-dependent regulation of syndecan gene expression. *Circ Res*. 1997;81:785-96.
166. Lin YZ, Yao SY, Veach RA, Torgerson TR, Hawiger J. Inhibition of nuclear translocation of transcription factor NF-kappa B by a synthetic peptide containing a cell membrane-permeable motif and nuclear localization sequence. *J Biol Chem*. 1995;270:14255-8.
167. la Cour T, Gupta R, Rapacki K, Skriver K, Poulsen FM, Brunak S. NESbase version 1.0: a database of nuclear export signals. *Nucleic Acids Res*. 2003;31:393-6.
168. la Cour T, Kiemer L, Molgaard A, Gupta R, Skriver K, Brunak S. Analysis and prediction of leucine-rich nuclear export signals. *Protein Eng Des Sel*. 2004;17:527-36.
169. Schneider TD, Stephens RM. Sequence logos: a new way to display consensus sequences. *Nucleic Acids Res*. 1990;18:6097-100.
170. Okamura H, Aramburu J, Garcia-Rodriguez C, Viola JP, Raghavan A, Tahiliani M, Zhang X, Qin J, Hogan PG, Rao A. Concerted dephosphorylation of the transcription factor NFAT1 induces a conformational switch that regulates transcriptional activity. *Mol Cell*. 2000;6:539-50.
171. Shibasaki F, Price ER, Milan D, McKeon F. Role of kinases and the phosphatase calcineurin in the nuclear shuttling of transcription factor NF-AT4. *Nature*. 1996;382:370-3.
172. Cunningham MD, Cleaveland J, Nadler SG. An intracellular targeted NLS peptide inhibitor of karyopherin alpha:NF-kappa B interactions. *Biochem Biophys Res Commun*. 2003;300:403-7.
173. Torgerson TR, Colosia AD, Donahue JP, Lin YZ, Hawiger J. Regulation of NF-kappa B, AP-1, NFAT, and STAT1 nuclear import in T lymphocytes by noninvasive delivery of peptide carrying the nuclear localization sequence of NF-kappa B p50. *J Immunol*. 1998;161:6084-92.
174. Aramburu J, Yaffe MB, Lopez-Rodriguez C, Cantley LC, Hogan PG, Rao A. Affinity-driven peptide selection of an NFAT inhibitor more selective than cyclosporin A. *Science*. 1999;285:2129-33.
175. Hogan PG, Chen L, Nardone J, Rao A. Transcriptional regulation by calcium, calcineurin, and NFAT. *Genes Dev*. 2003;17:2205-32.

176. Zhu J, McKeon F. NF-AT activation requires suppression of Crm1-dependent export by calcineurin. *Nature*. 1999;398:256-60.
177. Chow CW, Rincon M, Cavanagh J, Dickens M, Davis RJ. Nuclear accumulation of NFAT4 opposed by the JNK signal transduction pathway. *Science*. 1997;278:1638-41.
178. Yang TT, Xiong Q, Enslen H, Davis RJ, Chow CW. Phosphorylation of NFATc4 by p38 mitogen-activated protein kinases. *Mol Cell Biol*. 2002;22:3892-904.
179. Sheridan CM, Heist EK, Beals CR, Crabtree GR, Gardner P. Protein kinase A negatively modulates the nuclear accumulation of NF-ATc1 by priming for subsequent phosphorylation by glycogen synthase kinase-3. *J Biol Chem*. 2002;277:48664-76.
180. Zhu J, Shibasaki F, Price R, Guillemot JC, Yano T, Dotsch V, Wagner G, Ferrara P, McKeon F. Intramolecular masking of nuclear import signal on NF-AT4 by casein kinase I and MEKK1. *Cell*. 1998;93:851-61.
181. Hogan PG, Rao A. Transcriptional regulation. Modification by nuclear export? *Nature*. 1999;398:200-1.

7. Abbreviations

$^{R}_{....}$	resistant
µCi	micro Curie
µg	microgram
µM	micromolar
aa	amino acid
AB	aortic banding
ACE	Angiotensin-converting enzyme
AID	autoinhibitory domain
AKAP79	A-kinase anchoring protein 79
AMP	Adenosine monophosphate
AngII	Angiotensin II
ANP	Atrial natriuretic peptide
APS	Ammonium persulfate
ARM repeats	*armadillo* repeats
AS	aortic stenosis
ATP	Adenosine triphosphate
beta (β) -MHC	β-Myosin heavy chain
BIB	β-like import receptor binding
BNP	Brain natriuretic peptide
CAD	coronary artery disease
Cain/Cabin-1	Calcineurin inhibitor/Calcineurin binding protein1
CaM	Calmodulin
CAS	Cellular apoptosis-susceptibility
CBFHH	calcium and bicarbonate free Hanks' with HEPES
CCR	central conserved region
CDC25	Cycle protein 25
Cdk	Cyclin-dependent kinase
cDNA	copy DNA
CK1	casein kinase 1
cm	centimeter
CMV	Cyto Megalo Virus
Cn	Calcineurin
CnA	Calcineurin A
CnB	Calcineurin B
cNLS	classical NLS
Co-IP	co-immunoprecipitation
cpm (c.p.m.)	counts per milliliter
CREB	cAMP response element-binding protein
CRM1	Chromosome region maintenance protein 1
CsA	Cyclosporin A
ctr	control
Cy2 / 3	Carbocyanin 2 / 3
CyP	Cyclophilin P
d	day (s)
DAPI	4',6-Diamidino-2-phenylindol
DARPP-32	Dopamine- and cyclic AMP-regulated phosphoprotein with 32 kDa
DDT	Dichloro-diphenyl-trichloroethane
DMEM	Dulbecco´s Modified Eagle's Medium
DNA	desoxyribonuclein acid
DSCR1	Down-syndrome critical region 1
DSMZ	Deutsche Sammlung von Mikroorganismen und Zellkulturen
DSP	dual-specifity phosphatase
E. coli	*Escherichia coli*
e.g.	lat. *exemplum gratum*; for example
EDTA	Ethylenediaminetetraacetic acid.
eEF1A	eukaryotic translational Elongation Factor 1A
EGFP	enhanced green fluorescent protein

EGTA	Ethylene glycol tetraacetic acid
eIF5A	eukaryotic Initiation Factor 5A
eNOS	endothelial NO synthase
ER	endoplasmatic reticulum
ERK	Extracellularly responsive kinase
ET-1	Endothelin-1
FCS	foetal calf serum
FG	Phenylalanine-Glycin (amino acid pattern)
FKBP12	FK506 binding protein 12
FRET	Fluorescence resonance energy transfer
g	gram
g	G-force
GAPDH	Glycerin aldehyde phosphate dehydrogenase
GATA4	transcription factor
GDP	Guanine diphosphate
GFP	green fluorescent protein
GPCR	G-protein coupled receptor
GSK3β	Glycogen synthase kinase 3β
GTP	Guanosine triphosphate
h	hour (s)
HCM	hypertophic cardiomyopathy
HEAT	Huntingtin, Elongations factor 3, 'A' subunit of protein phospha-tase A, TOR1 lipid kinase)
HIV	Human immunodeficiency virus
hnRNPA1	heterogenous nuclear ribonucleoprotein A1
HRP	Horse-radish peroxidase
i.e.	lat. *id est*; that is
i.p.	intraperitoneal
IBB	Importinβ binding domain
IBP	Import Blocking Peptide
IGF-1	Insulin growth factor
Il-2	Interleukin-2
IP3	Inositol triphosphate
JNK	c-Jun N-terminal kinase
kb	kilo bases
k_D	Michaelis-Menten constant
kDa	kilo dalton
LAD	left anterior descending
LMB	Leptomycin B
LV	left ventricular / left ventricle
m	month
MAPK	Mitogen-activated protein kinase
MCIP1	Myocyte-enriched Cn-interacting protein 1
MCS	multiple cloning site
MDa	mega dalton
MEF2C	Myocyte enhanced factor 2C
MEK	Mitogen-acitvated protein kinase kinase
MEM	Minimal Essential Medium
mg	milligram
MI	myocard infarction
min	minute (s)
ml	milliliter
mM	millimolar
mm	millimeter
mRNA	messenger RNA
n.s.	non significant
ncNLS	nonclassical NLS
NES	nuclear export sequence
NFAT	Nuclear factor of activated T-cells

NF-κB	Nuclear factor kappa B
NLS	nuclear localization sequence
nm	nanometer
NMD3	Nonsense-mediated mRNA decay protein 3
NMDA	N-methyl-D-aspartat
NPC	nuclear pore complex
NRCM	neonatal rat cardiomyocyte
NTF2	Nuclear transport factor 2
P	Promotor
p	plasmid
p	probability
PAGE	Polyacrylamide gel electrophoresis
PBS	Phosphate buffered Saline
PCR	Polymerase chain reaction
PE	Phenylephrine
PFA	Paraformaldehyde
PKA	Protein kinase A
PKC	Protein kinase C
PKI	Protein kinase inhibitor
PLB	Phospholamban
PMSF	Phenylmethanesulphonylfluoride
PP	Protein phosphatase
PPM	Phosphoprotein phosphatases M
PPP	Phosphoprotein phosphatases P
PTHrP	Parathyroid hormone-related protein
PTK	Protein tyrosine kinase
PTP	Protein tyrosine phosphatases
RanBP	Ran binding protein
RanGAP	Ran GTPase activating protein
RanGEF	Ran guanine exchange factor
rel.	relative
RIPA	RadioImmuno PrecipitationAssay
RNA	ribonuclein acid
RNP	Ribonucleoprotein
rpL23a	ribosomal protein L23a
rpL25	ribosomal protein L25
rpm	revolutions per minute
RPTP	receptor-like PTP
RyR	Ryanodine receptor
s	second (s)
SDS	Sodium Dodecyl Sulfate
SEM	Structural Equation Modelling
SERCA	SR Ca^{2+} ATPase
Smad-3 (=Mad3)	Mothers against decapentaplegic homolog 3
SOD	Superoxide dismutase
SR	sarcoplasmatic reticulum
SRP	Signal recognition particle
SV40	Simian virus 40
T & D	Trypsine and DNase
TAE	Tris - acetic acid - EDTA
TCA	Trichloracetic acid
Tcn1p (Crz1p)	transcription factor
TEMED	N,N,N',N'-Tetramethylethylenediamine
TGFβ	Transforming growth factor β
TNFα	Tumor necrosis factor α
tRNA	tranport RNA
U	unit (s)
WT	wildtype

8. Publications and Presentations from this work

8.1. Original articles

- Wu R, Laser M, Han H, Varadarajulu J, Schuh K, **Hallhuber M**, Hu K, Ertl G, Hauck C, Ritter O. (2006). Fibroblast migration after myocardial infarction is regulated by SPARC expression. *J Mol Med.* Mar; 84(3): 241-252.

- **Hallhuber M**, Burkard N, Wu R, Buch MH, Engelhardt S, Hein L, Neyses L, Schuh K, Ritter O. (2006). Inhibition of calcineurin prevents myocardial hypertrophy. *Circ Res*. Sep 15; 99(6):626-635.

- **Hallhuber M** and Ritter O. 2007. A new approach to prevent myocardial hypertrophy: the import blocking peptide. *Fut Cardiol*. Jan; 3(1):91-98.

- Burkard N, Rokita AG, Kaufmann SG, **Hallhuber M**, Wu R, Hu K, Hofmann U, Bonz A, Frantz S, Cartwright EJ, Neyses L, Maier LS, Maier SK, Renne T, Schuh K, Ritter O. 2007. Conditional neuronal nitric oxide synthase overexpression impairs myocardial contractility. *Circ Res*. Feb 16; 100(3):e32-44. Epub Feb 1.

8.2. Poster Presentations

- Erhöhte Calcineurinaktivität durch Proteolyse mit Calpain. 2005 Feb. 25th. *4. Bad Brückenauer Wintertagung* (Medizinische Klinik und Poliklinik I, Universität Würzburg). Würzburg, Germany.

- Erhöhte Calcineurinaktivität durch Proteolyse mit Calpain. 2005 Mar. 31th. *71. Jahrestagung der Deutschen Gesellschaft für Kardiologie* (Deutsche Gesellschaft für Kardiologie (DGK)). Mannheim, Germany.

- Myocardial Calcineurin activity is increased by Calpain-induced proteolysis. 2005 Jun. 11th. *Heart Failure 2005* (European Society of Cardiology (ESC)). Lissabon, Portugal.

- Targeted proteolysis activates Calcineurin. 2005 Sep. 3rd. *ESC Annual Congress 2005.* (European Society of Cardiology (ESC)). Stockholm, Sweden.

- Inhibition of nuclear import of Calcineurin prevents myocardial hypertrophy. 2007 Feb. 8th. *5th Dutch-German Joint Meeting of Molecular Cardiology Groups*. (Rudolf Virchow Zentrum, Netherlands Society of Cardiology, Deutsche Gesellschaft für Kardiologie (DGK)). Würzburg, Germany.

8.3. Oral Presentations

- NLS-Analogon IBP verhindert die nukleäre Translokation von Calcineurin A. 2005 Apr. 20th. *72. Jahrestagung der Deutschen Gesellschaft für Kardiologie* (Deutsche Gesellschaft für Kardiologie (DGK)). Mannheim, Germany.

- Inhibition of nuclear import of Calcineurin prevents myocardial hypertrophy. 2006 Sep. 2nd. *World Congress of Cardiology 2006, ESC Annual Congress 2006* (European Society of Cardiology (ESC)). Barcelona, Spain.

- Inhibition of nuclear import of Calcineurin prevents myocardial hypertrophy. 2006 Nov. 12th. *79th Scientific Sessions American Heart Association 2006* (American Heart Association (AHA)). Chicago, USA.

- Inhibition der nukläre Translokation von Calcineurin A verhindert myokardiale Hypertrophie. 2007 Mar. 16th. *5. Bad Brückenauer Wintertagung* (Medizinische Klinik und Poliklinik I, Universität Würzburg). Würzburg, Germany.

- Inhibition of Calcineurin / importin interaction disrupts Calcineurin / NFAT cascade *in vivo*. 2007 Apr. 12th. *73. Jahrestagung der Deutschen Gesellschaft für Kardiologie* (Deutsche Gesellschaft für Kardiologie (DGK)). Mannheim, Germany.

Curriculum vitae

Person Details

name	Matthias Hallhuber
date of birth	25.10.1979
place of birth	Vilshofen
resident in	Am Schulzengraben 2 97723 Oberthulba / Hassenbach
family status	single
nationality	german
e-mail	matthias_hallhuber@web.de Hallhuber_M@klinik.uni-wuerzburg.de

Current

01/2007 – today	research associate at the Bayerischen Julius-Maximilians-University of Wuerzburg, Clinic of the University of Wuerzburg, Department of Medicine I, Molecular Cardiology; working group PD Dr. med. Oliver Ritter

Tertiary Education

since 02/2007	written compilation of PhD thesis
08/2004 - 03/2007	graduation at the Bayerischen Julius-Maximilians-University of Wuerzburg, Clinic of the University of Wuerzburg, Department of Medicine I, Molecular Cardiology; supervised by PD Dr. med. Oliver Ritter topic: „Inhibition of Nuclear Import of Calcineurin Prevents the Development of Myocardial Hypertrophy“
10/1999 - 07/2004	study in biology at the Bayerischen Julius-Maximilians-University of Wuerzburg (main subject: microbiology; minor subjects: biotechnology and biochemistry *certificate*: Diplom-Biologe Univ. diploma thesis in microbiology; supervised by Prof. Dr. Jürgen Kreft topic: „Konstruktion diverser *prfA*-Mutanten von *Listeria monocytogenes* und Vergleichende Genomanalysen verschiedener Stämme von *Listeria monocytogenes* mittels Makro-Array DNA-Hybridisierungsversuchen“

School Education

1990 – 1999:	Jack-Steinberg Gymnasium Bad Kissingen; Bad Kissingen, Germany *certificate*: general qualification for university entrance
1986 – 1990:	Grundschule Aura; Aura, Germany

Würzburg, den 12.04.2007

Matthias Hallhuber

Eidesstattliche Erklärungen

Hiermit erkläre ich ehrenwörtlich, dass ich die vorliegende Dissertation in allen Teilen selbständig angefertigt und keine anderen als die von mir genannten Quellen und Hilfsmittel verwendet habe.

Weiterhin versichere ich, dass ich bisher keinen Promotionsversuch unternommen oder die vorliegende Dissertation weder in gleicher noch in ähnlicher Form in einem anderen Prüfungsverfahren vorgelegt habe.

Hiermit bewerbe ich mich erstmals um den akademischen Grad *„Doctor rerum naturalium“* (Dr. rer. nat.) durch ordentliche Promotion an der Bayerischen Julius-Maximilians-Universität Würzburg.

Würzburg, den 12.04. 2007

Matthias Hallhuber